8-2006

Mechanisms for Increasing Respiratory Capacity through Ontogeny in the Blastoid Genus *Pentremites*

Troy A. Dexter
University of Tennessee - Knoxville

To the Graduate Council:

I am submitting herewith a thesis written by Troy A. Dexter entitled "Mechanisms for Increasing Respiratory Capacity through Ontogeny in the Blastoid Genus *Pentremites*." I have examined the final electronic copy of this thesis for form and content and recommend that it be accepted in partial fulfillment of the requirements for the degree of Master of Science, with a major in Geology.

Michael L. McKinney, Major Professor

We have read this thesis and recommend its acceptance:

Colin D. Sumrall, Edmund Perfect

Accepted for the Council:
Carolyn R. Hodges

Vice Provost and Dean of the Graduate School

(Original signatures are on file with official student records.)

To the Graduate Council:

I am submitting herewith a thesis written by Troy A. Dexter entitled "Mechanisms for Increasing Respiratory Capacity through Ontogeny in the Blastoid Genus *Pentremites*." I have examined the final electronic copy of this thesis for form and content and recommend that it be accepted in partial fulfillment of the requirements for the degree of Master of Science, with a major in Geology.

Michael L. McKinney
Major Professor

We have read this thesis
and recommend its acceptance:

Colin D. Sumrall

Edmund Perfect

Accepted for the Council:
Anne Mayhew
Vice Chancellor and
Dean of Graduate Studies

(Original signatures are on file with official student records.)

MECHANISMS FOR INCREASING RESPIRATORY CAPACITY THROUGH ONTOGENY IN THE BLASTOID GENUS *PENTREMITES*

A Thesis Presented
for the Master of Science
Degree
The University of Tennessee, Knoxville

Troy A. Dexter
August 2006

Acknowledgements

I would like to thank Dr. Colin Sumrall for creating this project and for all the help and guidance he has given throughout the process, including traveling into the field, sample collection, sample preparation, interpretation of results, expanding the project beyond the blastoid clade, and revising the first few poorly written drafts of this thesis. He has coerced me to present my research a number of times and has introduced me to other researchers in my field whose help has significantly benefited this project. Beyond this project, he is responsible for my education in geology field methods, scientific principles, how to excel at teaching, and just about everything I know in paleontology. Dr. Colin Sumrall has ensured that I am prepared for my upcoming PhD work as well as my future career.

I would like to thank my committee for their advice on this project and their hasty revisions of this thesis. Dr. Michael McKinney was essential for the morphometric interpretations and statistical methods used on this project. Dr. Michael McKinney is also responsible for my original application into this department all those years ago, and without his counsel I would never have come to the University of Tennessee and would likely never have returned to academia. Dr. Ed Perfect not only helped with the revisions of this thesis, but also assisted in shaping the project and its direction in the early stages of its proposal. Dr. Ed Perfect's knowledge of hydrodynamics was necessary for the interpretation of hydrospire biomechanics.

There are a number of people who I would like to thank for their involvement in this project. Dr. Kula Misra allowed the use of his thin bladed Buehler® rock saw, which

I proceeded to break. Dr. Claudia Mora and Dr. Zheng-Hua Li graciously allowed the use of their microtome which was originally to be used on the small samples and which I also proceeded to break. Bill Deane helped me track down and run equipment. Dr. Lawrence Taylor allowed me to use his thin bladed rock saw and Allan Patchen helped me with any issues I had with the saw and was considerate enough to try to fix Kula's rock saw. Dr. Linda Kah was essential in kicking my ass into gear any time I started to slack on the writing of this thesis. Dr. Jonathon Evenick's assistance was essential for the formatting of this thesis and for help with general Microsoft Word© issues (of which there are many). Jeff Nettles helped expand the possible methods I could use for this project and gave much of his time working through methodological issues with me. My personal secretary, Whitney Kocis, read over anything I had written and gave valuable advice for the clarity of my writing. Beyond the department, I had numerous talks with Dr. Johnny Waters and Dr. James Sprinkle about my project focus and what difficulties I would have to address during my research.

Paleontology is not the most economic of geologic disciplines and requires a great deal of begging and borrowing. I would like to thank those organizations who have assisted this degree monetarily. The Geological Society of America provided me with a 2005 Student Grant and the Paleontological Society provided me with a Stephen Jay Gould Grant. This money was invaluable for conducting this research project. I also greatly appreciate scholarship money that I have received from the Mayo Foundation and from the Department of Earth and Planetary Sciences at the University of Tennessee. That money helped offset the great expense of attaining an advanced degree.

Abstract

This study was conducted to determine how the hydrospires in blastoids (the respiratory channels through which blastoids respire) change in shape and capacity during ontogeny. As the volume of a blastoid increases ontogenetically, the respiratory capacity of the hydrospires must increase to match the additional respiratory requirements. Ontogenetically, volume increases at a cubic rate, therefore the surface area of the respiratory structures should increase at a similar rate. Using transverse cross sections of the theca through an ontogenetic series in two species of the blastoid Pentremites*, the surface area and volume of the hydrospires was quantified. The data demonstrated that the hydrospires increased surface area with increasing volume to maintain respiratory capacity and that this was accomplished using different mechanisms depending upon the species. In the species* Pentremites godoni*, increased hydrospire surface area was developed through increased length of the hydrospires through ontogeny. In the species* Pentremites pyriformis*, increased surface area of the hydrospires was accomplished by increasing the number of hydrospire folds within the body through ontogeny.*

Table of Contents

List of Tables

List of Figures

1. Introduction

Biomechanics of extinct animals are often difficult to quantify because of the lack of preservation of soft internal organs. This study was conducted to investigate the respiratory structures in a group of fossilized echinoderms called blastoids. The respiratory structures of blastoids, called hydrospires, are thin, porous folds of high Mg-calcite stereom on the thecal interior. During diagenesis, secondary precipitation of calcite occurs within the pores of the hydrospires, which further preserves these lightly skeletized respiratory structures. Consequently, the measurement of surface area and the quantification of respiratory capacity can be calculated through serial sections.

Blastoids are a group of extinct, stalked echinoderms in the Class Blastoidea that range from Middle Ordovician to Late Permian. The only modern echinoderm analog to blastoids are the generally deep water, stalked crinoids that respire through tube feet, or podia, found externally on the feeding arms. Blastoid respiration occurred through the pumping of seawater internally along the hydrospires within the theca or body cavity. Consequently, little comparison can be made between the mode of respiration in modern echinoderms and internal structures of extinct blastoids. The hydrospires in blastoids represent a general model for endothecal, or internal, respiration common among many groups of extinct, stalked echinoderms including hemicosmitid rhombiferans, glyptocystitoid rhombiferans, “rhomb” bearing crinoids, and parablastoids. This study will advance the understanding of a mode of respiration that can be fit to many other groups outside of the blastoid clade.

There are a number of difficulties involved in interpreting the effects of changing respiratory capacity through ontogeny. The morphology that a species evolves is affected by a number of factors besides the configuration of the hydrospires, including the capacity of the food gathering structures and hydrodynamics of the theca. The respiratory structures have to maintain the metabolic requirements of the blastoid as morphology evolves over time. By studying the hydrospires of two different morphotypes of blastoids, the role of the hydrospires can be clarified.

2. Background

Blastoids are benthic, epifaunal marine animals that required a substrate for attachment and slow water current for capturing food particles (Beaver, 1967a). The minute size of the food groove of the brachioles, suggests that the food was limited to small particles, possibly planktonic organisms (Beaver, 1967a). The oldest known blastoid, *Macurdablastus*, dates back to the Middle Ordovician, and blastoids attained a global distribution by the Devonian period (Macurda, 1967a). Blastoids are an abundant echinoderm component of Mississippian Age rocks. However, by the Permian period, where blastoids show extreme diversity, they were limited to eastern Asia, primarily the island of Timor with a few exceptions outside of Asia (Sprinkle, 1980a, Macurda, 1967a, Macurda, 1967b). Blastoids went extinct at the end of the Permian period (Sprinkle, 1980a, Macurda, 1967a).

Morphology

Blastoids attached to marine substrates with rootlets, and were held up above the substrate by a short, thin column or "stem" and the internal organs were housed within a theca or "head" (Fig. 1) (Fay, 1967). The theca is encased by 19-20 mesodermal skeletal plates, which are composed of unicrystalline, high Mg-calcite, microporous stereom. Five long food canals extend down along the theca called the ambulacra. The area between each of these ambulacra is known as the interambulacral area. The area from the aboral (away from the mouth) edge of the ambulacra to the mouth at the top of the theca is called the vault, whereas the area from the bottom of the ambulacra to the bottom of the basals on the theca is called the pelvis (Fig. 2).

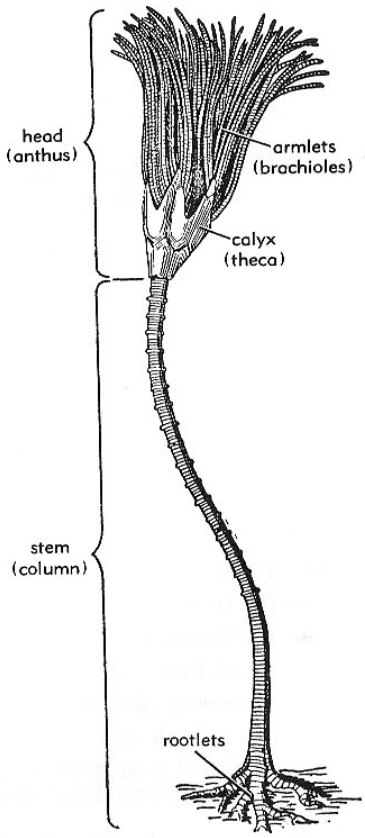

Figure 1: Drawing of the entire blastoid animal as it would appear in life. *From Fay,1967.*

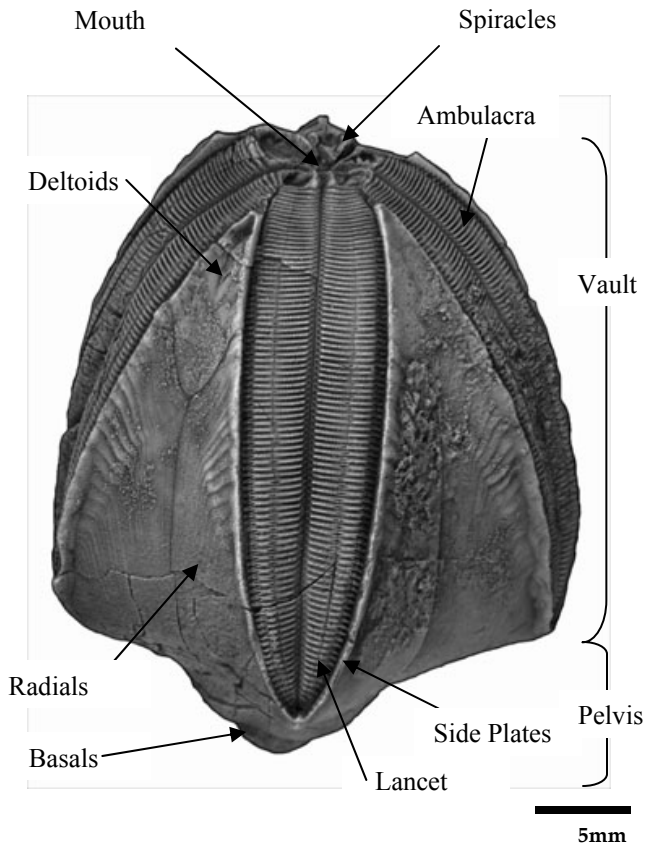

Figure 2: Features of the blastoid theca based on a large specimen of *Pentremites robustus*.

All blastoids have three thecal plates above the column called basals, followed adorally (toward the mouth) by five radials and then five deltoids (Fig. 2). The basals connect the theca to the stem. The radials are cleft to surround five long thin lancet plates, upon which the food groove-bearing ambulacra, are held (Fig. 2). In the interambulacral area and adorally from the radials are deltoid plates (Fig. 2). The deltoid plates, which form later in ontogeny, extend adaxially (toward the polar axis) internally to form the edges of the mouth frame (Fig. 2).

The ambulacra sit within each radial plate and between each deltoid plate. The ambulacra are held on a lancet plate that is partially exposed in Pentrimitid blastoids. The edges of the ambulacra are plated by numerous small plates known as side plates (Fig. 2). The side plates acted as supports for the thin accessory feeding appendages called brachioles (Fig. 1) (Beaver, 1967). Each side plate is composed of a primary and secondary plate. The primary side plates are arranged in a biserial pattern along the ambulacra. The secondary side plates are smaller plates located between each primary side plate toward the radial on either side of the ambulacrum. The brachioles are long, thin, biserially plated appendages extending out from the theca (Fig. 1) (Beaver, 1967).

Brachioles are numerous feeding appendages that extend from the body into the water column. The base of the brachiole, called the brachiole facet, is located at the juncture of the primary and secondary side plates. Brachioles captured food particles and transported the nutrients into food grooves between the side plates. The nutrients were then transported along the main food groove in the center of the ambulacra toward the mouth at the top of the theca (Beaver, 1967).

Pores or slits pass through the plates along both sides of the ambulacra. These are known as hydrospire pores in spiraculate blastoids or hydrospire slits in fissiculate blastoids (Fig. 3). These structures allowed water to enter into the hydrospires (Beaver, 1967). The hydrospires are internal respiratory canals through which respiration occurred (Fig. 4 and 5) (Beaver, 1967). After diffusion of gases occurred along the hydrospire, the water would be expelled through the either the spiracles in order Spiraculata or spiraculate slits in order Fissiculata at the top of the theca (Fig. 2) (Macurda, 1965, Macurda, 1967). The genus *Pentremites* used in this study is a spiraculate blastoid that has hydospire pores and spiracles.

A pair of hydrospires are positioned behind each ambulacrum and are separated into various numbers of corrugated folds (Figs. 4 and 5). In *Pentremites*, water passing in through the hydrospire pores would have been transported up along these thin, porous hydrospire folds and out through the spiracles (Fig. 5) (Macurda, 1965). The thin walls of the hydrospire folds are constructed of permeable, mesh-like stereom and were likely structures through which respiration took place (Beaver, 1996, Macurda, 1967). In order to increase the efficiency of respiration, it is likely that fluid from the water vascular system was transported aborally within the visceral cavity along the walls of the hydrospire folds as suggested by Paul (1968). This counter-current flow of coelomic fluid would increase the oxygen gradient between the respiratory structures and sea water thus increasing the rate of oxygen diffusion through the hydrospires. Countercurrent respiration allows the diffusion of 80 to 90% of the oxygen in sea water as opposed to the maximum of 40 to 50% with concurrent respiration (Campbell, 1996, Paul, 1968).

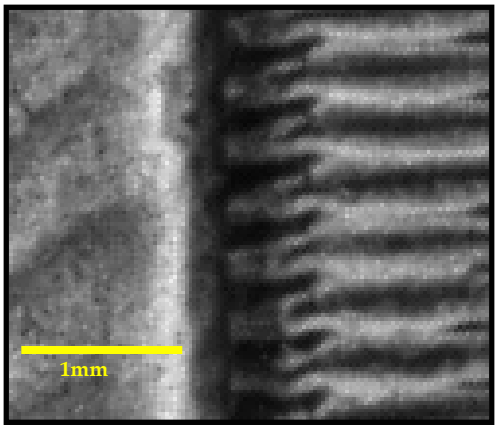

Figure 3: Hydrospire pores found between the side plates at the edges of the ambulacra on a *P. Robustus*.

Figure 4: Transverse cross section through *P. godoni* (Sample F8) revealing the corrugated folds of the hydrospires.

Figure 5: Abaxial side of a broken radial plate form a *P. robustus* revealing the hydrospire folds extending up along the theca behind the ambulacrum.

Although the soft tissue of the water-vascular system is unlikely to preserve in the fossil record, the significant difference in oxygen diffusion efficiency makes it highly probable that countercurrent respiration was employed in blastoids. Spiracles or spiraculate slits, which are found around the mouth directly above the deltoids at the top of the theca, would allow effluent water from the hydrospires to be expelled (Fig. 2).

Phylogeny and Development

There are a number phylogenetic hypothesis for the blastoid clade. Possible relationships include a direct ancestry from coronoids (Brett et al. 1983, Sprinkle, 1980), that coronoids and blastoids are direct descendants of eocrinoids (Brett et al. 1983), or that blastoids are a sister taxa to coronoids (Koverman and Sumrall, 2003, Sumrall, 1997). The spiraculate blastoid genus *Pentremites* also has a number of potential phylogenetic placements. It has been suggested that *Pentremites* is descended from the spiraculate genus *Hyperoblastus,* which is argued to have been descended from the fissiculate blastoid *Heteroschisma* (Galloway and Kaska, 1957). Another possibility is the spiraculate blastoid *Petaloblastus*, with either *Devonblastus* or *Cordyloblastus* as ancestor of *Petaloblastus* (Fay, 1967a). It has also been argued that *Pentremites* is directly descended from the fissiculate blastoid family phaenoschismatidae without a spiraculate intermediate, making the spiraculate order polyphyletic (Macurda, 1975). Using stratocladistic analyses, *Pentremites* has been linked to a fissiculate ancestor, with both Spiraculata and Fissiculata as polyphyletic clades (Bodenbender and Fisher, 2001). However, this hypothesis reached using stratocladistic analysis has a number of unresolved issues and is considered tenuous at best (Sumrall and Brochu, 2003).

Echinoderm reproduction is thought to be primarily sexual with the release of eggs and sperm into the water column. Indeed, fossilized eggs are believed to have been found in *Pentremites rusticus* (Katz and Sprinkle, 1976). This species has two morphotypes; one normal and one with an expanded hydrospire cavity where the internal gonads would likely have been located (Katz and Sprinkle, 1976). Early life stages of echinoderms include a free swimming larval stage. It is believed that the attachment to the ocean floor and metamorphosis into a stalked echinoderm occurs after this larval stage in blastoids. This early, post larval stage in blastoids has been attributed in the fossil record to genus *Passalocrinus*, which was formerly interpreted as a crinoid (Sevastopulo, 2005). This genus has identical plating to blastoids and is interpreted to be equivalent to the cystidean stage in crinoid development (Sumrall and Waters, 2006).

The calcite plates of the blastoid theca were secreted by mesoderm tissues. Growth occurred by the periodic secretion of small amounts of calcite to each plate by tissues in between the sutures of plates (Macurda, 1967). This pattern of growth left minute growth lines visible along the external plates of the theca (Fig. 2), and the stereom mesh of each plate is optically a single calcite crystal (Macurda, 1967).

3. Current Study

Hypothesis

The clade Blastoidea is characterized by a homologous arrangement of plates. This facilitates comparison of structures between species, but it also constrains morphological alterations in response to shifting evolutionary patterns as well as potential ecophenotypical change. Since diffusion of gases occurred along the hydrospire folds, the surface area of the hydrospire folds was likely the limiting factor in the amount of oxygen that could be absorbed. Consequently, increases in total respiratory need resulting from increased body size through ontogeny should be recognizable as increases in the hydrospire fold surface area. This could be accomplished by changing any of three parameters for hydrospire folds: number, length, or shape. Previous investigations have indicated that hydrospire fold number tends to remain constant within each species and is not likely to change through ontogeny (Macurda, 1967, Beaver, 1967, J. Sprinkle, pers. comm.), suggesting that changes in shape and length are more important. However, variation in hydrospire fold number through ontogeny has been observed in certain fissiculate blastoids (Macurda, 1967).

Assuming isometry (no change in shape during ontogeny), as an organism grows, linear dimensions increase at a linear rate, surface area increases at a squared rate, and volume increases at a cubic rate. Consequently, during ontogeny, certain properties of organisms should vary linearly (height, length, width), at a squared rate (diffusional membranes, external casing), or at a cubic rate (volume, mass, food intake, respiration). In organisms with isometric growth, an increase in length will cause the surface area to increase as a square function and the volume to increase as a cubic function (Fig. 6)

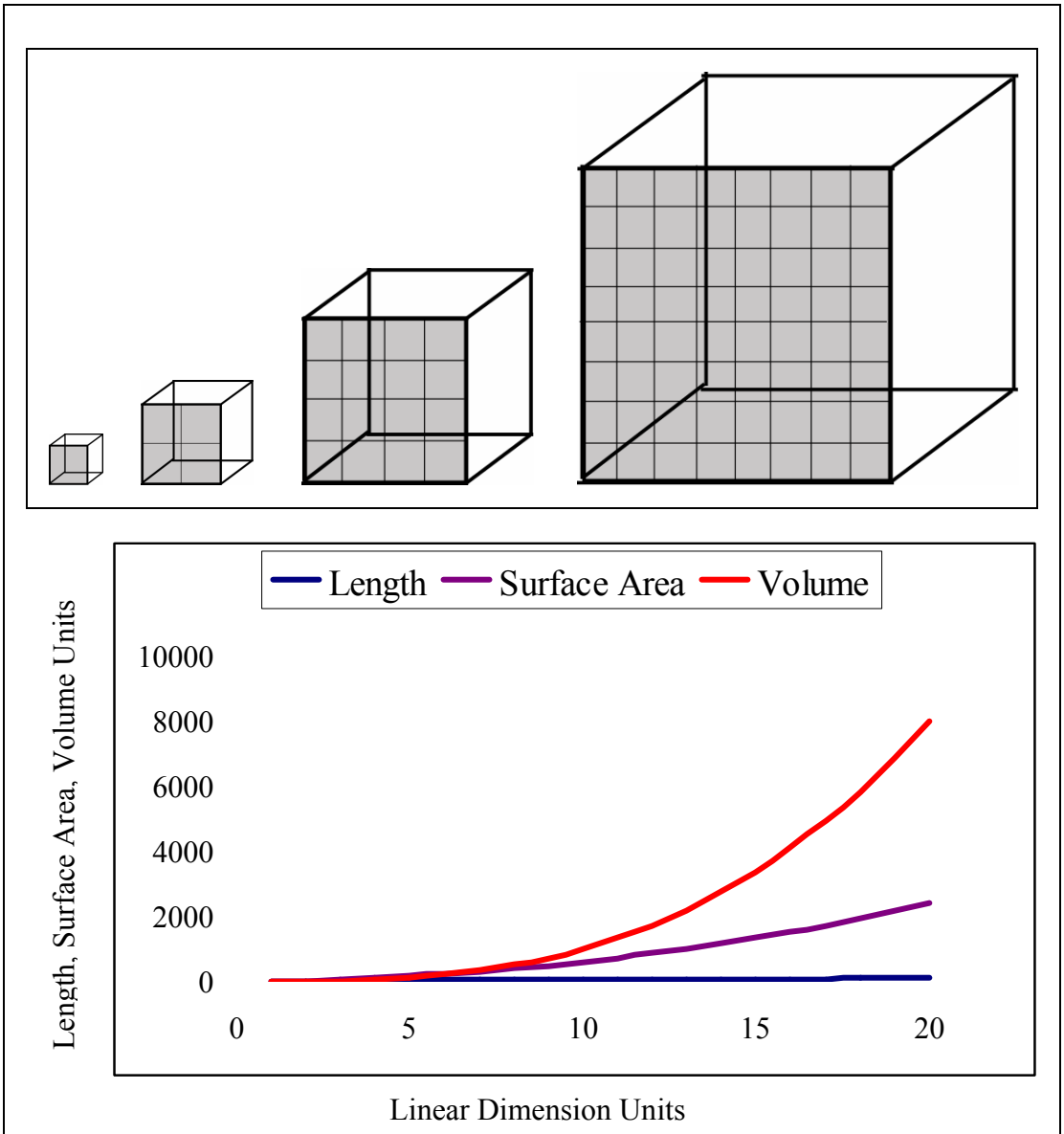

Figure 6: Graphical depiction of increases in surface area and volume relative to length for a geometric shape increasing in size isometrically.

(Becker et al.,2000). In a living organism, an increase in volume should be proportional to an increase in the number of cells within that individual. Therefore, if the nutrient requirement for each individual cell remains constant, an increase in volume of an individual should produce a cubic relationship for nutrient uptake relative to the length of the individual. However, since diffusion occurs over the surface area of respiratory organs, it should increase as a squared rate relative to the height of the animal unless allometric changes in size and shape occur in the respiratory organs (Becker et al.,2000). Ontogenetic increases in blastoid thecal volume should be met with a concomitant increase in respiratory surface area to allow the metabolism of the increased nutrient uptake.

If the rate of surface area growth through ontogeny creates a curve significantly less than a cubic function, other factors are necessary to explain where oxygen for metabolism is obtained. There are a number of factors that could explain this pattern. (1) Oxygen diffusion and circulation could occur within organs other than the known respiratory structures, such as the brachiole feeding appendages. A long standing question about brachioles is whether or not they have a water vascular system running up their length similar to the podia of modern echinoderms (Briemer and Macurda, 1972, Sprinkle, 1973). The thin width of the brachioles may have allowed them not only to maintain their own metabolic requirements but also to increase the oxygen uptake for the entire organism and decrease the requirements on the hydrospires. (2) The metabolic requirements are far exceeded in younger individuals and only become adequate at mature stages of development. (3) Oxygen diffusion becomes more efficient at mature

stages as flow rate through the wider hydrospire pores becomes less restricted. (4) The metabolic rate of the individual may decrease through ontogeny. By comparing data on the surface area of the hydrospires and the visceral volume, each of these possibilities can be tested for their validity.

The plates of a blastoid are composed of porous stereom with organic material filling in the pores. The external plates likely required very little oxygen and could probably diffuse what they needed directly from the water column. The brachioles, stems, and rootlets are also thin and likely respire through diffusion. For this reason, the brachioles, stems, and rootlets were not measured for this study.

Localities

Two species in the genus *Pentremites* were collected for this study. The species collected were *Pentremites godoni* and *Pentremites pyriformis*. These species were selected for their close relationship to each other as well as their different growth strategies resulting in dissimilar morphotypes. Both populations were collected from localities of Late Mississippian, Chesterian Age.

One population was collected at Floraville in Saint Claire County, Illinois. The samples were gathered from the Lower Chesterian, Ridenhower Formation of the Paint Creek Group (Beaver and Fabian, 1998). This site is located at 38º 22’ 54.35” north latitude, 90º 04’ 51.18” west longitude. The outcrops were found along the banks of a streambed located at either side of the Prairie Du Long Creek. The outcrops were composed of highly weathered, fissile, fossiliferous, light green shale with very minor limestone interbedding. Blastoids found at this locality were primarily *Pentremites*

godoni. The faunal components included common Paleozoic marine organisms, such as crinoids, various brachiopod species, encrusting bryozoa, and horn corals. This unit was deposited in a muddy, shallow, lagoonal environment. The blastoids at this locality displayed excellent external preservation with little flattening, distortion, or silicification. Blastoids were preserved in secondarily precipitated calcite spar with some geopedal micrite infilling.

The other population of blastoids was collected from a Middle Chesterian rock from Sulphur in Crawford County, Illinois. The samples were gathered from the Indian Springs Shale Member of the Big Clifty Formation in the Stephensport Group (Blake and Elliott, 2003). This site was located at 38º 14' 33.28" north latitude, 86º 28' 09.43" west longitude. The outcrops were located at road cuts around the intersection of Interstate 64 and Indiana Highway 37. The outcrops were composed of fossiliferous gray shale interbedded with limestone. Blastoids at this locality were mostly *Pentremites pyriformis*. Other faunal elements at this locality besides blastoids were crinoids, brachiopods, trilobites, horn corals, and the bryozoan *Archimedes*. This locality was also likely a muddy, shallow water, lagoonal environment at the time of deposition. Blastoids showed decent preservation with a limited number of samples being flattened or distorted and some minor silicification. Blastoids were preserved in calcite spar and occasionally filled with geopedal micrite.

Species Description

Pentremitid blastoids are in the Family Pentremitidae in the Order Spiraculata (Fay and Wanner, 1967). Spiraculate blastoids are diagnosed by the possession of

hydrospire pores along to either side of the ambulacra and spiracles around the mouth (Fay and Wanner, 1967). *Pentremites* Say is diagnosed by the presence of four spiracles and an anispiracle (a pore formed by the merging of the anus and the spiracle) and for its exposed lancets centered in the ambulacra (Fay and Wanner, 1967).

The blastoid specimens collected from Floraville, Illinois, were almost exclusively *Pentremites godoni*. The blastoid specimens collected from Sulphur, Indiana, were primarily *Pentremites pyriformis* with small number of *Pentremites godoni*. *Pentremites godoni* are recognized by long, wide ambulacra that compose most of the height of the theca (Fig. 7). *Pentremites pyriformis* have much shorter ambulacra relative to the theca (Fig. 8). *Pentremites godoni* tend to have wider, squatter theca with an obtuse pelvis angle whereas *P. pyriformis* tend to be thinner (nearly subconical) with a sharp pelvis angle (Fig. 9). In *Pentremites pyriformis*, the vault height to pelvis height ratio (V/P ratio) tends to remain the same throughout ontogeny, growing from 1.0 to a maximum of 1.5 (Waters et al., 1985). *Pentremites godoni* have a strongly allometric V/P ratio that starts at around 1.0 in juveniles and increases from 4.0 to 10.0 in adults (Waters et al., 1985). By using the diagnostic characteristics of each species, samples of *P. godoni* found at the Sulphur locality were removed from the population and samples of *P. pyriformis* found at the Floraville locality were removed from the population. This became increasingly difficult at small sizes. All morphometric comparisons between the two populations graphed noticeably separate, and outliers were used to uncover any *P. pyriformis* found at Floraville or *P. godoni* found at Sulphur (Figs. 9 and 10).

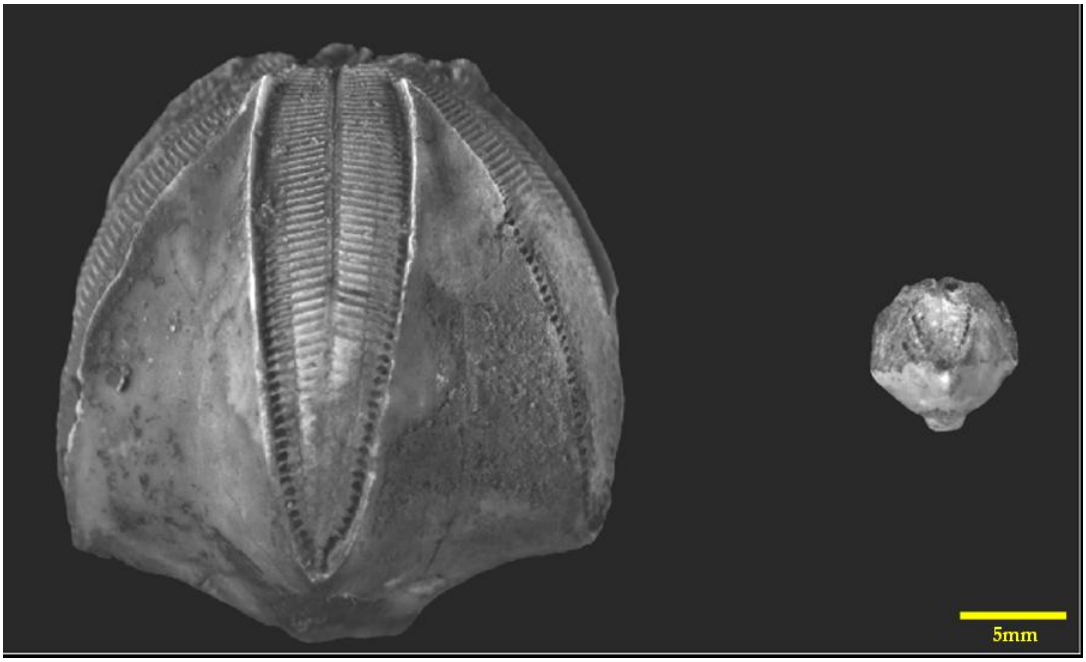

Figure 7: Adult and Juvenile *Pentremites godoni* (Samples F1 and F15).

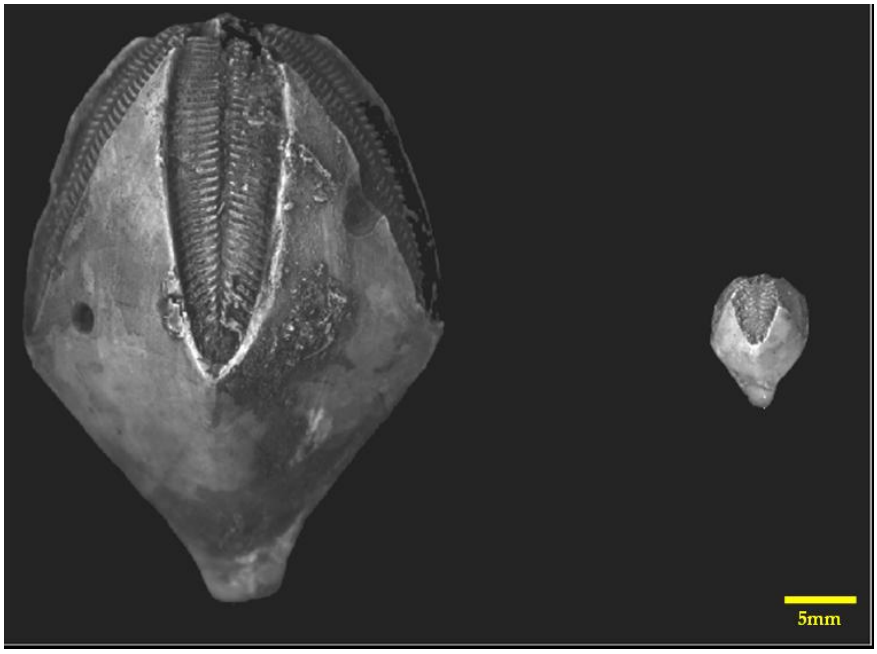

Figure 8: Adult and Juvenile *Pentremites pyriformis* (Samples S2 and SA13).

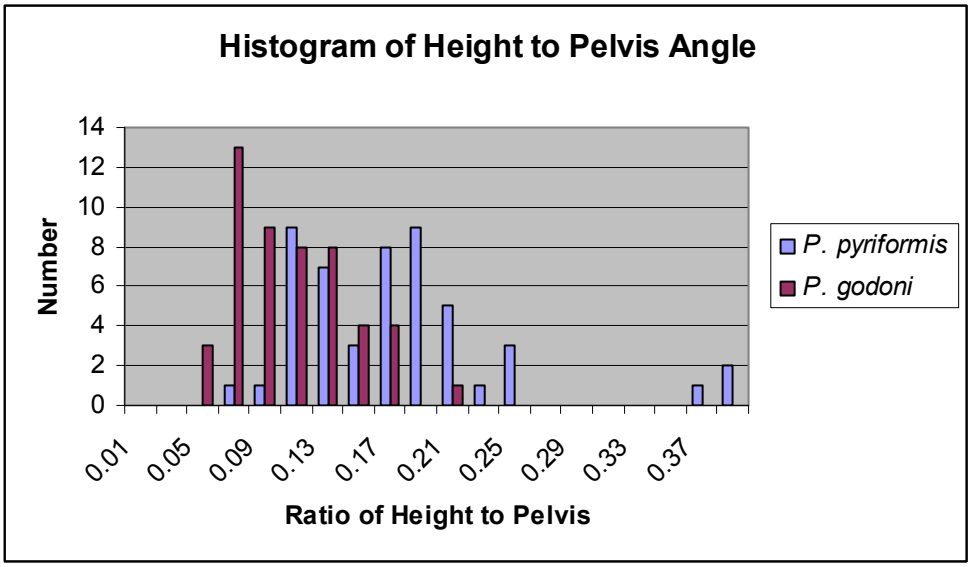

Figure 9: Histogram of the ratios between thecal height and pelvis angle.

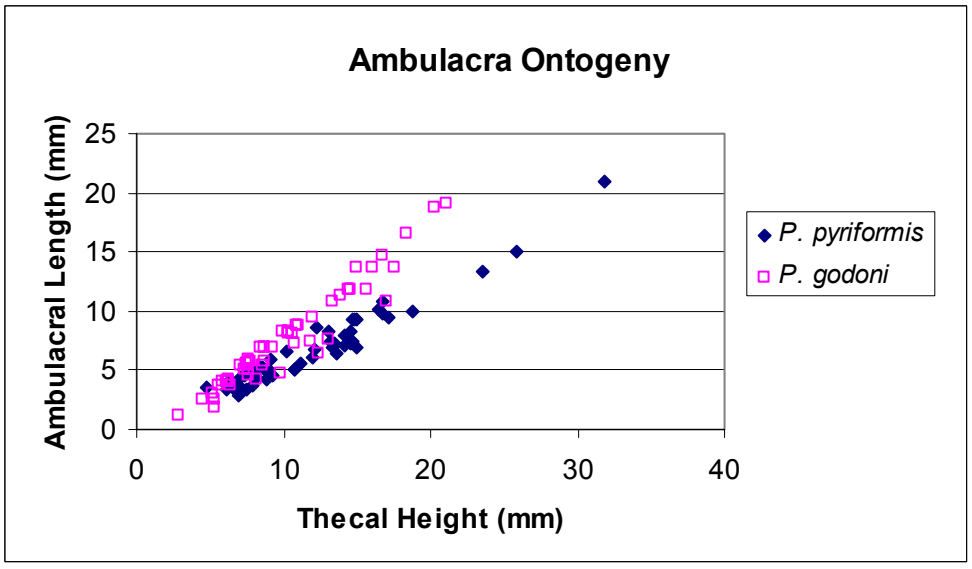

Figure 10: Comparison of ambulacral length between Sulphur *P. pyriformis* and Floraville *P. godoni.*

4. Methodology

Sample Collection

Specimens were collected individually as well as from bulk samples of weathered shale gathered in buckets at the two localities. Two five-gallon buckets of bulk material were collected at each locality. The bulk samples were rinsed and agitated a number of times with water to remove clay-sized particles. Hydrogen peroxide was added to the water, left to react overnight, and the material was periodically agitated. The hydrogen peroxide helped break down the organic matter which, as it effervesced, helped disaggregate the shale. The samples were thoroughly agitated and wet-sieved at a decreasing phi size. The sieve sizes used started at a maximum of -2.75 Φ (6.73 mm) and decreased continuously through -1.75 Φ (3.36 mm) and +0.5 Φ (1.19 mm) to a minimum of +3.0 Φ (0.125 mm) to facilitate searching for small specimens. Clay particles were rinsed through the sieves leaving behind primarily bioclastic residue. The remaining material was sorted by size and left out to dry on paper. Each size fraction of the dry material was carefully searched for blastoids at the various stages of ontogeny.

All the blastoids from the bulk samples and from individually collected samples were sorted by completeness. Fragmented or disarticulated samples would have been unacceptable for hydrospire or volumetric measurements and were thus removed from the sample population. Severely flattened or distorted blastoids were also removed from the sample population, as they would not have accurately preserved the measurements made on the blastoid. Complete samples were cleaned primarily with a toothbrush and warm water. More tenacious matrix was removed with a dental pick and a few of the samples were cleaned with an S. S. White Airabrasive® Jet Machining Unit using

sodium bicarbonate abrasive powder to remove matrix material that was firmly cemented on the specimens. From the cleaned, complete samples, fifty individuals were selected along a complete ontogenetic series from both *Pentremites* species.

Specimens of *Pentremites pyriformis* from the Sulphur locality were labeled numerically as S1 to S20, SA1 to SA14, and SB1 to SB16. Specimens of *Pentremites godoni* from the Floraville locality were labeled F1 to F15, FA1 to FA11, and FB1 to FB24. An additional *P. godoni* specimen from Floraville used for the visceral volume measurements was labeled GRand1. Specimens were kept in individual bins within plastic fishing tackle boxes from which the numbering system was derived. Small samples were contained in small sealable plastic bags that were kept within the tackle boxes.

Morphometric Analysis

All measurements are recorded in the appendix. Specimens were measured primarily with calipers. For small samples, measurements were taken using a gradicle in the eyepiece of a Bausch and Lomb® dissection microscope. The gradicle was calibrated using a metric ruler and was recalibrated following any change to the focus or zoom between samples. The following characteristics were measured for morphometric analysis: thecal height, thecal width, pelvis height, ambulacral length, ambulacral width, radial length, radial width, radial-radial (RR) suture length, radial-deltoid (RD) suture length, pelvis angle, side plates per millimeter, side plates per ambulacrum, and mass. Total brachiole number, vault height, and volume were calculated from the measurements. Blastoids, like most echinoderms, have radial symmetry, so plates are

repeated five times around the theca. Since samples were not flattened or distorted, only one measurement was taken and recorded for symmetric characteristics that were repeated around the theca (such as ambulacral length or radial length).

Height was measured from the bottom of the basals to the top of the oral face (Fig. 11). Width was measured from the ambulacrum on one side of the axis to the two opposing radials on the other side where it was greatest (Fig. 11). For example, width would be measured from the A ambulacrum to the contact suture of the C and D radials. Width was always measured at the location of greatest width on the individual, usually found at the distal end of the ambulacra. Pelvis height was measured from the aboral base of the ambulacra to the bottom of the basals (Fig. 11). Vault height, the distance from the adoral end of the ambulacra to the top of the oral face, was calculated by subtracting the pelvis measurement from the height. The ambulacral length was measured from the base of the ambulacra to the top of the oral face (Fig. 11). The ambulacral length was measured at a forward angle to the theca to accommodate the curvature of the ambulacra. The ambulacra width was measured at the location of greatest width along the ambulacra (Fig. 11).

The radial-radial (RR) suture, was measured along the contact formed between adjacent radials on the individual (Fig. 12). The radial-deltoid (RD) suture was measured along the edge of contact formed between the adoral side of the radial and the lower side of the adjacent deltoid (Fig. 12). Radial length was measured from the upper edge of the radial in contact with the deltoid and the lower edge of the radial in contact with the

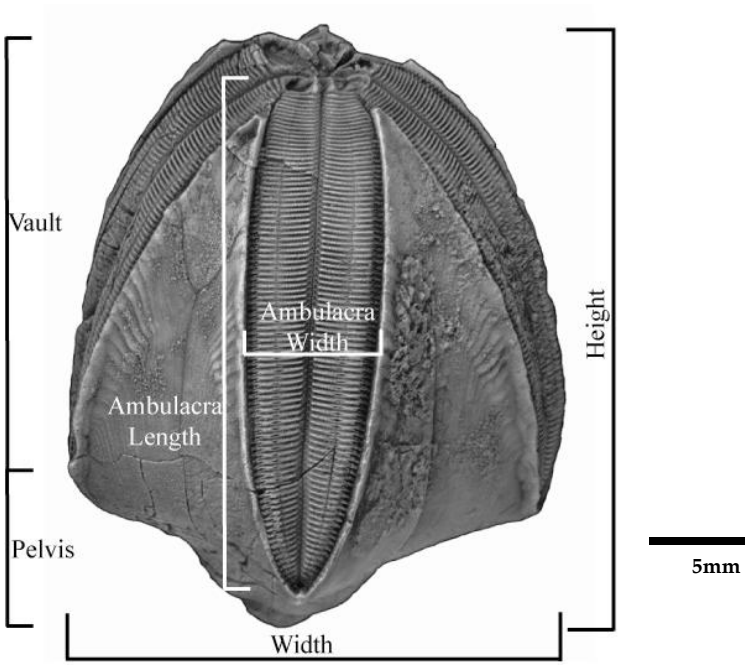

Figure 11: Diagram of morphometric measurements on the theca of a *P. robustus*.

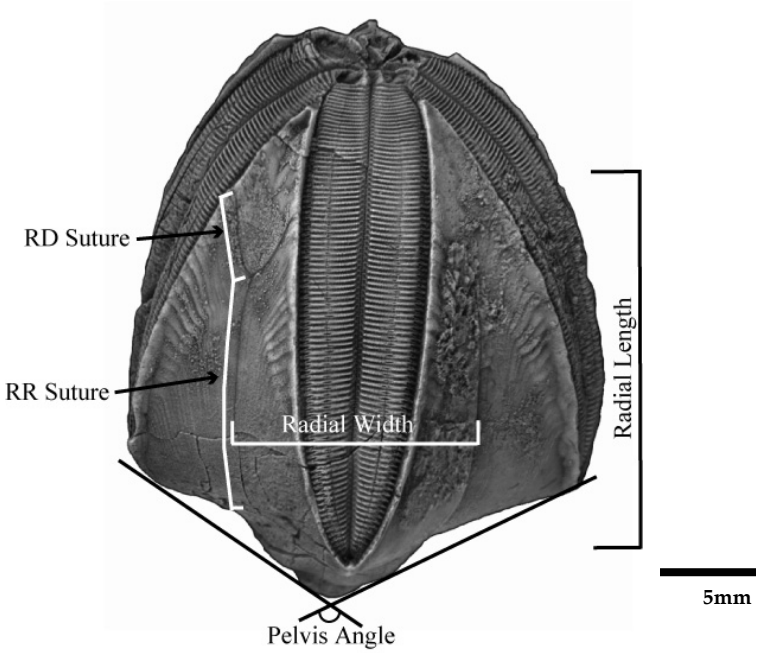

Figure 12: Continued diagram of measurements on the theca of a *P. robustus*.

basals (Fig. 12). Radial width was measured at the location of greatest width on the radial plate between the RR sutures on either side (Fig. 12).

The pelvis angle is the angle formed by the basals and lower portion of the radials at either side (Fig. 12). Pelvis angle was measured using a modified camera lucida technique. A protractor was placed on a piece of white paper and moved into focus under the camera lucida mirror while the blastoid was placed under the microscope. This allowed the sample to be visible in one eyepiece and the protractor to be visible in the other eyepiece. With the transparent appearance created by this technique, the protractor appeared to be inside the blastoid. This permitted accurate measurement of the pelvis angle without the difficulty created by measuring a two dimensional characteristic on a three dimensional object.

The number of side plates per millimeter was calculated by measuring 1.0 millimeter in gradicle units with a ruler under a dissection scope and then visually determining how many primary side plates fit within that millimeter. Side plates per ambulacrum were counted for the primary side plates on both sides of the ambulacrum for two ambulacra on an individual. If the count was different, then a third ambulacrum was counted and the average of all three was calculated. Brachioles were calculated by multiplying the number of primary side plates per ambulacrum by five.

Mass was measured with an Ohaus® Explorer mass scale with a 0.1 microgram resolution. Volume for the entire individual was calculated by dividing the mass of the sample by the density of calcite or 2.71 grams/cubic centimeter. The density was then converted to millimeters cubed with one cubic centimeter equal to 1000 mm^3.

All the Sulphur radial-deltoid sutures were measured under the dissection microscope except samples S1 through S7, which were measured using calipers. All the Sulphur radial-radial sutures were measured using calipers with the exception of samples SA7 through SA14, which were measured under the dissection microscope. Radial-deltoid sutures for all Floraville samples were taken under the microscope. The radial-radial sutures, radial width, and radial length measurements for Floraville samples FA1 through FA11 were taken using a microscope. Every measurement for Floraville samples F11 through F15 was taken using a microscope.

Large Sample Sectioning

The species were sectioned transversely to calculate the volume and surface area of the internal hydrospires. Each section was made by the removal of material from the oral side of the theca leaving a flat internal surface and the remaining aboral portion of the theca. The individual sample was destroyed using this sectioning process. Large samples were any specimen with a thecal height greater than 7 millimeters. Specimens were attached to glass slides so that they could be sectioned perpendicular to the thecal polar axis. The basal area of each sample was removed with a rock saw and ground down to create a plane that was perpendicular to the polar axis. Ward's® Etched Petrographic Microscope Slides (27mm by 46 mm by 1.5mm) were scribed with the sample number. The sample was then attached by the basal side to the slide with Loctite® 3335 UV/Cationic Epoxy. The samples were left under a Raytech® Ultraviolet lamp (Model LS7CB) for at least twenty minutes for the epoxy to cure. This resulted in a properly oriented specimen that could then be sectioned.

A Buehler® Isomet Low Speed Saw with micrometer and a 0.5 millimeter thick diamond blade was used to section the samples. The micrometer on the Buehler® rock saw was calibrated with calipers and determined to move the sample two millimeters every three rotations or 0.66 millimeters every rotation. A slide holder attachment was fastened to the arm of the Buehler® rock saw to hold the specimen in place while sectioning. A maximum of 0.33 millimeters was ground off for each section on specimens measuring 7 to 9 millimeters in height. A maximum of 0.66 millimeters was ground off for each section on specimens measuring 9 to 12 millimeters in height. A maximum of 1.0 millimeters was ground off for each section on specimens measuring 12 to 16 millimeters in height. A maximum of 2.0 millimeters was ground off for each section on specimens greater than 16 millimeters in height. Thinner sections were removed at the top of each specimen where the hydrospires undergo considerable change. After the removal of a section using the Buehler® rock saw, samples were processed for digital imaging. The samples were polished with 600 grit, rinsed, and briefly etched with 0.1 molar Hydrochloric acid. This process smoothed out the photographed surface allowing higher resolution of the minute hydrospires.

Samples were photographed using a digital camera with lighting after each serial grind was removed. The A-ambulacrum was marked on the slides and the position of each slide was outlined on a piece of paper on the copy stand to keep the sample orientation consistent and to insure that all of the blastoid would remain within the frame of the picture. A ruler was placed beside the sample and was held at the level of the each section of the blastoid with a block of clay. This kept the ruler in focus with the rest of

the picture. The ruler was used to calibrate the measurements in the image analysis package Scion Image.

Specimens were ground starting at the oral face perpendicular to the axis and material was removed downward toward the basals. Slices were made until the spiracles with a thick walled, tube-like morphology had graded into the hydrospires with a thin walled, corrugated morphology. The thickness of each section was recorded. The total number of sections was kept at approximately 10 for each sample. Slices were made removing material up to the aboral edge of the ambulacra until the hydrospires ended and that final cut thickness was recorded.

Small Sample Sectioning

Small samples were individuals whose thecal heights were less than 7 mm. Specimens were mounted in small pieces of clay with the basals down in small rubber cups oriented to keep the polar axis perpendicular to the bottom of the cup. The rubber cups were then filled with epoxy and cured. The rubber cups had a non-adhesive internal surface and were coated in Vaseline. The cups were filled with Buehler® Epoxicure Resin (20-8130) and Buehler® Hardener (20-8132), entirely surrounding the blastoid. The epoxy was left overnight to cure and the samples were removed. A rock saw was used to square off the rounded edges of epoxy and to remove the epoxy above the oral face to save time grinding the sample down. Two minute holes were drilled parallel to the axis of the blastoid in the epoxy with a 0.5 mm drill bit on the flattened oral face (Fig. 13). These holes were used as reference points to calibrate measurements in the Scion Image analysis package. The distance between the holes was measured under the

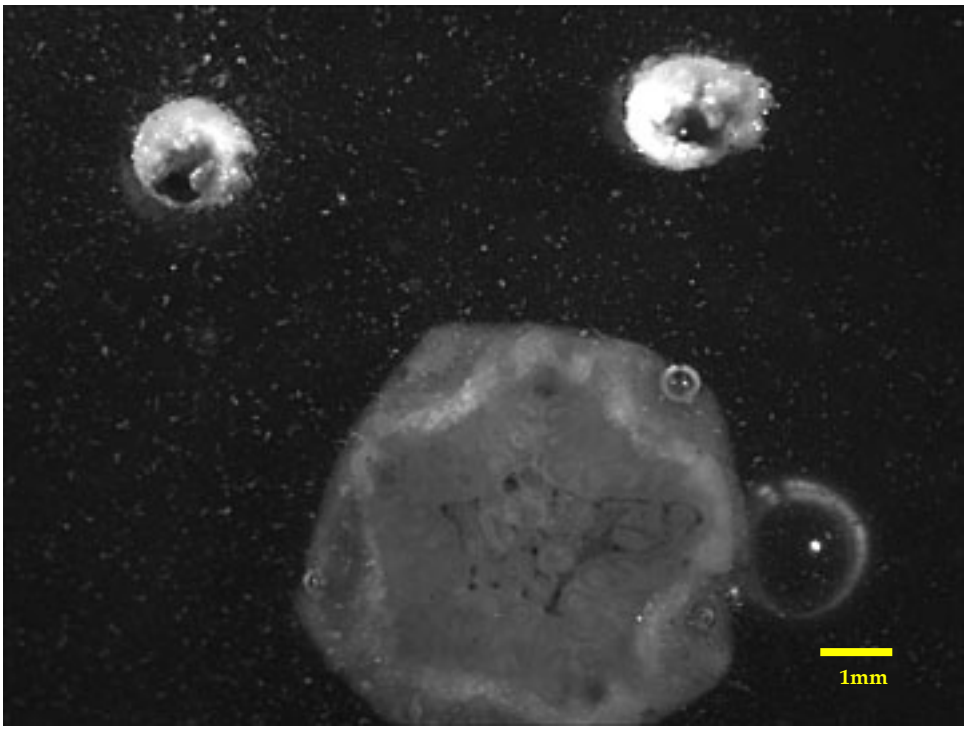

Figure 13: Small sectioned sample showing small parallel drill holes at the top used as reference points for the image analysis package (Sample FA11).

microscope and recorded. Since the holes may not have been precisely parallel to one another, the distance between them was taken after each section was removed. This kept the calibration in Scion Image precise. Another minute hole was drilled into the side of the specimen in epoxy parallel with the flattened oral face. This was used as a reference point for the thickness of each section. The thickness of each section was measured with a microscope between the hole and the photographed surface of the specimen. This distance was recorded after each section was ground off to keep track of the removed thickness of each transverse cross section.

Each section was ground down perpendicular to the polar axis aborally from the top using 240 grit and the grinding blade of a Hillquist® thin section maker. Samples were ground from the oral surface until the first occurrence of the hydrospire folds. The thickness prior to the section that revealed the hydrospires was recorded. The sections were removed perpendicular to the polar axis. Sections were removed until the hydrospire folds were no longer visible, and this final thickness was recorded. After removing each section, the samples were polished in 600 grit and then briefly etched with 0.1 molar hydrochloric acid. This enhanced the visibility of the hydrospires. Images were digitally captured through a microscope with an attached camera mount. Approximately 7 sections were removed from each individual specimen using this method.

Photographic Measurements

The images captured for each sample were measured using an image analysis program Scion Image from Scion Corporation which is a derivative of NIH Image developed for use on a Personal Computer. The program was set to record only area and

perimeter measurements. For each image, a line was drawn with the Line Tool marking the length of the reference points (ruler marks for larger samples or drill holes in epoxy for smaller samples), and the scale was calibrated to make measurements. The Pencil tool was selected to outline each half of the hydrospire pairs as well as the area connecting all the folds on a single hydrospire together, and the measurement was recorded (Fig. 14). If the ten hydrospires were not visible or complete in a photograph, only the visible hydrospires were recorded. Measurements were exported to a Microsoft® Excel worksheet. This process was repeated for each photograph of each sample.

Calculating Surface Area

The following procedure was used on both the area and perimeter measured in cross section to determine the total hydrospire volume and surface area for each individual blastoid. The average of the visible hydrospire fold measurements was calculated. Each average was then multiplied by half of the thickness of the previous cross section from the photographed surface (Fig. 15). Then each average was multiplied by half the thickness of the next occurring cross section from the photographed surface (Fig. 15). These numbers were then summed to get the area and volume of the average hydrospire fold for that photograph. There are ten total hydrospires in a blastoid, with one at either side of the five ambulacra. Since the average hydrospire fold was used in this method, this number was multiplied by ten to calculate the entire hydrospire surface area and volume for the individual. The volume of the hydrospires was subtracted from the total volume (calculated from the mass) for each individual.

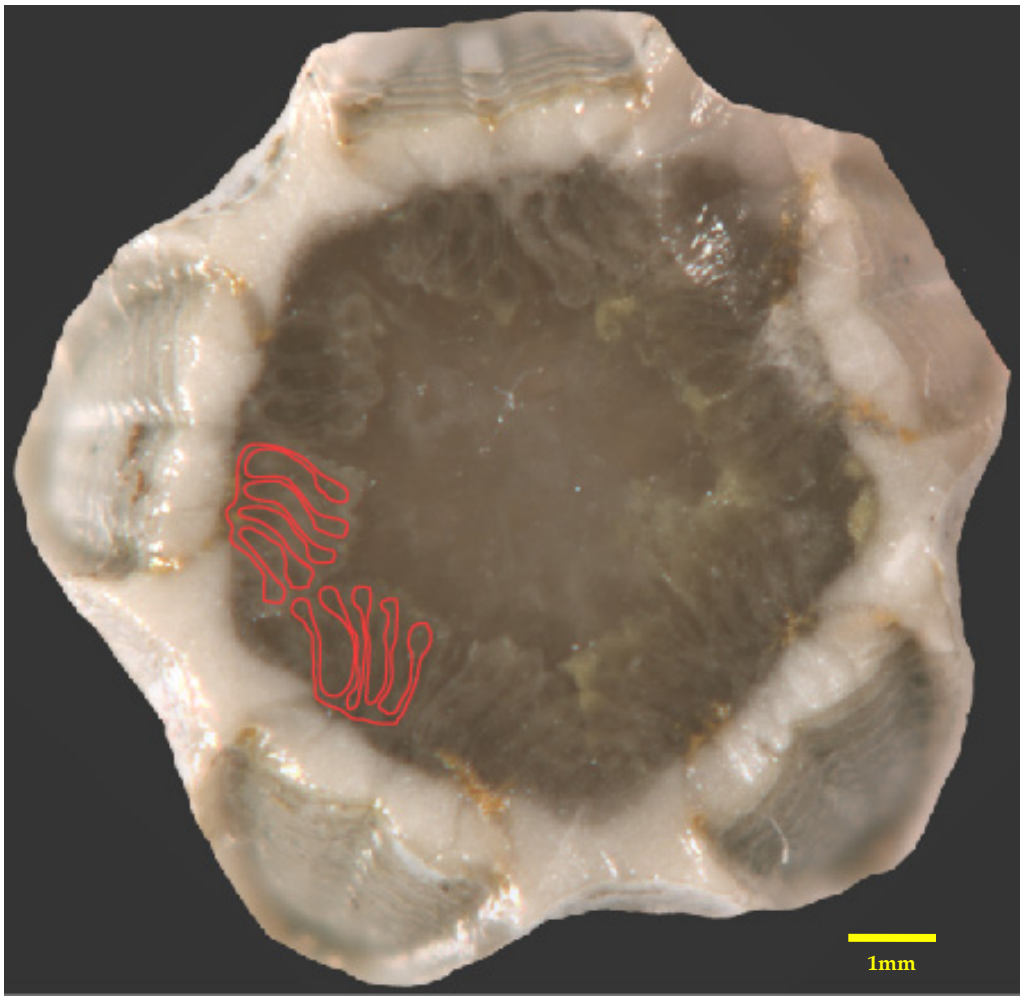

Figure 14: Transverse cross section showing clearly defined, circular visceral cavity and outline of hydrospire fold perimeter (Sample F8).

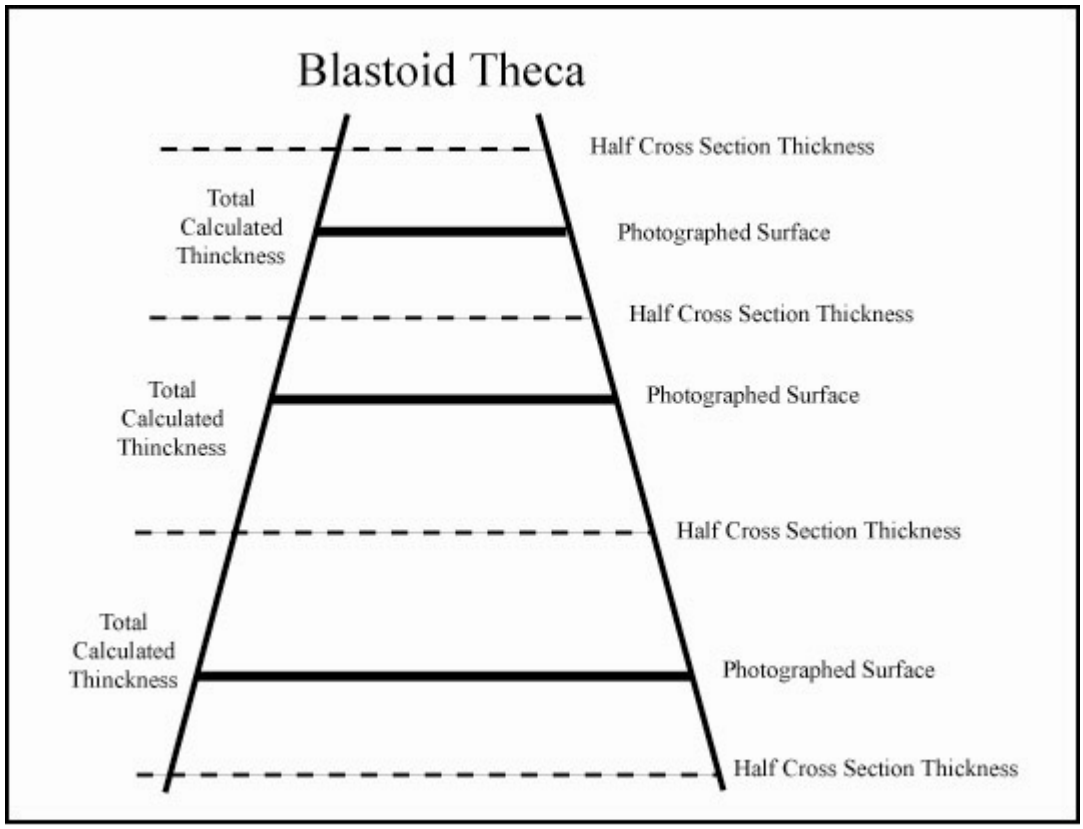

Figure 15: Total thickness for measuring hydrospire surface area and volume. This method uses half the thickness of the previous section and half the thickness of the following section.

Occasionally the blastoid would not be centered precisely perpendicular to the axis. This would cause some of the hydrospire folds to not be revealed on one side, while showing up clearly on the other side during the initial cross sections. This would also cause some of the hydrospire folds on one side to disappear earlier than on the other side during the later cross sections. In these situations, those hydrospire folds that were not yet visible were given an area and perimeter of zero. To keep the hydrospire folds that were not present from adding to the total surface area and volume of the individual, their averages were multiplied by the number of hydrospire folds present rather than by ten. This could only occur at the top or bottom of the ambulacra.

Calculating Visceral Volume

Visceral volume could not be calculated on specimens that were sectioned because the basals were removed to attach the samples to glass slides and the visceral cavity extends down into the basals. Visceral volume was calculated on four specimens from each species and a linear equation was calculated relative to mass. This allowed the visceral volume to be extrapolated to all sectioned specimens using the mass of the samples.

Four specimens were selected along the ontogenetic series for each of the species. The specimens were longitudinally sectioned through the center of one of the ambulacra and the opposing interradials (Fig. 16). This created a plane bisecting the center of the mouth and the center of the basals. This surface was digitally photographed along with a ruler which was used to calibrate measurements in Scion Image. Adobe® Photoshop CS

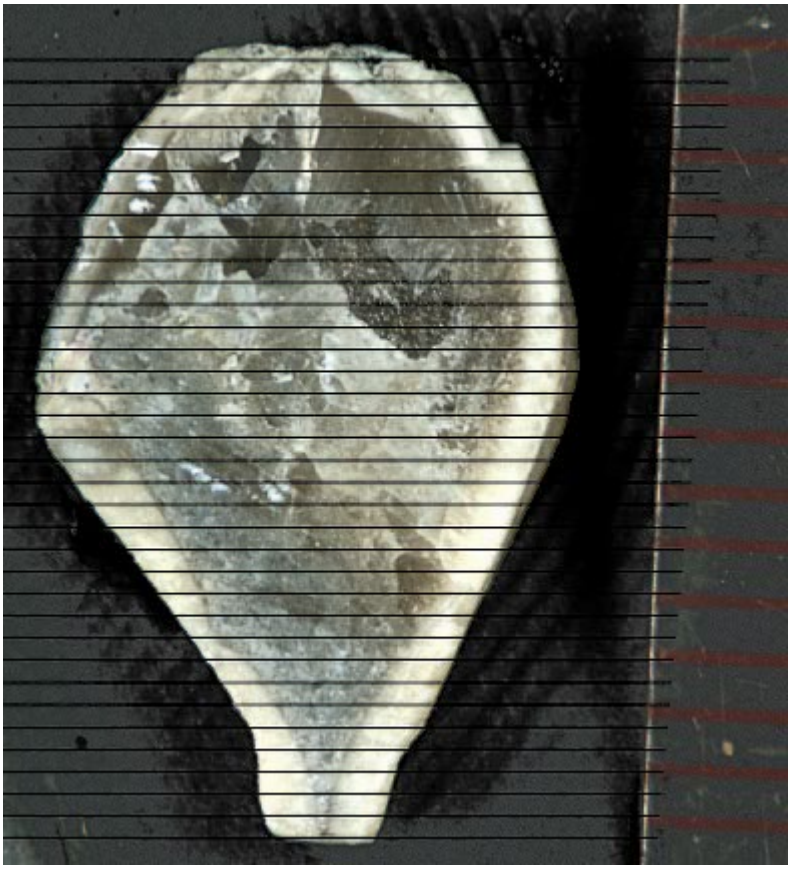

Figure 16: Transverse section through a specimen used to calculate visceral volume (Sample S10).

was used to create a horizontal grid over the photograph perpendicular to the polar axis (Fig. 16).

The visceral cavity is nearly circular in transverse cross section (Fig. 14). The lines drawn along the longitudinal section images are equivalent to the diameter of the visceral cavity circles in transverse cross section. The thickness between each line represents the thickness of each of these circular cylinders of visceral cavity. Scion Image was calibrated with the photographed ruler. The distance from the edges of the visceral cavity at each of the drawn lines was measured as well as the thickness between each line (Fig. 16). The distance above the top line to the mouth and the bottom line to the bottom of the basals was also measured and recorded. Using the geometric formula for the area of a circle, $A=\pi r^2$, and radius of each section as half the diameter, the area of the visceral cavity at each section was calculated. The volume of each circular cylinder was calculated by multiplying the area by half the thickness of the section before the drawn line and half the thickness of the section after the drawn line. The volume at the top and bottom were calculated by multiplying the thickness by the area of the line above or below as in the equation: $V = \sum_{i=2}^{N} \pi * r_i^2 * \left(\frac{h_i + h_{i-1}}{2} \right)$.

The total visceral volume was calculated by summing the volume of all the sections together. The visceral volumes were graphed against the mass and a linear equation was derived in Microsoft© Excel. By inserting the mass of the specimens into the linear equation, an approximate visceral volume for all the sectioned samples was calculated.

Data Analysis

All data from the morphometric analyses were entered into a Microsoft® Excel spreadsheet. Comparisons of features for the two populations were graphed on X-Y scatter plots. Microsoft® Excel was used to add trend lines, calculate linear and power equations and calculate R^2 values. The R^2 values, or the coefficient of determination, indicate how well the X and Y values correlate with one another. The t-tests were calculated using the formula: $T = \frac{\overline{X}_{pyr} - \overline{X}_{god}}{\sqrt{\frac{Var_{pyr}}{N_{pyr}} + \frac{Var_{god}}{N_{god}}}}$, where $\overline{X}_{pyr}$ and $\overline{X}_{god}$ are the mean of the character ratios for *P. pyriformis* and *P. godoni* respectively, Var_{pyr} and Var_{god} are the variance of species' characters, and N_{pyr} and N_{god} are the number of samples for each species. The t-tests were two tailed and homoscedastic. An α of 0.05 was used to determine significance unless otherwise noted. An α equal to 0.05 indicates that the statistic is significant to 95%. Microsoft® Excel's Data Analysis ToolPak was used to run linear regressions and to determine residuals for comparisons between hydrospire surface area and thecal volume or visceral volume. SAS® was used to compute Shapiro Wilk statistical tests for normality on the residuals and to determine the F statistic of ANOVA for the linear regressions.

Data were compiled to compare differences between the two species and to ascertain allometric changes through ontogeny. A power function was used to determine the allometric relationship between characteristics through ontogeny for both species. The power function, $Y = \underline{b}\, X^{\underline{a}}$, uses Y and X as the variables (Y and X equal the characteristics under comparison), with b as the intercept and the exponent a as the ratio

of allometric growth (Brower, 1987, Brower, in press). The exponent of allometric growth represents the change in the rate between Y and X. Thecal height was used to determine relative stage of ontogeny among the individuals in both species.

Discussion of Procedures

Although echinoderm stereom is composed of high Mg-calcite, the volume calculated from the mass used the density of calcite. Magnesium comprises little of the total mass in high Mg-calcite (approximately 4%). Furthermore, the pores in the stereom as well as the entire visceral cavity are permineralized with calcite leaving only a minute amount of Magnesium in the total mass (Fig. 17). The samples selected from the population also had very little silicification present externally. Any minor amount of silicification would not affect the results greatly since the difference in density between silica and calcite is minimal (2.63 g/cc compared to 2.71 g/cc).

Sections were removed using consistent thicknesses with the exception of the top and occasionally the bottom of the specimen where sections were purposely made to add detail. Thinner sections were ground off at the top of all samples and at the bottom of less mature samples to increase resolution at these critical locations. The hydrospires show extensive change near the top of the specimen where the hydrospire folds are merging together to form the spiracles. Specimens with small thecal heights showed the hydrospires grading down in size at the bottom of the ambulacra whereas more mature specimens maintained hydrospire size at the bottom of the ambulacra. If the consistent, thicker sections were removed through these locations where the hydrospires go through considerable change, the measurements would underestimate the total hydrospire surface

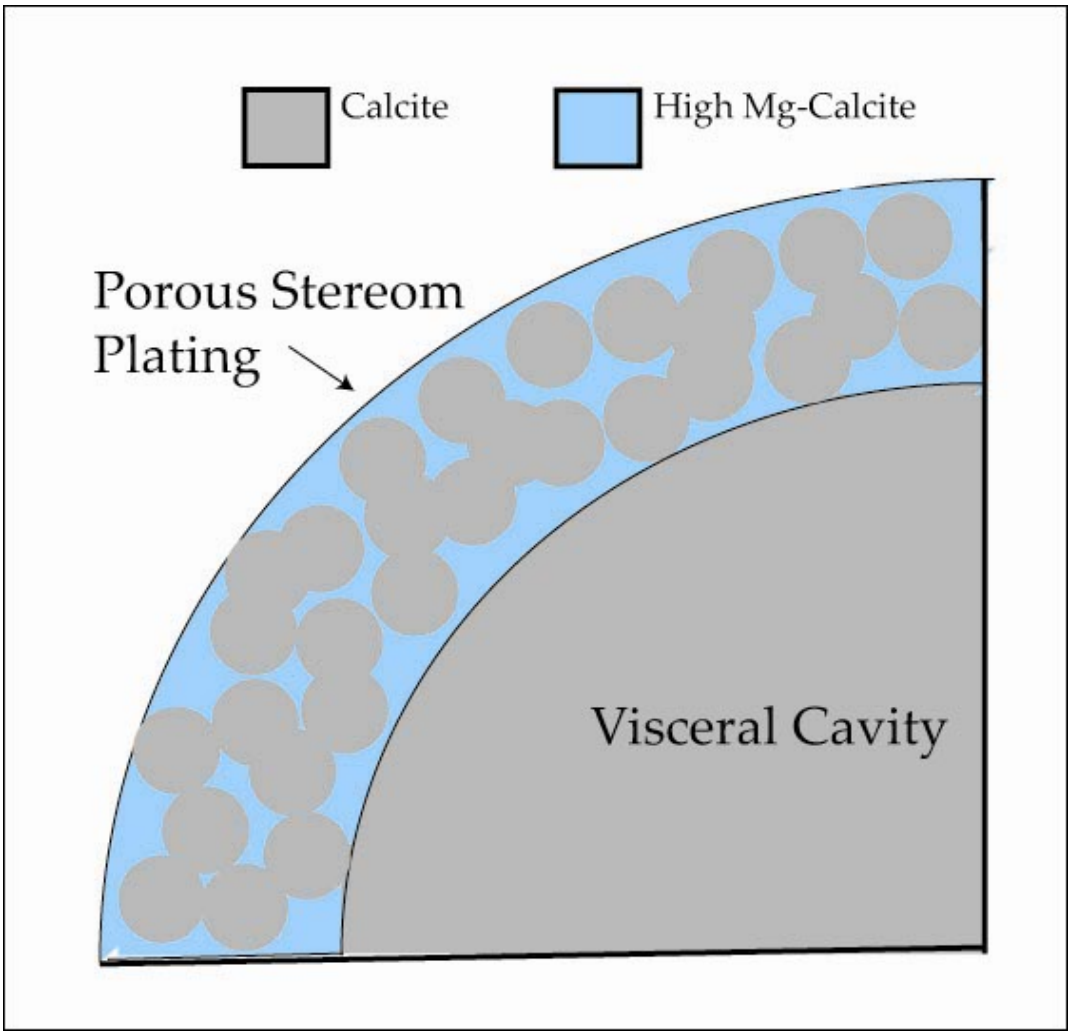

Figure 17: Graphical depiction of the ratio between secondarily precipitated calcite and the high Mg-calcite of thecal plating to demonstrate the limited affect of Magnesium on total mass.

area. Occasional increases in the thickness of sections occurred when the specimen accidentally slipped off the slide arm attachment of the rock saw and a new cut was needed to create an even surface.

The hydrospire volume was subtracted from the calculations of total volume and visceral volume. Since the hydrospires are cavities open to the outside environment, they have no living tissue within them that needed to respire. This adjusted volume is a closer representation of the total volume of the theca. The adjusted volume was calculated only in samples that had been cross sectioned, so any morphometric analyses comparing the volume of all samples in the population used the total thecal volume data.

On larger samples, the bottom of some of the hydrospires would occasionally lose their folds but retain small, circular, abaxial tubes that continued on to the bottom of the ambulacra (Fig. 18). These hydrospires were not in contact with the visceral cavity and were surrounded by the radials (Fig. 18). They would usually occur in a few of the hydrospires for a section and then would be lost as the next section reached the bottom of the ambulacra. Although they probably were not capable of transporting oxygen into the body, they did add to the total volume of the hydrospires. These areas were measured for both surface area and volume. Since the procedure took the average of the hydrospire folds in a photographed section, the addition of the tubes would have a limited effect on the total surface area if they did not transport oxygen into the body. Their spotty nature also suggests that these tubes have a rather limited vertical expression. The hydrospire folds were likely still in contact with the visceral cavity directly above these tubes and

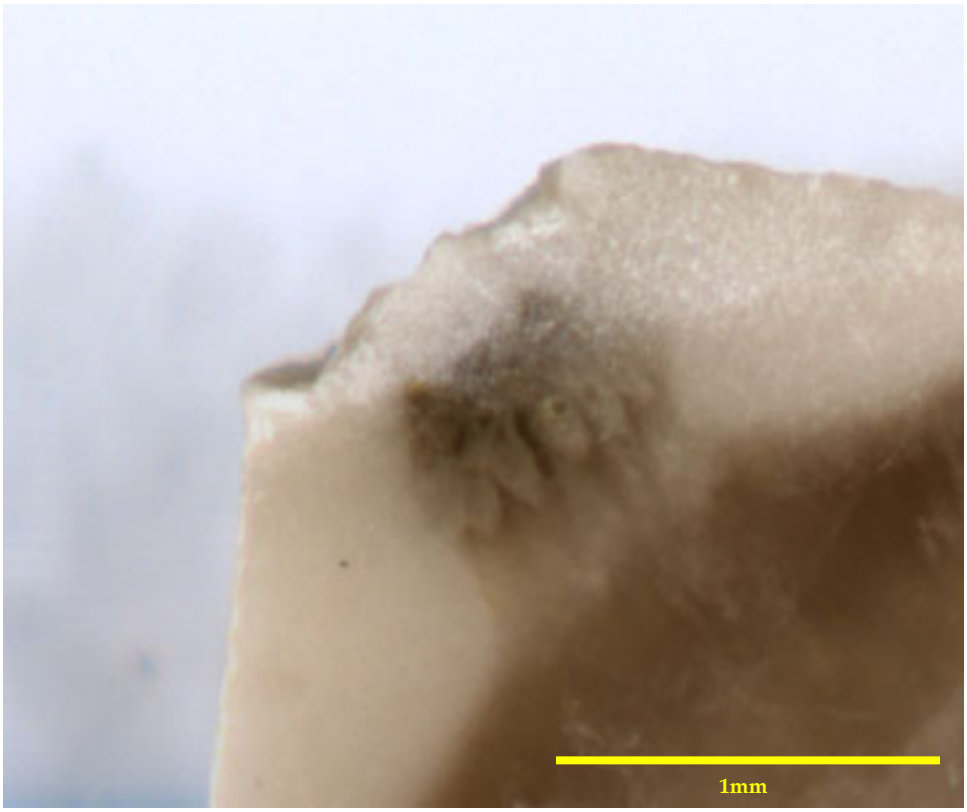

Figure 18: Cross section at the bottom of the ambulacra revealing minute hydrospire tubes that were not in contact with the visceral cavity (Sample F8).

removal of the tubes from the calculations would underestimate the actual hydrospire surface area within that section.

The serial grinding of an individual blastoid separated it into a number of truncated cylinders in which the surface area and volume were calculated (Fig. 15). These cylinders were then summed to determine the total hydrospire surface area and volume for the specimen. The calculated measurements found in Scion image were not simply multiplied by the thickness of each section, but rather by half the thickness of the section above and half the thickness of the section below (Fig. 15). If the cross section measurements were multiplied by the thickness of the next cut, the surface area and volume near the bottom of that cylinder would be different from the known measurement at the top and more similar to the next cross section measurement. By multiplying the measurements by half the thickness of the previous cross section and half the thickness of the following cross section, thus centering the known measurements, each cylinder provides a closer representation of the actual hydrospire surface area and volume (Fig. 15). Since smaller sections were used at the top of each specimen, the photographed surface was not always at the exact midpoint of each cylinder (Fig. 15). This method should still reduce the error that would have occurred had the measurements occurred at the top or the bottom of each cylinder.

5. Results

Morphometric Data

A number of t-tests were run on various characteristic ratios to insure that the visually separated populations being compared to one another represented two distinct species. The t-tests for the morphometric data use an α equal to 0.002. Length of the ambulacra and shape of the theca were the primary characteristics used to visually distinguish the two species. The means of thecal height to ambulacral length were 1.8 for *Pentremites pyriformis* and 1.5 for *Pentremites godoni*. The ratios of thecal height to ambulacral length produced a t of 5.6 with 98 degrees of freedom, which were significantly different. When the ratios of thecal height to thecal width were analyzed, the t value was 11 with 98 degrees of freedom which was also significant. The means were 1.4 for *P. pyriformis* and 1.1 for *P. godoni*. The t-test for thecal height by pelvis height was significantly different with a t of -4.8. The means for thecal height to pelvis height were 1.8 for *P. pyriformis* and 2.7 for *P. godoni*. The t-test for thecal height by radial plate length was significant different with a t value of -11. The means were 1.6 for *P. pyriformis* and 2.0 for *P. godoni*.

In *Pentremites pyriformis* and *Pentremites godoni*, thecal width, ambulacral length, and vault height appeared to increase at a linear rate through ontogeny as demonstrated in Figures 10, 19, and 20 (Tables 1 and 2). In *P. pyriformis*, the thecal height to ambulacral length produced an R^2 value of 0.9429, thecal height to thecal width produced an R^2 value of 0.9555, and thecal height to vault height produced an R^2 value of 0.9180 (Figs. 10, 19, and 20, Table 1). In *P. godoni*, thecal height to ambulacral length produced an R^2 value of 0.9342, thecal height to thecal width produced an R^2 value of

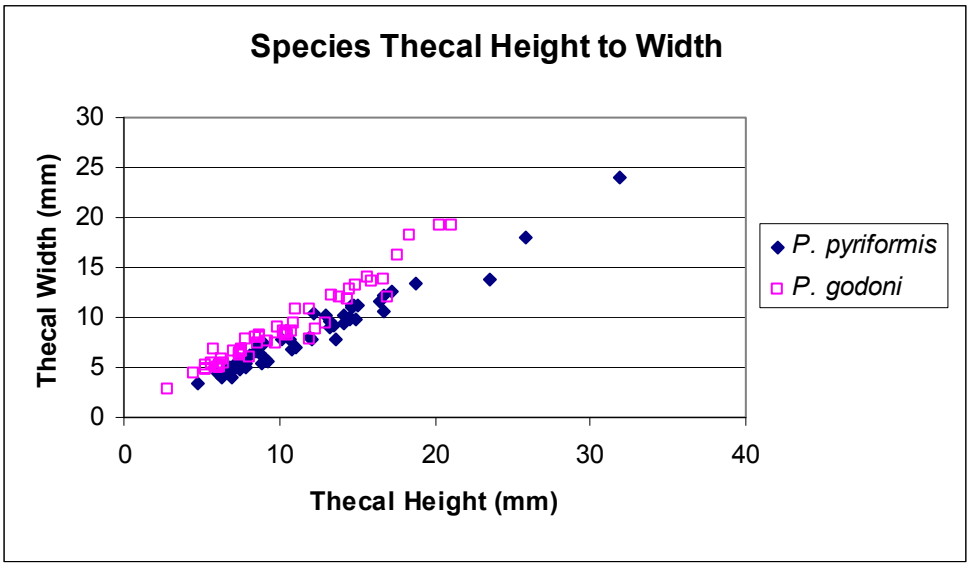

Figure 19: Comparison of thecal height to thecal width between *P. pyriformis* and *P. godoni*.

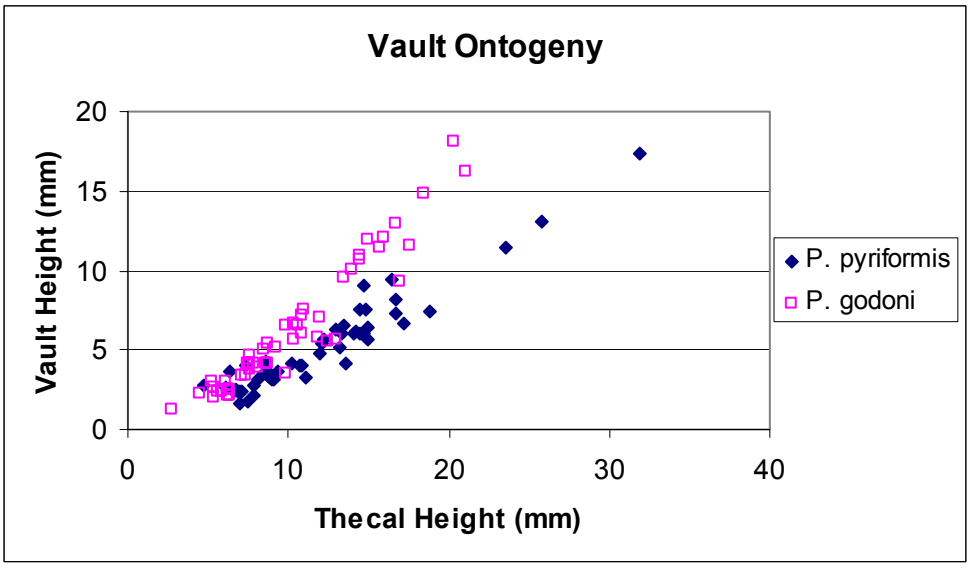

Figure 20: Comparison of thecal height to vault height between *P. pyriformis* and *P. godoni*.

Table 1: Calculated R^2 for linear transgressions and allometric exponents from a power function for *Pentremites pyriformis*.

X Axis	Y Axis	r^2 of Linear Trend	Intercept of Power Function	Exponent of Power Function
Thecal Height (mm)	Ambulacral Length (mm)	0.9429	0.53	1.1
Thecal Height (mm)	Pelvis Angle (º)	0.1086	54	0.12
Thecal Height (mm)	Thecal Width (mm)	0.9555	0.70	1.0
Thecal Height (mm)	Vault Height (mm)	0.9180	0.26	1.2
Thecal Height (mm)	Pelvis Height (mm)	0.8837	0.75	0.89
Thecal Height (mm)	Thecal Volume (mm^3)	0.7080	0.19	3.0
Thecal Height (mm)	Radial Plate Length (mm)	0.9801	0.48	1.1
Thecal Height (mm)	R-R Suture Length (mm)	0.9554	0.43	1.1
Thecal Height (mm)	Radial Plate Width (mm)	0.9401	2.5	.97
Thecal Height (mm)	Brachiole Number	0.8514	20	0.87
Thecal Volume (mm^3)	Brachiole Number	0.7209	31	2.8
Thecal Height (mm)	Hydrospire Surface Area (mm^2)	0.8933	0.71	2.5
Thecal Volume (mm^3)	Hydrospire Surface Area (mm^2)	0.9833	2.9	0.84
Thecal Mass (g)	Hydrospire Surface Area (mm^2)	0.9849	390	0.83
Thecal Mass (g)	Visceral Volume (mm^3)	0.9831	0	1.0
Visceral Volume (mm^3)	Hydrospire Surface Area (mm^2)	0.9820	4.5	0.84

Table 2: Calculated R^2 for linear transgressions and allometric exponents from a power function for *Pentremites godoni*.

X Axis	Y Axis	r^2 of Linear Trend	Intercept of Power Function	Exponent of Power Function
Thecal Height (mm)	Ambulacral Length (mm)	0.9342	0.34	1.3
Thecal Height (mm)	Pelvis Angle (º)	0.2360	72	0.18
Thecal Height (mm)	Thecal Width (mm)	0.9409	1.0	0.93
Thecal Height (mm)	Vault Height (mm)	0.9214	0.23	1.4
Thecal Height (mm)	Pelvis Height (mm)	0.1550	1.7	0.36
Thecal Height (mm)	Thecal Volume (mm^3)	0.7735	0.38	2.9
Thecal Height (mm)	Radial Plate Length (mm)	0.9522	0.57	1.0
Thecal Height (mm)	R-R Suture Length (mm)	0.8944	0.46	1.0
Thecal Height (mm)	Radial Plate Width (mm)	0.9525	2.1	.98
Thecal Height (mm)	Brachiole Number	0.8661	18	1.1
Thecal Volume (mm^3)	Brachiole Number	0.8199	24	2.5
Thecal Height (mm)	Hydrospire Surface Area (mm^2)	0.8697	0.76	2.7
Thecal Volume (mm^3)	Hydrospire Surface Area (mm^2)	0.9835	2.1	0.88
Thecal Mass (g)	Hydrospire Surface Area (mm^2)	0.9840	370	0.88
Thecal Mass (g)	Visceral Volume (mm^3)	0.9894	0	1.0
Visceral Volume (mm^3)	Hydrospire Surface Area (mm^2)	0.9833	2.7	0.88

0.9409, and thecal height to vault height produced an R^2 value of 0.9214 (Figs. 10, 19, and 20, Table 2). The equation of the power function for thecal height to ambulacral length in *P. pyriformis* was $Y = 0.53\ X^{1.1}$ and for *P. godoni* was $Y = 0.34\ X^{1.3}$ (Tables 1 and 2). The equation of the power function for thecal height to thecal width in *P. pyriformis* was $Y = 0.70\ X^{1.0}$ and for *P. godoni* was $Y = 1.0\ X^{0.93}$. The allometric equation for thecal height to vault height was in *P. pyriformis* was $Y = 0.26\ X^{1.2}$ and $Y = 0.23\ X^{1.4}$ in *P. godoni* (Tables 1 and 2).

Pelvis ontogeny is dramatically different between the two species. *Pentremites pyriformis* displayed a somewhat linear rate of increase in pelvis height through ontogeny, with an R^2 value of 0.8837 (Fig.21, Table 1). The power function for *P. pyriformis* was $Y = 0.75\ X^{0.89}$ with an exponent of 0.89 (Table 1). *Pentremites pyriformis* increased pelvis height at a similar rate as thecal height, so there was no allometry through ontogeny. Visual inspection of Figure 21 showed *P. godoni* to be very variable in pelvis height and to have little change after a certain ontogenetic stage. *P. godoni* displayed no correlation with an R^2 value of 0.1550 (Fig. 21, Table 2). The significant differences in pelvis height between the two species are further supported by the t-test for the ratio of thecal height to pelvis height with a t value of 4.8 and 98 degrees of freedom (significant at $t \geq 2.6$).

By graphing thecal volume to thecal height, it is visually apparent that volume is increasing at the expected cubic rate (Fig. 22). The volume used for the following morphometric tests do not have the volume of the hydrospires subtracted from the total since not all samples had been cross sectioned. The formula derived from the graph for *P.*

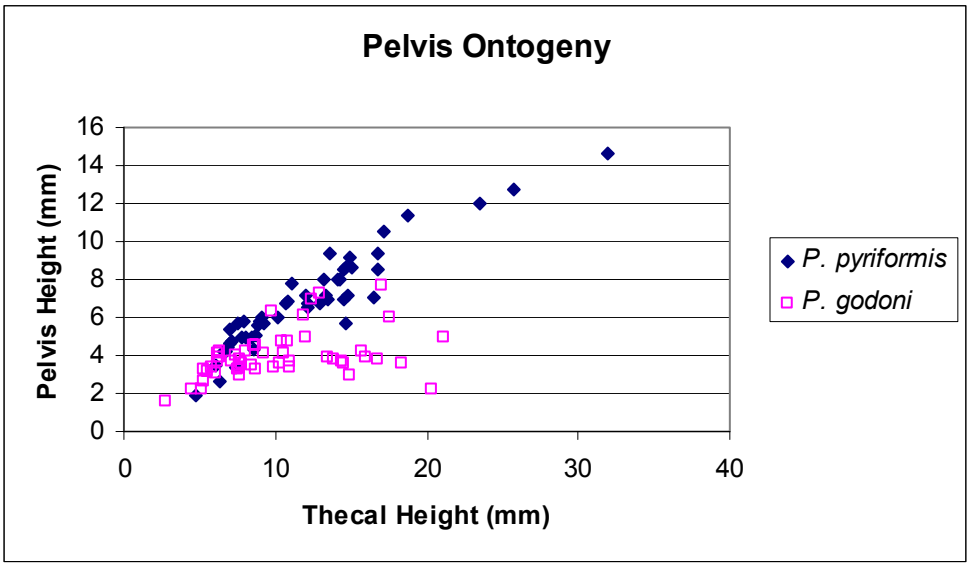

Figure 21: Comparison of thecal height to pelvis height between *P. pyriformis* and *P. godoni*.

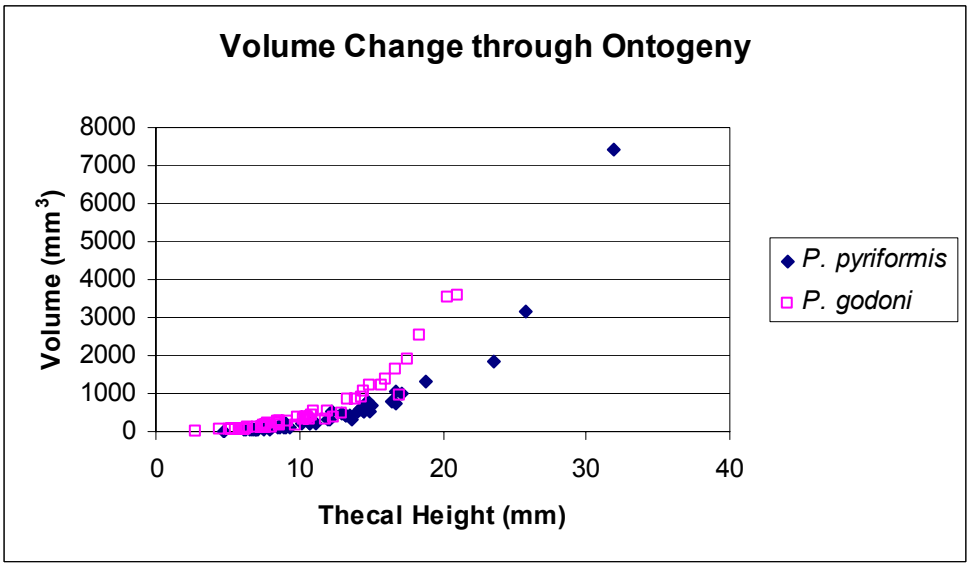

Figure 22: Comparison of volume to thecal height between *P. pyriformis* and *P. godoni.*

pyriformis was $Y = 1.4 X^{3.0}$ and the formula derived from *P. godoni* was $Y = 2.8 X^{2.9}$ (Tables 1 and 2). The exponent of growth for height for *P. pyriformis* was 3.0 and the exponent of growth for *P. godoni* was 2.9 both of which were extraordinarily close to the expected cubic rate of volume increase (Tables 1 and 2).

When the thecal height was compared with the radial plate lengths, the growth rates appeared to increase at a nearly isometric rate through ontogeny. In *Pentremites pyriformis*, the radials remained relatively morphologically unchanged through ontogeny, maintaining the same shape as in juvenile forms. In *Pentremites godoni*, the adoral sides increased in length while the aboral edge remained relatively unchanged as the ambulacral length increased through ontogeny. The line extracted from the graph for *P. pyriformis* had an R^2 value of 0.9801 and the line for *P. godoni* had an R^2 value of 0.9522 (Fig. 23, Tables 1 and 2). The power function for the species are $Y = 0.48 X^{1.1}$ for *P. pyriformis* and $Y = 0.57 X^{1.0}$ for *P. godoni*. The RR suture length, or the length of contact between two radial plates, when compared to height displayed R^2 value of 0.9554 for *P. pyriformis* and R^2 value of 0.8944 for *P. godoni* (Fig. 24, Tables 1 and 2). When the widths of the radial plates are compared to height, they also produce descent R^2 values. *Pentremites pyriformis* had an R^2 value of 0.9401 and *P. godoni* had an R^2 value of 0.9525 (Fig. 25, Tables 1 and 2).

Changing brachiole number through ontogeny did not increase in a linear fashion (Fig. 26). The R^2 value for *P. pyriformis* was 0.8514 and the R^2 value for *P. godoni* was 0.8661 (Fig. 26, Tables 1 and 2). The allometric exponent for *P. pyriformis* was 0.87 and for *P. godoni* was 1.1 (Tables 1 and 2). When the total number of brachioles on an

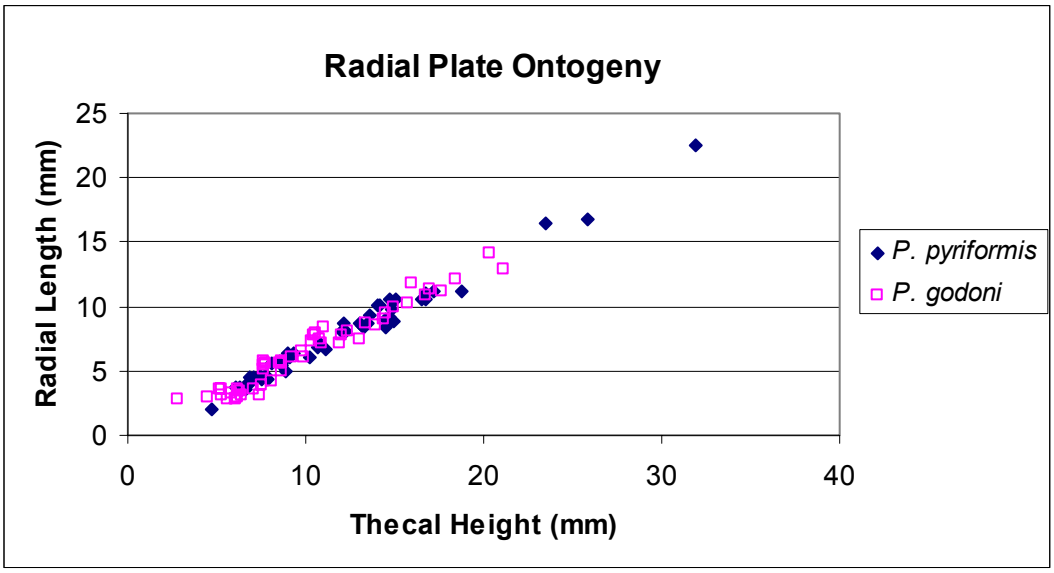

Figure 23: Comparison of thecal height to radial plate length in *P. pyriformis* and *P. godoni*.

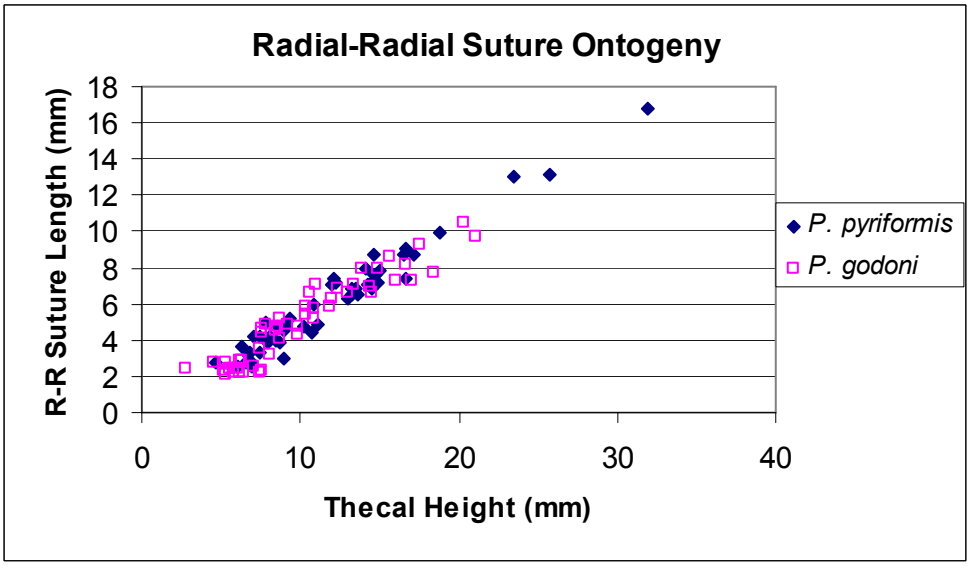

Figure 24: Lengthening of radial-radial suture through ontogeny.

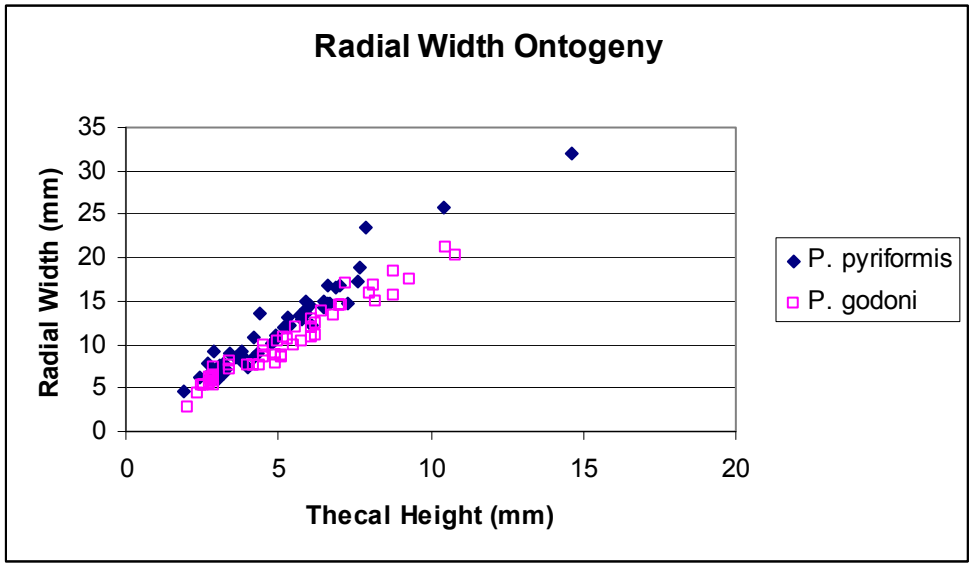

Figure 25: Comparison of thecal height to radial plate width in *P. pyriformis* and *P. godoni*.

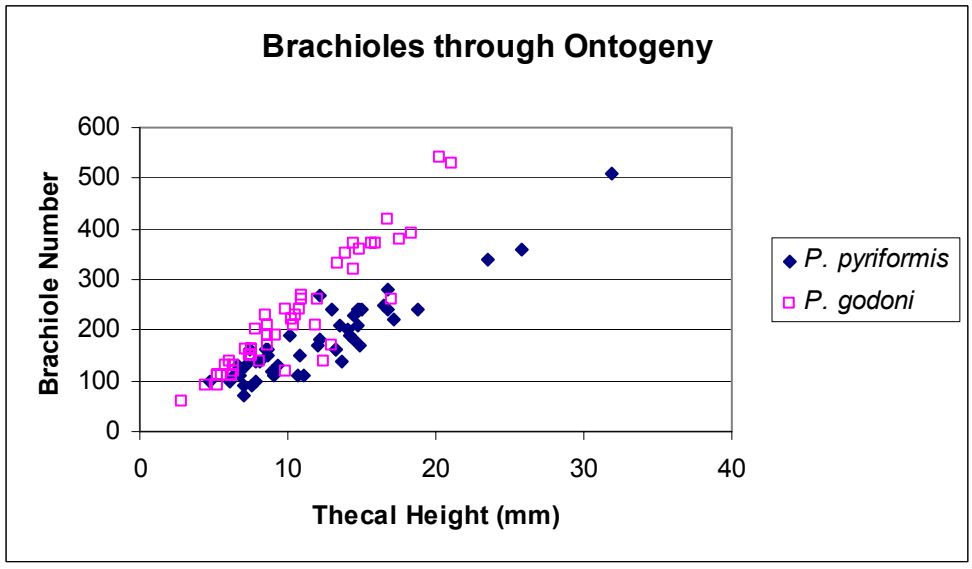

Figure 26: Increasing brachiole number through ontogeny.

individual was compared to the volume of the individual, the R^2 values for a linear equation were 0.7209 in *P. pyriformis* and 0.8199 in *P. godoni* (Fig. 27, Tables 1 and 2). When a power function was used to determine allometry, the equation derived for *P. pyriformis* was $Y = 31 X^{2.8}$ and the equation for *P. godoni* was $Y = 24 X^{2.5}$, where X is the volume and Y is the number of brachioles. The brachiole number appears to taper off in mature samples (Fig. 27, Tables 1 and 2).

Analysis of Hydrospire Surface Area

The number of cross sections used to calculate hydrospire surface area for large samples (thecal height greater than 7 mm) was approximately 10 with a minimum of 9 sections per individual and a maximum of 15 sections. The number of cross sections used to calculate hydrospire surface area for small samples (thecal height less than 7 mm) was approximately 7 with a minimum of 4 sections per individual and a maximum of 10 sections. The large specimens had a sample size of 27 and the small specimens had a sample size of 7, counting only the samples whose hydrospires were decently visible and presented no preservation issues. Eighteen cross sectioned samples were *Pentremites pyriformis* while 15 cross sectioned samples were *Pentremites godoni*. Approximately one third (15 out of 48) of the sample attempts failed to produce visible hydrospires in cross section.

Hydrospire surface area increased at an exponential rate compared to height (Fig. 28). The equation for the power curve for *P. pyriformis* was $Y = 0.71 X^{2.5}$ and the equation for *P. godoni* was $Y = 0.76 X^{2.7}$ where X is the height and Y is the hydrospire surface area (Fig. 28, Tables 1 and 2). When the data for hydrospire surface area

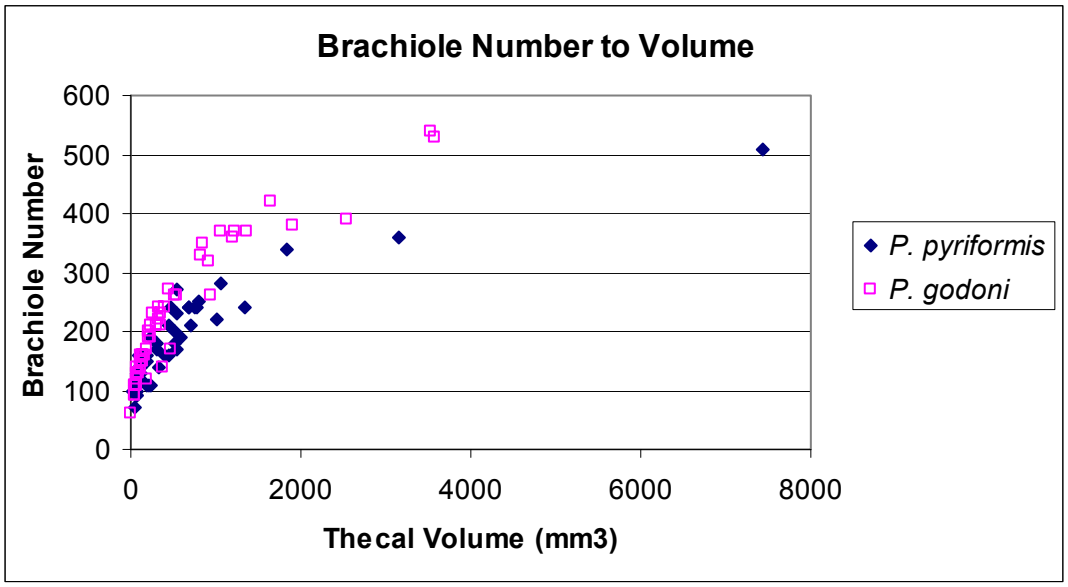

Figure 27: Increasing brachiole number relative to thecal volume.

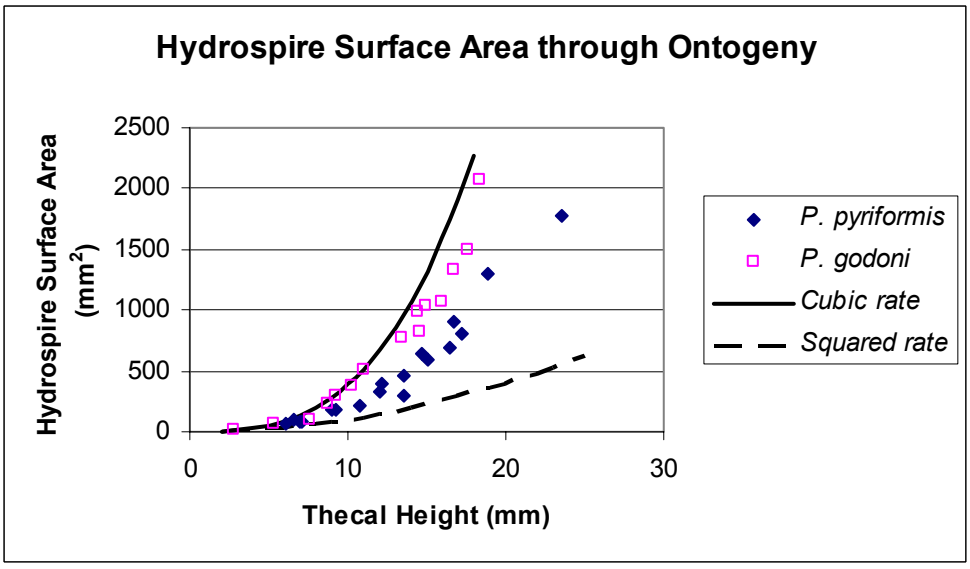

Figure 28: Hydrospire surface area increase through ontogeny. Curves show hypothetical cubic rate and squared rate of increase.

compared to height was fit to a power curve, the R^2 value for *P. pyriformis* was 0.9746 and the R^2 value for *P. godoni* was 0.9874. The expected exponent for the rate of increase in hydrospire surface area relative to height is 3 assuming anisometric surface area growth to match volume, and the experimental result for *P. pyriformis* was 2.5 and for *P. godoni* was 2.7 (Tables 1 and 2).

The volume calculated for the hydrospires was subtracted from the total volume (Fig. 29). A t-test was calculated between the two species for the ratio of hydrospire surface area to volume and returned a value of 0.7871. With 32 degrees of freedom and an α of 0.1, this is not significantly different ($t \geq \approx 1.310$). When hydrospire surface area was compared to volume, the R^2 values produced for a line in *P. pyriformis* was 0.9833 and for *P. godoni* was 0.9835. When the curve of the graph was fit to a power function, the equation for *P. pyriformis* was $Y = 2.9\ X^{0.84}$ and for *P. godoni* was $Y = 2.1\ X^{0.88}$, where Y is the hydrospire surface area and X is the volume (Tables 1 and 2). The R^2 value for the power functions are 0.9816 for *P. pyriformis* and 0.9882 for *P. godoni*. The exponent of volume (X) for *P. pyriformis* was 0.84 and for *P. godoni* was 0.88, both of which are less then one. This indicates that the hydrospire surface area is increasing at a slower rate than volume. A T-test between comparing the ratio of surface area to volume between the two species did not show a significant difference and had a P value of 0.4466 ($t \geq 2.75$ at alpha of 0.05).

The comparison of hydrospire surface area to mass presented similar results as the comparison of hydrospire surface area to volume, as would be expected since volume was derived from mass (Fig. 30). The R^2 value of the line for *P. pyriformis* is 0.9849 and

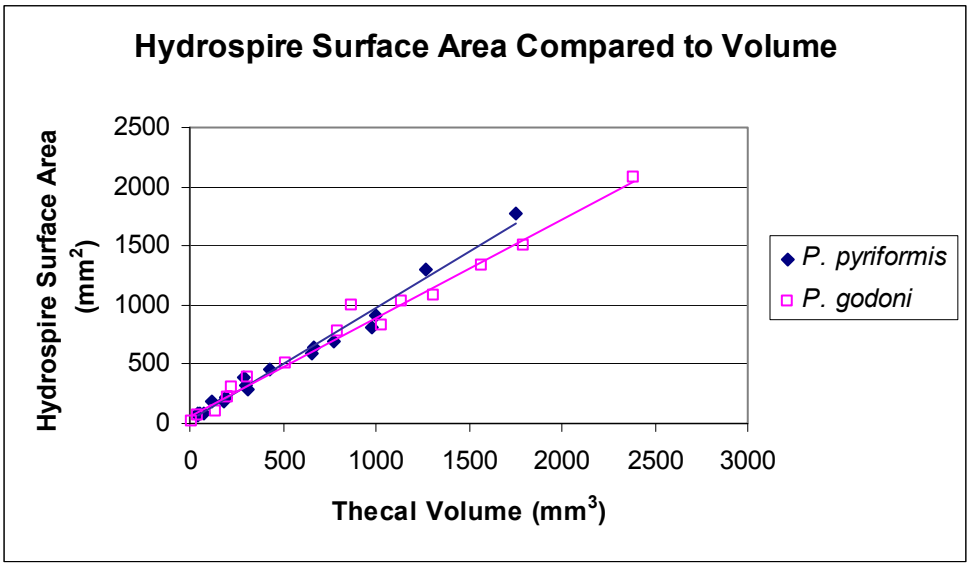

Figure 29: Hydrospire surface area relative to volume.

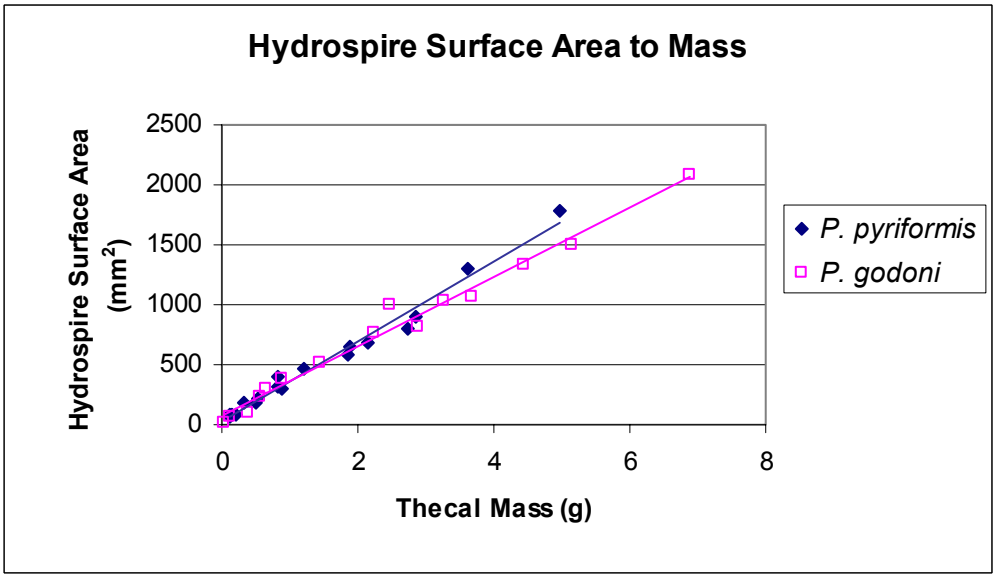

Figure 30: Hydrospire surface area compared to the individuals' mass.

for *P. godoni* is 0.9840. The exponent of a power curve where X is the mass and Y is the hydrospire surface area produced an exponent of 0.83 for *P. pyriformis* and 0.88 for *P. godoni* (Tables 1 and 2). The R^2 values for the power curve were 0.9834 for *P. pyriformis* and 0.9888 for *P. godoni*.

Analysis of Visceral Volume

Specimens at different stages of ontogeny were measured for total visceral volume for each species. Five *Pentremites godoni* samples and four *Pentremites pyriformis* were measured. There were no large *P. pyriformis* specimens left to measure. These specimens were plotted against mass (Fig. 31). The origin at (0,0) and the points from the measured specimens were used to calculate the equation of the line formed by visceral volume to thecal mass for each species. The origin is included because a specimen with zero mass should have no visceral volume. The equation of the line for *Pentremites pyriformis* was Y = 222.85X and for *Pentremites godoni* was Y = 278.58X, where X is thecal mass and Y is visceral volume (Fig. 31). The R^2 values for these lines were 0.9799 for *P. pyriformis* and 0.9810 for *P. godoni* (Fig. 31).

Thecal mass was used as the proxy for interpolating visceral volume. Thecal mass was entered into the linear equations for each of the cross sectioned samples to calculate a total visceral volume for each species. The t-test between the two species using the ratio of hydrospire surface area to visceral volume produced a t value of 3.163 with 32 degrees of freedom. This is significant at $\alpha < 0.01$. When the data of hydrospire surface area is compared to visceral volume, the exponent of the power function is 0.84 in *Pentremites pyriformis* and is 0.88 in *Pentremites godoni* (Fig. 32, Tables 1 and 2). The R^2 values of

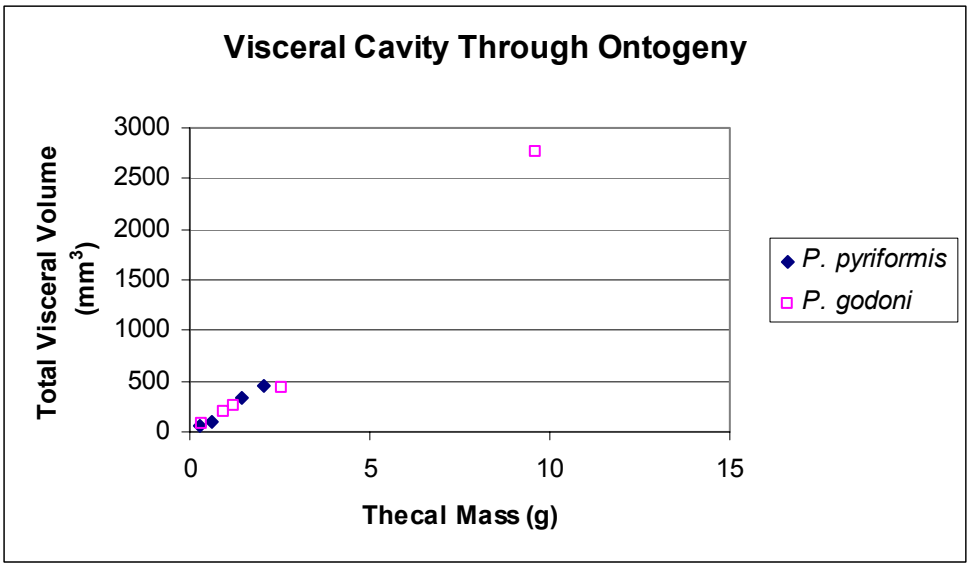

Figure 31: Total visceral volume plotted against mass to calculate the development of the visceral cavity through ontogeny.

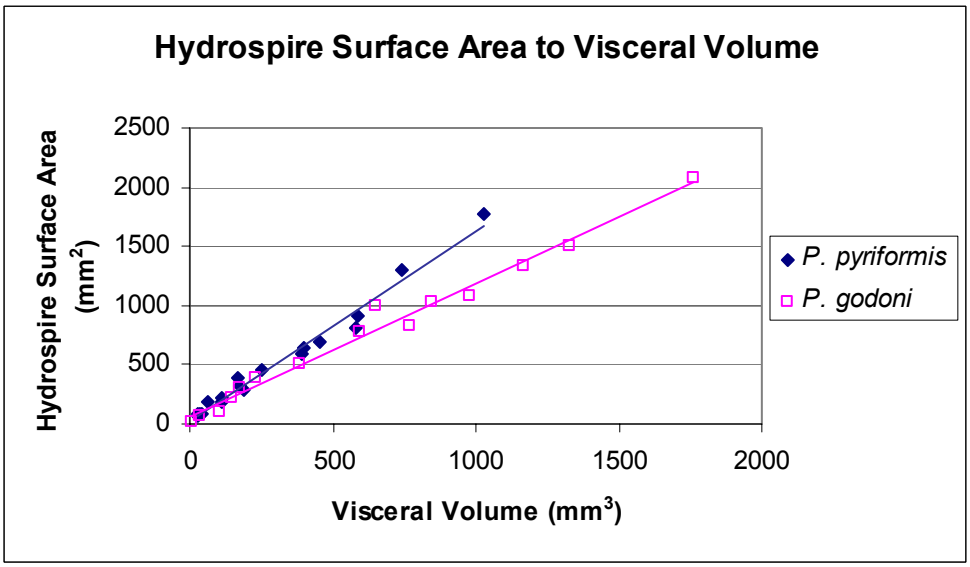

Figure 32: Hydrospire surface area compared to visceral volume through ontogeny.

the linear equations produced when comparing hydrospire surface area to visceral volume were 0.9820 in *P. pyriformis* and 0.9833 in *P. godoni* (Fig. 32).

Normalizing Surface Area and Thecal Volume

Linear regression was calculated to determine the relationship between hydrospire surface area and volume. If both values are increasing at the same rate, then a slope of one is expected. Both characteristics use different units of measurement which changes the shape of the slope depending upon an unknown conversion factor between the characteristics. In order to test the slope of the linear regression for a one to one ratio, the values for both characteristics had to be normalized. This was accomplished by dividing the values by the standard deviation of the population. A linear regression was then calculated on the normalized values. The linear regression of hydrospire surface area to thecal volume and visceral volume in both *Pentremites pyriformis* and *Pentremites godoni* was statistically significant at $\alpha < 0.001$ as demonstrated in the F statistic (Table 3). The slope of lines for hydrospire surface area to thecal volume and visceral volume in *P. pyriformis* were 0.9916 and 0.9910 respectively with standard errors of approximately ± 0.03 (Table 3). The slope of lines for *P. godoni* of hydrospire surface area to thecal volume was 0.9917 and for visceral volume was 0.9916 with standard errors of approximately ± 0.04 (Table 3). To further test the significance of the hypothesis that the slope is equal to one, the following formula was used: $t = \frac{b-1}{SE}$, where b is the coefficient of the x variable (or slope), one is the predicted value of the slope, and SE is the standard error of coefficient (Table 3). The hypothesis that the slopes of the lines are

Table 3: Statistical analysis of linear regression after values were normalized.

Species	Linear Regression of Normailized Values	F Statistic	Slope of X-Variable	Standard Error (±)	t-test for b=1	Significance
P. pyriformis	Hydrospire Surface Area to Thecal Volume	940.1311	0.9916	0.0323	-0.2598	Not rejected
P. pyriformis	Hydrospire Surface Area to Visceral Volume	872.0843	0.9910	0.0336	-0.2697	Not rejected
P. godoni	Hydrospire Surface Area to Thecal Volume	776.7019	0.9917	0.0356	-0.2323	Not rejected
P. godoni	Hydrospire Surface Area to Visceral Volume	765.0285	0.9916	0.0359	-0.2340	Not rejected

equal to one as demonstrated with the t values that could not be rejected at alpha of 0.40 (Table 3).

To further test the significance of the linear regression, the residuals of the data points from the interpolated line were examined for normality. This procedure tests the hypothesis that the scattering of points around the predicted line should be normally distributed around that line. If the data tended towards a curved line, the residuals would not be normally distributed. The Shapiro Wilk statistical test for normality was chosen for the small sample size of internal measurements. In *Pentremites pyriformis*, hydrospire surface area returned a P-value of 0.6692 when compared to thecal volume and 0.7067 when compared to visceral volume (Table 4). Both P-values are well above alpha of 0.05, therefore the hypothesis that the residuals are normally distributed cannot be rejected. In *Pentremites godoni*, hydrospire surface area to thecal volume returned a P-value of 0.0717 and compared to visceral volume returned a P-value of 0.0939. The P-values are slightly above the alpha of 0.05, suggesting that the residuals are normally distributed (Table 4).

Interspecies Variation in Hydrospire Folds

Pentremites godoni developed 5 hydrospire folds early in ontogeny and maintained this fold number through maturity (Fig. 33). *Pentremites pyriformis* developed additional folds at the mature stages of ontogeny (Fig. 33). The preceding cross sections of *Pentremites godoni* and *Pentremites pyriformis* demonstrate the development of hydrospire folds within the theca. Early ontogeny of both species showed

Table 4: Testing residuals for normalized distribution using Shapiro Wilk statistic.

Species	Examined Residuals for Normal Distribution	Shapiro Wilk w-Stat	Shapiro Wilk P-value	Shapiro Wilk Significance
P. pyriformis	Hydrospire Surface Area to Thecal Volume	0.9634	0.6692	Not rejected
P. pyriformis	Hydrospire Surface Area to Visceral Volume	0.9653	0.7067	Not rejected
P. godoni	Hydrospire Surface Area to Thecal Volume	0.8919	0.0717	Not rejected
P. godoni	Hydrospire Surface Area to Visceral Volume	0.8996	0.0939	Not rejected

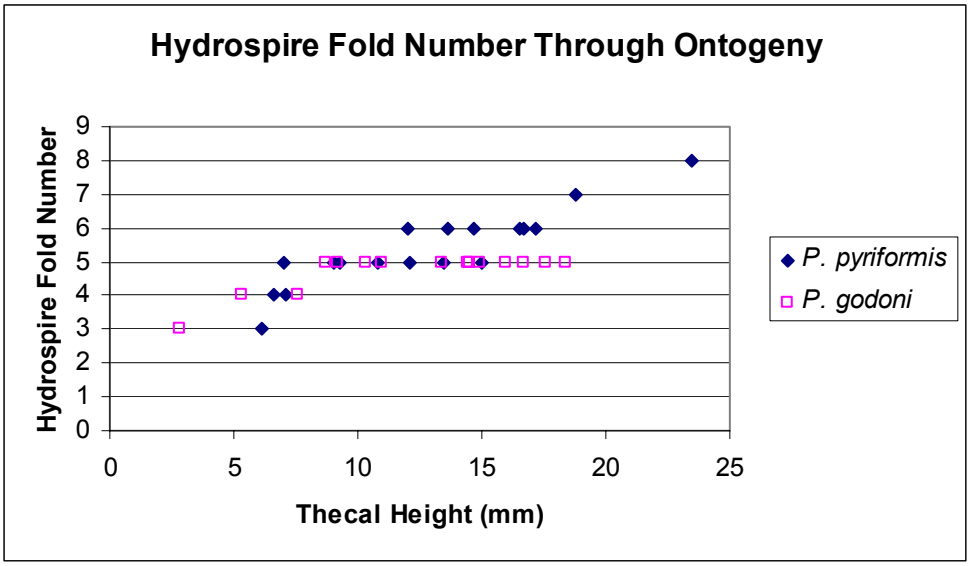

Figure 33: Changing hydrospire fold number through ontogeny in *P. pyriformis* and *P. godoni*.

a small number of hydrospire folds than at later stages of ontogeny. *Pentremites godoni* appeared to develop hydrospire folds more rapidly through ontogeny than *Pentremites pyriformis* (Fig. 33). *Pentremites godoni* had three hydrospire folds at a thecal height of 2.79 mm and a thecal volume of 8.046 mm^3 (Fig. 34). *Pentremites godoni* developed four hydrospire folds at a thecal height of 5.33 mm and a thecal volume 45.85 mm^3 (Fig. 35). When *P. godoni* reached a height of 8.7 mm and a volume of 199.9 mm^3, the hydrospire fold number reached five folds and that count was maintained through ontogeny (Figs. 36 and 37).

Pentremites pyriformis had three hydrospire folds at a thecal height of 6.1 mm and a volume of 46.43 mm^3 (Fig. 38). *Pentremites pyriformis* developed four hydrospire folds at a thecal height of 6.6 mm and a thecal volume of 57.06 mm^3 (Fig. 39). The hydrospire fold number reached five in one sample of *P. pyriformis* that had a thecal height of 9.0 mm and a thecal volume of 183.5 mm^3 and in another sample of *P. pyriformis* that had a thecal height of 9.3 mm and a thecal volume of 115.0 mm^3. Five hydrospire folds were maintained until a thecal height of 12 mm (Fig. 40). Unlike *P. godoni, P. pyriformis* continued to increase hydrospire fold number beyond five throughout ontogeny. From the thecal heights of 12.0 to 13.5 mm, *P. pyriformis* had five to six hydrospire folds (Figs. 41). From the thecal heights of 13.5 mm to 18.8 mm, *P. pyriformis* had six to seven hydrospire folds (Figs. 42). At a thecal height of 18.8 mm and a thecal volume of 1274 mm^3 or greater, *P. pyriformis* had eight hydrospire folds (Figs. 33 and 43).

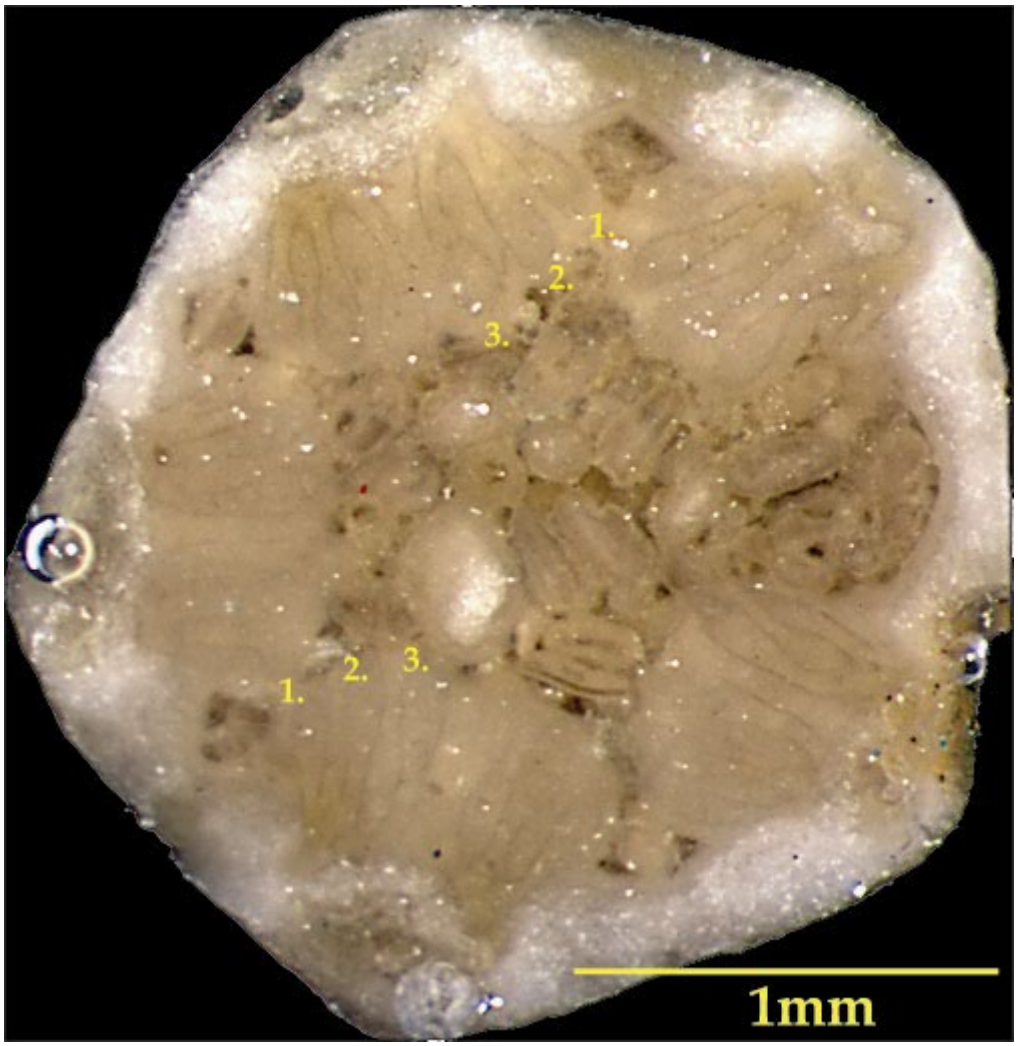

Figure 34: *Pentremites godoni* (Sample F13) with a thecal height of 2.79 mm showing three hydrospire folds.

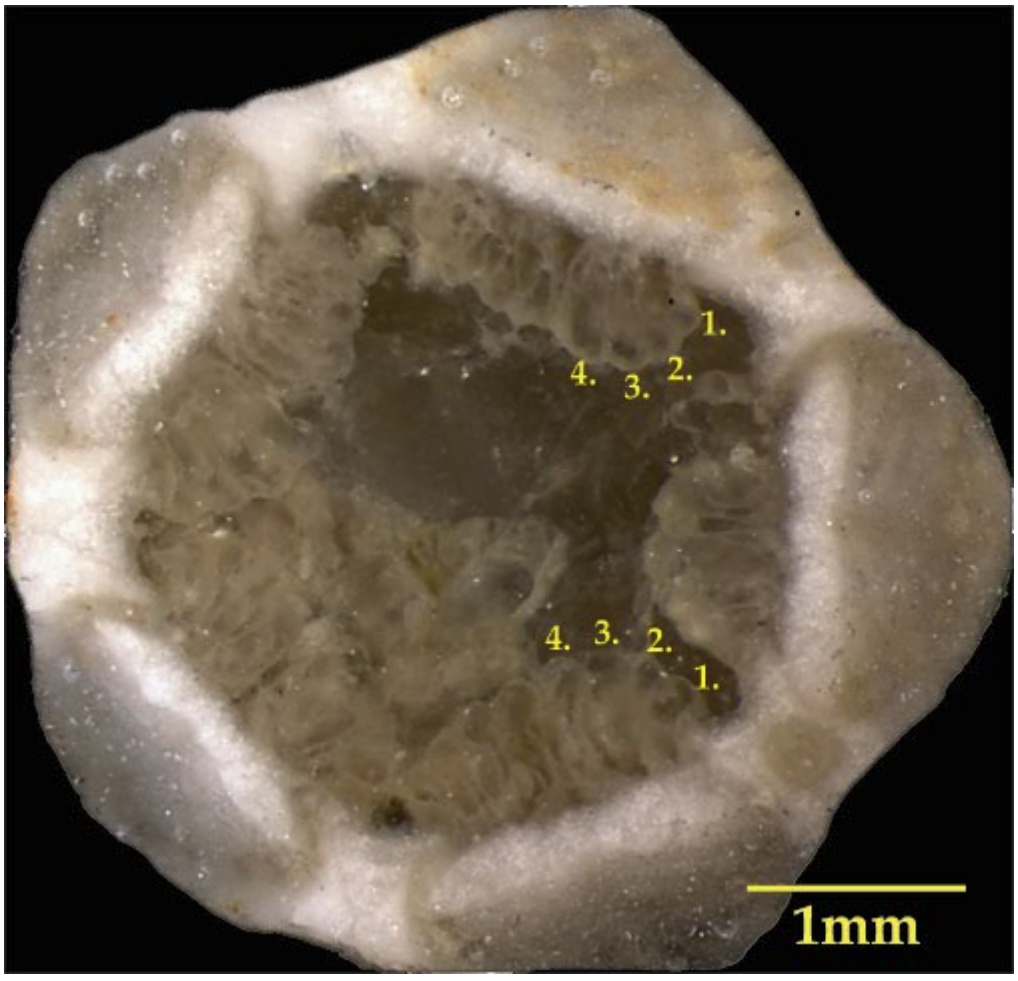

Figure 35: *Pentremites godoni* (Sample F15) with a thecal height of 5.33 mm showing four hydrospire folds.

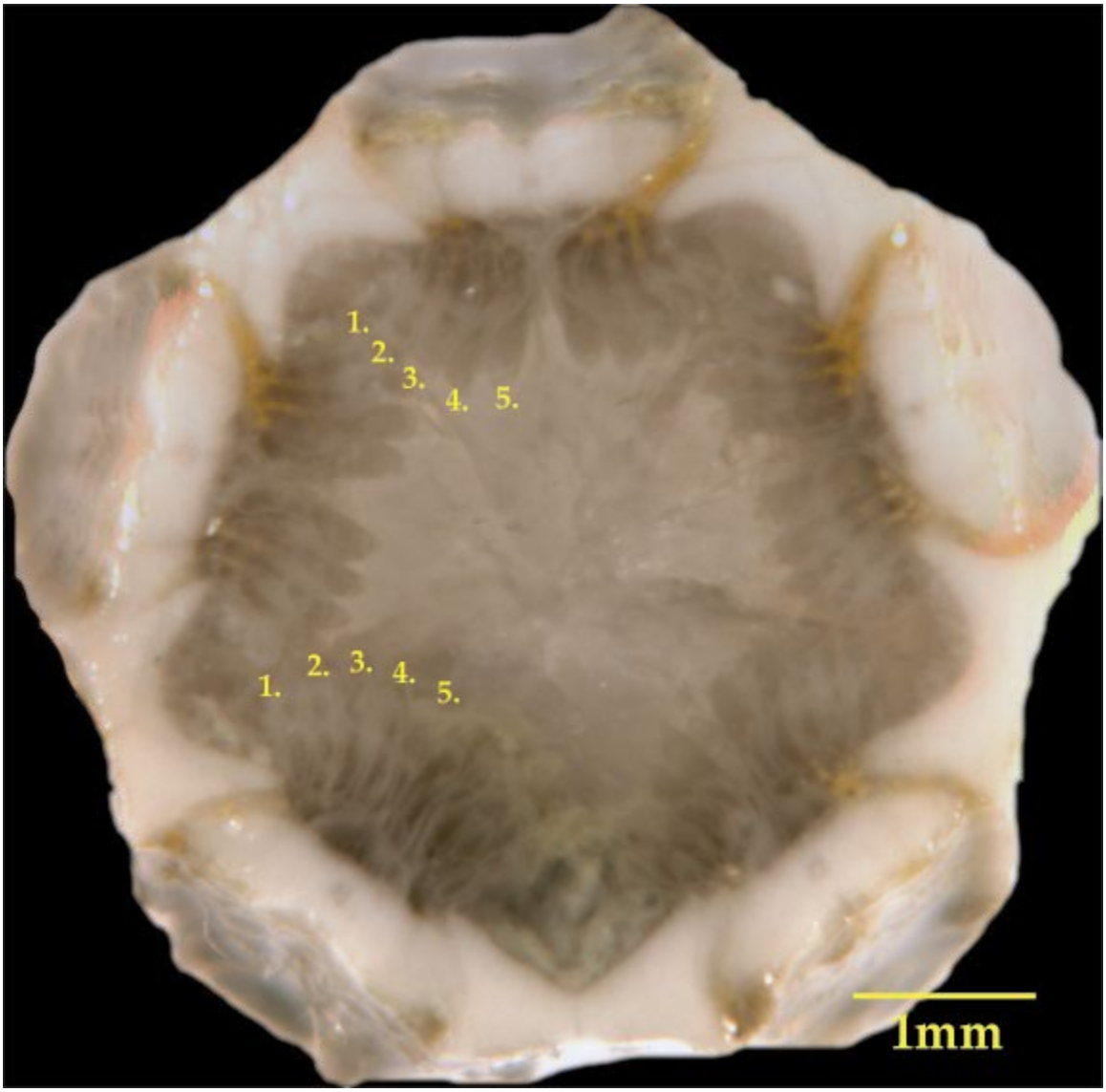

Figure 36: *Pentremites godoni* (Sample F9) with a thecal height of 9.2 mm showing five hydrospire folds.

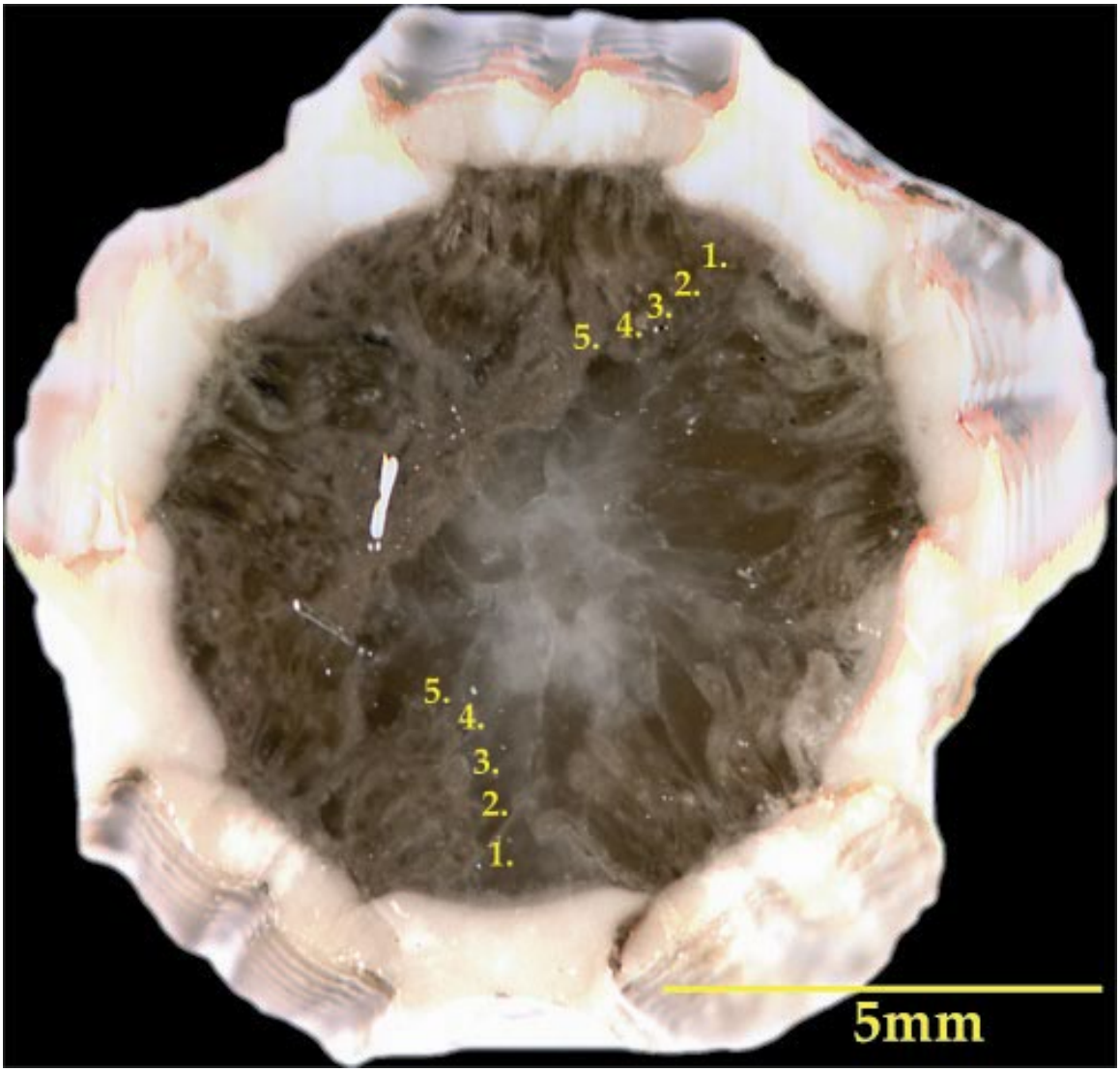

Figure 37: *Pentremites godoni* (Sample FB5) with a thecal height of 14.4 mm showing five hydrospire folds.

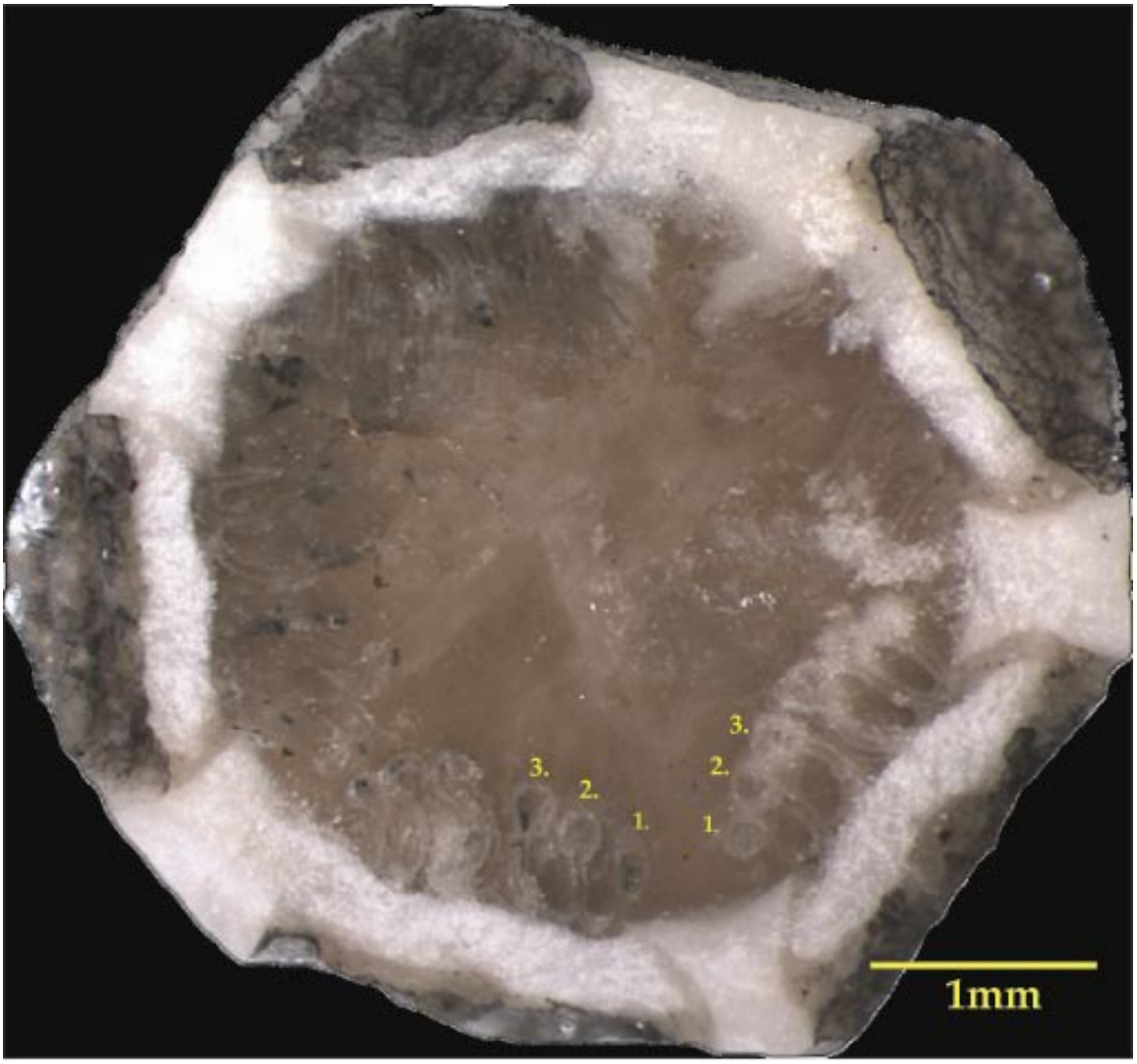

Figure 38: *Pentremites pyriformis* (Sample SA13) with a thecal height of 6.1 mm showing three hydrospire folds.

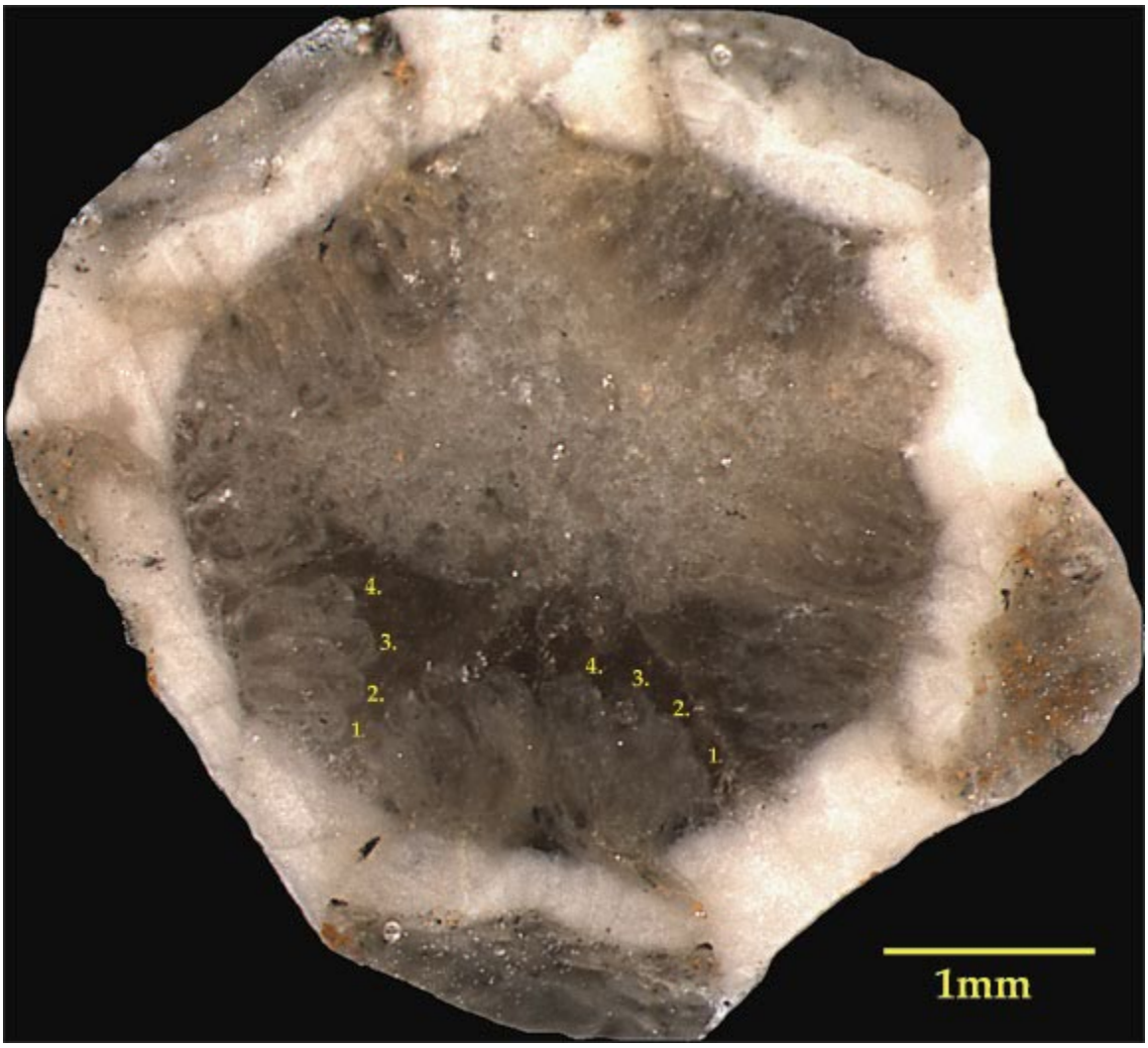

Figure 39: *Pentremites pyriformis* (Sample SA14) with a thecal height of 6.6 mm showing four hydrospire folds.

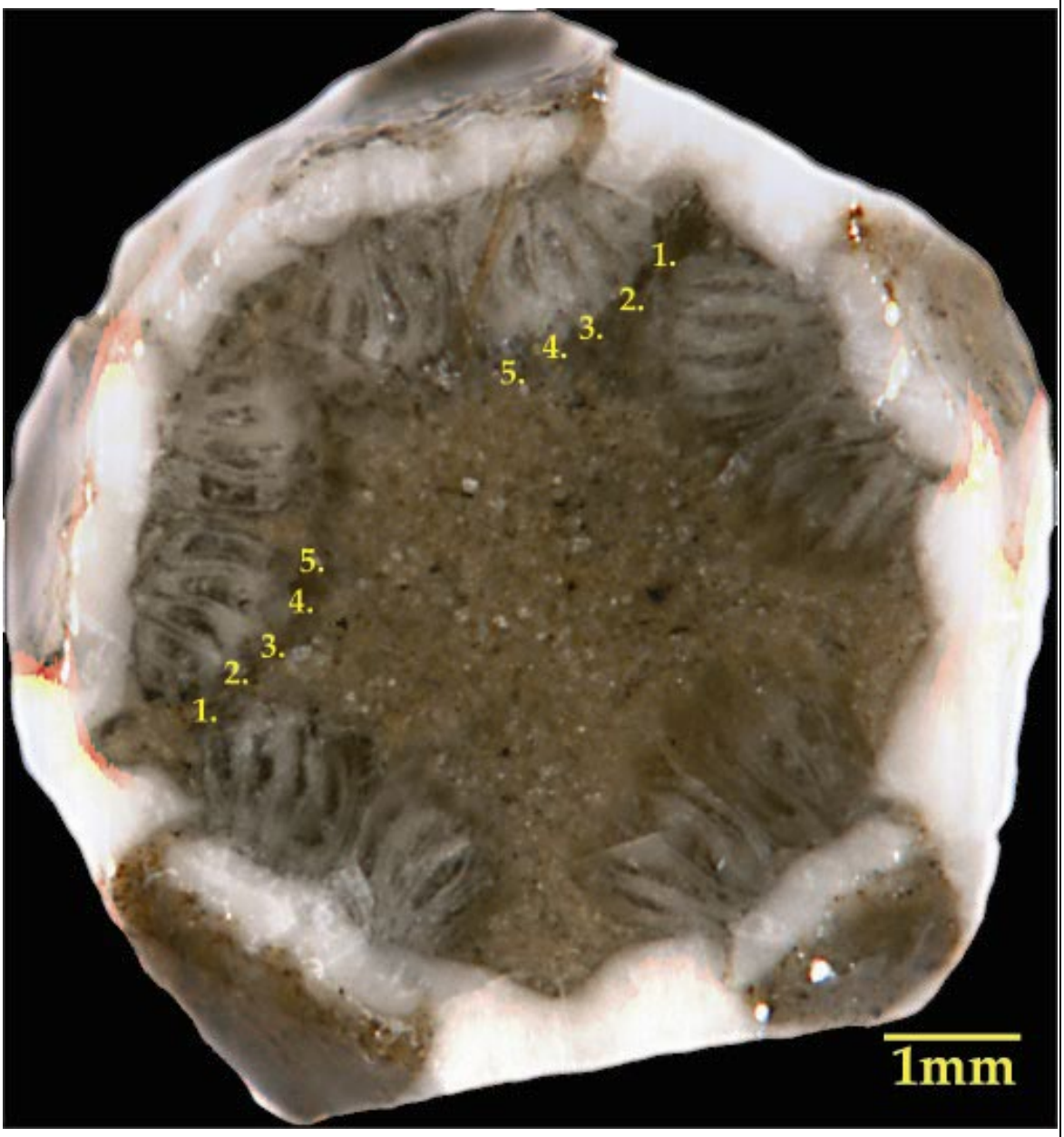

Figure 40: *Pentremites pyriformis* (Sample S15) with a thecal height of 10.8 mm showing five hydrospire folds.

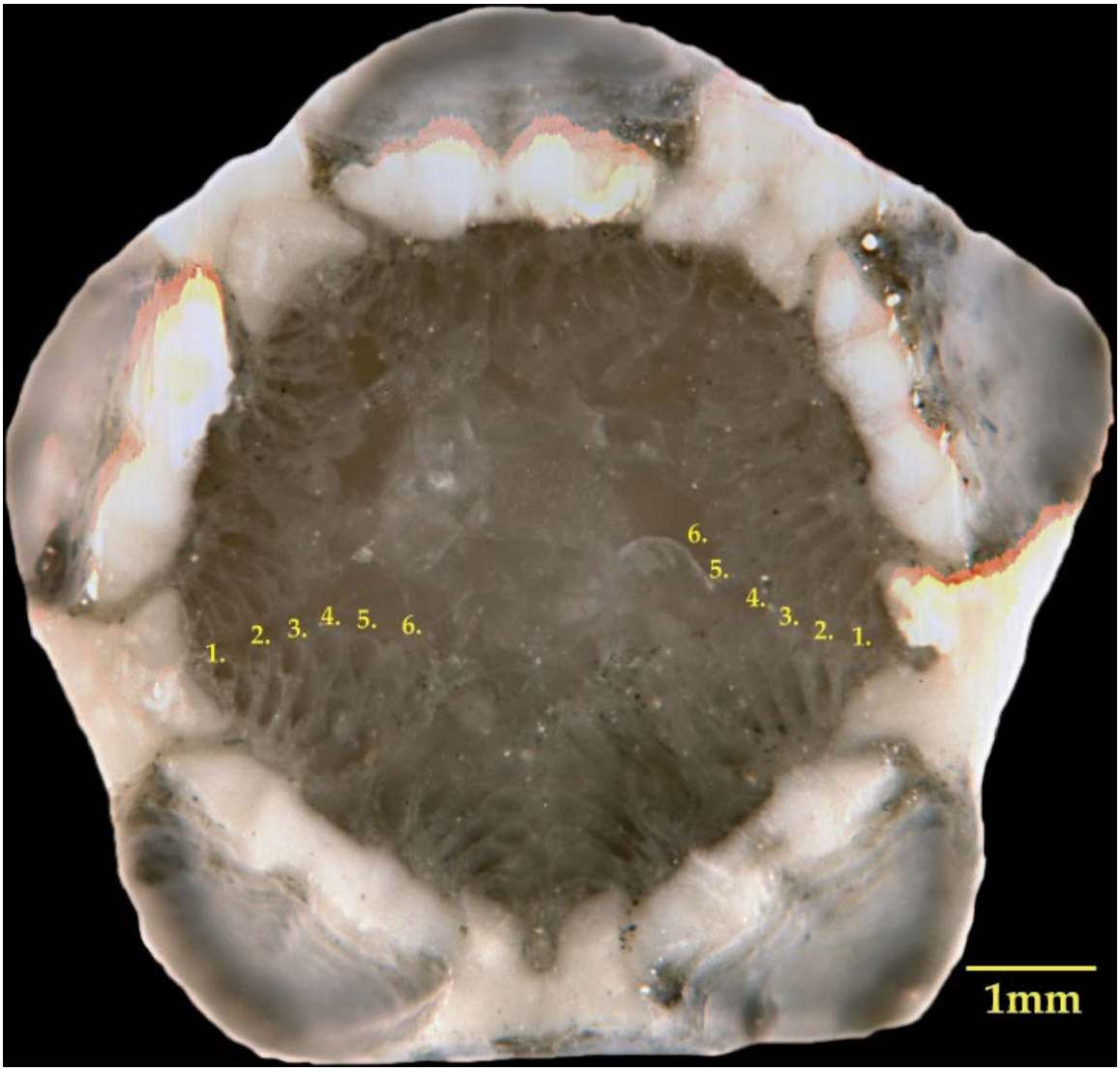

Figure 41: *Pentremites pyriformis* (Sample S14) with a thecal height of 12.0 mm showing six hydrospire folds.

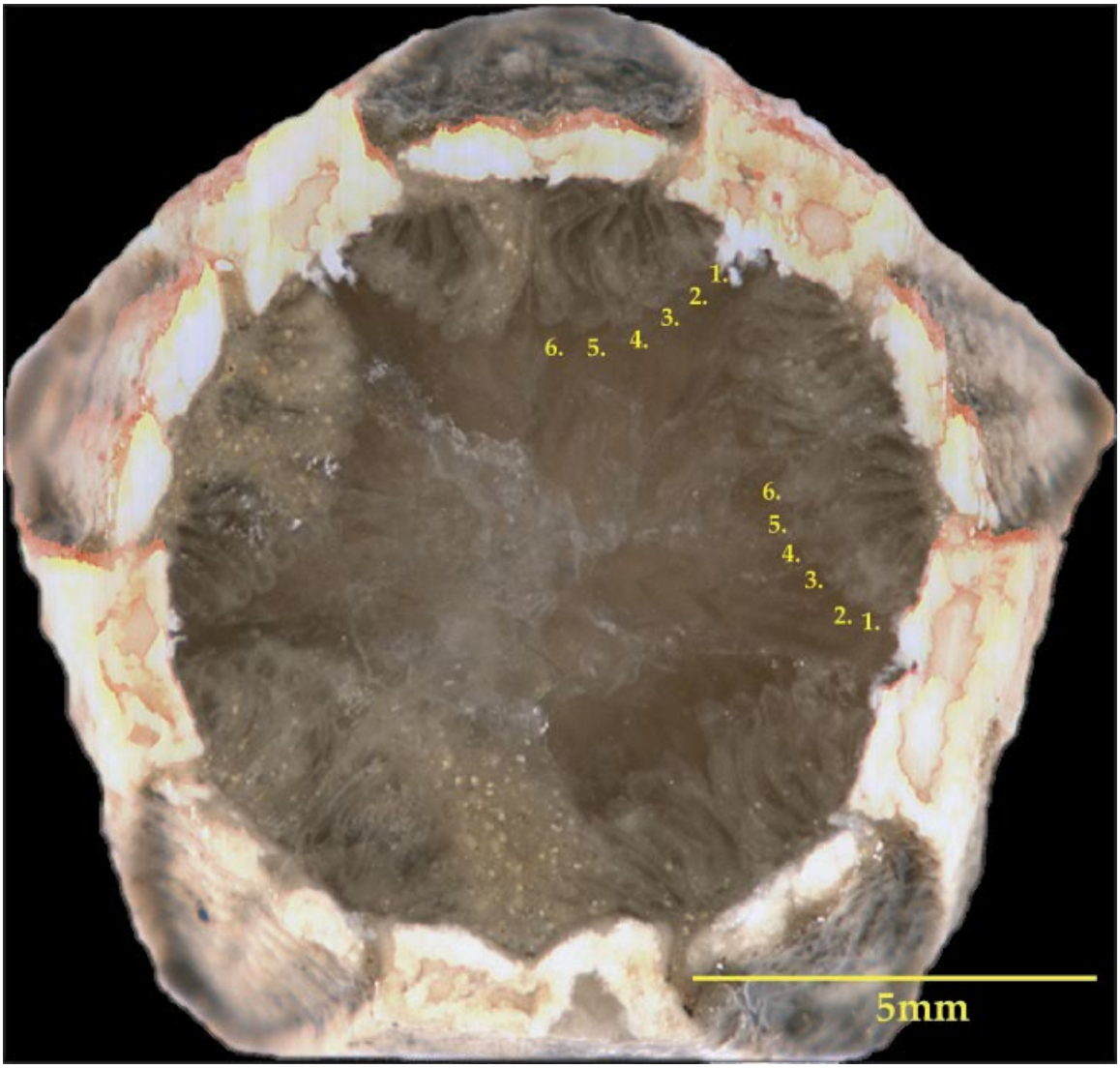

Figure 42: *Pentremites pyriformis* (Sample S5) with a thecal height of 17.2 mm showing six hydrospire folds.

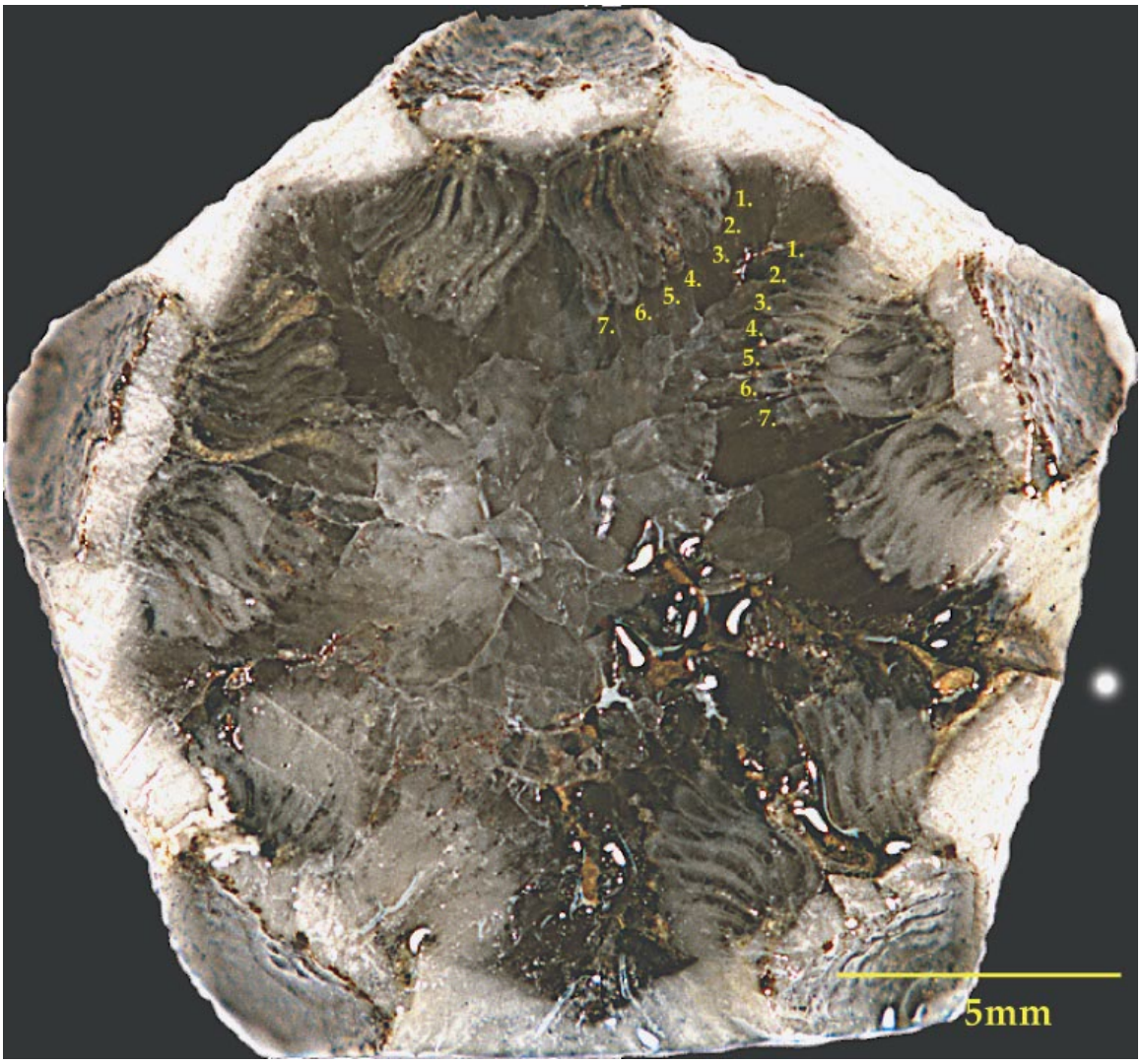

Figure 43: *Pentremites pyriformis* (Sample S4) with a thecal height of 18.8 mm showing seven hydrospire folds.

6. Discussion

Ontogeny

Using thecal height as a proxy for ontogenetic stage, a number of characteristics showed little allometry. Thecal width, ambulacral length, and vault height all increase at a linear rate in both species with high R^2 values (Figs. 10, 19, and 20, Tables 1 and 2). The pelvis height in *Pentremites pyriformis* appears fairly isometric; however the R^2 value of 0.88 was a little low (Fig. 21). A fairly isometric rate of growth between the vault and pelvis in *P. pyriformis* is expected from previous studies that show a fairly consistent P/V ratio through ontogeny (Waters et al., 1985). The pelvis height in *Pentremites godoni* showed no linearity (Fig. 21). Pelvis height also never increased beyond a certain height throughout ontogeny (Fig. 21). The maximum pelvis height was 7.7 mm in *P. godoni* whereas the maximum pelvis height in *P. pyriformis* was 14.6 mm. There was no linearity in mature stages with both larger and smaller pelvis heights associated with older samples. There is a slight trend of increasing pelvis height with thecal height at the juvenile stages. This suggests that pelvis height in *P. godoni* has little trend in mature specimens and is based on intraspecific variation.

The theoretical Euclidean relationship between height and volume in an isometric shape should be a cubic increase in volume (Fig. 6). Although certain characteristics of blastoids display considerable allometry, the data suggests that the individuals as a whole are rather isometric. When volume is compared to height in both species, the experimental result is extraordinarily close to the theoretical expectation (Fig. 22). The expected exponent of curve is 3.0, and the experimental result for *P. pyriformis* was 3.0 and the result for *P. godoni* was 2.9. The near precision between ontogenetic stage and

volume means that volume can be interpolated to any sample with a known height, including broken or incomplete samples.

The radial plates of blastoids surround the ambulacra and include sections of both the vault and pelvis. The primary distinctions between the two species are the ambulacral lengths and the pelvis heights. With the essential involvement of the radial plates in the species distinction, it seems highly unusual that the radial plates of both species could be so similar (Fig. 23). The comparison of height to radial length produced linear equations that were too similar between the species to be coincidence. The slope for the rate of increase through ontogeny for *P. pyriformis* was 1.4 and for *P. godoni* was 1.4 (Fig. 23). The similarity between radial plates is further supported by the measures of the radial-radial sutures (Fig. 24). The slopes of the RR suture were 1.8 in *P.* pyriformis and 1.8 in *P. godoni* (Fig. 24). The widths of the radial plates are not as similar between the two species as the lengths, which is to be expected since *P. godoni* tends to be squatter and wider in general than *P. pyriformis* (Fig. 25).

Brachioles

Brachioles show unexpected growth through ontogeny. As the food gathering structures for blastoids, it would be expected that brachioles increase in an anisometric manner to keep pace with increasing volume through ontogeny. One constant in the measurements is that *P. godoni* has more brachioles at each life stage then *P. pyriformis*, which is to be expected with the longer ambulacra on *P. godoni* (Figs. 26 and 27). The increase in the number of brachioles had low R^2 values and was not linear through ontogeny (Fig. 26). When compared to volume, the exponent for brachiole number was

close to three rather than the expected one (Fig. 27). Therefore, if brachioles show no positive allometry through ontogeny, it seems unlikely that they would be able to provide enough food for the individual.

Part of the problem has to be the comparison between brachiole count and food gathering capacity. Food gathering capacity should be based on the total length and number of brachioles. However, measuring brachiole length is a nearly impossible task because brachioles are rarely found preserved on blastoids as their minute thickness makes them extraordinarily fragile and preserved brachioles have yet to be found with their complete length intact. Brachiole width is believed to remain constant through ontogeny as suggested by the constant size of the brachiole facets between the side plates (Macurda, 1975). What little information that is available on the brachioles suggests that their length tends to be about twice the height of the theca (J. Sprinkle, pers. comm.). If it is assumed that each brachiole on an individual is approximately twice the length of the theca, a hypothetical total brachiole length can be calculated for the samples in this study through ontogeny (Figs. 44 and 45). The hypothetical values for *P. pyriformis* for the brachioles relative to volume produce an allometric exponent of 1.5 and an R^2 value of 0.96 (Fig. 45). The hypothetical values for *P. godoni* for the brachioles relative to volume produce an exponent of 1.4 and an R^2 value of 0.99 (Fig. 45). Although an allometric exponent of 1.0 is expected, the brachioles are much closer to matching volume than when comparing numbers and measurements.

With so little information available on blastoid brachiole length, the rough estimate of brachiole length as twice the height is rather tenuous. As the metabolic

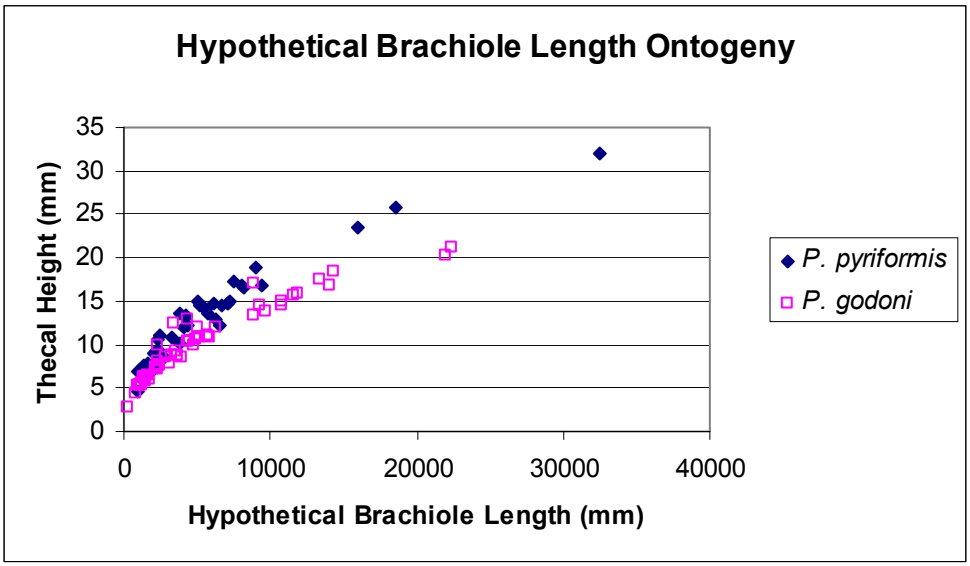

Figure 44: Hypothetical total brachiole length through ontogeny assuming brachiole length to be twice the height of the theca.

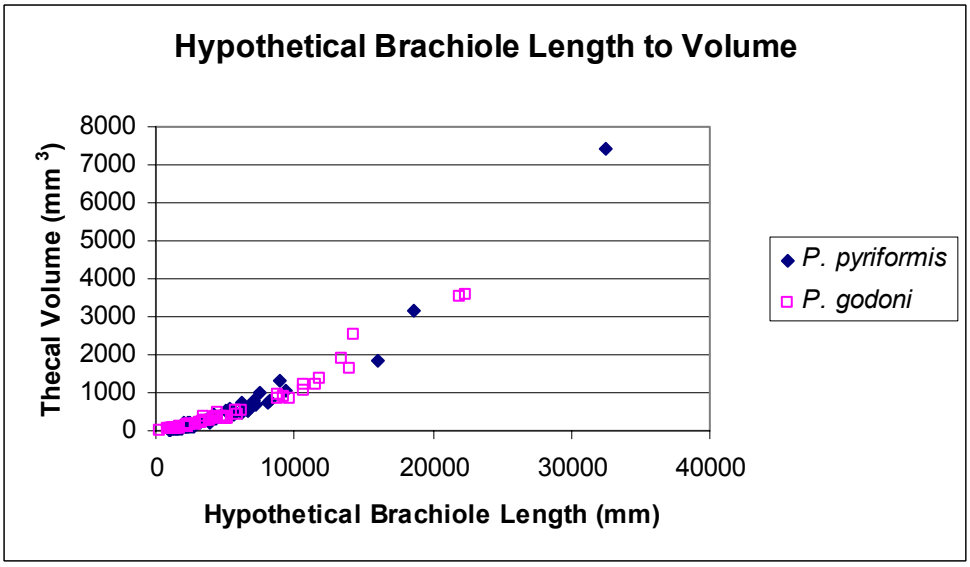

Figure 45: Hypothetical total brachiole length relative to volume assuming brachiole length to be twice the height of the theca.

requirements increase with volume, so should the capacity to capture food. If hydrospire surface area is used as a proxy for total respiratory requirement, then food gathering capacity of the brachioles should be equivalent to hydrospire surface area because the oxygen derived from the hydrospires is used to metabolize incoming food. Food gathering capacity in brachioles is based on the number and length of brachioles in an individual.

By utilizing the power function derived for hydrospire surface area to thecal height, the food gathering capacity can be estimated. This equation for *Pentremites pyriformis* is $Y = 0.7116\ X^{2.483}$ and for *Pentremites godoni* is $Y = 0.7577\ X^{2.656}$, where X is the thecal height and Y is the total hydrospire surface area. If hydrospire surface area is used as a proxy for food gathering capacity, then Y is proportional to the brachiole length multiplied by the number of brachioles, assuming brachiole length is the same for each brachiole on an individual. The formula can then be divided by the number of brachioles to calculate the individual brachiole length. This formula requires a constant to convert hydrospire surface area to food gathering capacity, so one complete brachiole on a pentremitid blastoid of known height is still necessary. Once found, the total brachiole length for the individual can be calculated by multiplying the total number of brachioles by the length of one brachiole. This known total length can then be divided by the food gathering capacity calculated from the formula to derive the constant which would allow estimation of brachiole length for all individuals through ontogeny. Brachiole length would have to be known for two or more samples to test the validity of this approach.

These formulas can be graphically demonstrated if a particular brachiole length is assumed at a certain point in ontogeny to convert the formulas to millimeters (Fig. 46). Three points along the ontogeny of a blastoid at thecal heights of 10 mm, 15 mm, and 20 mm were assumed to have brachiole lengths equal to twice the height of the theca and used for the conversion in the formula for *Pentremites godoni* (Fig. 46). The linear growth was calculated using a consistent brachiole length of twice the height of the theca as suggested by J. Sprinkle (pers. comm.). The rate of growth for anisometric brachiole length is dependant upon the constant used for conversion, and the earlier in ontogeny that the brachiole length reaches twice the height of the theca, the longer the brachiole length will be later in ontogeny (Fig. 46). This work is entirely speculative and would require a number of completely preserved brachioles to disprove.

Hydrospire Surface Area

When hydrospire surface was compared to height, the exponent was 2.5 for *P. pyriformis* and 2.7 for *P. godoni* (with high R^2 values), both of which were less than three (Fig. 28). This result demonstrates that the hydrospire surface area is increasing above a squared rate relative to a linear measure and that a positive allometry occurs within the hydrospires. This occurs because the hydrospires have to increase above a squared rate to compensate for the increased volume and increased metabolic need. The comparison of mass to hydrospire surface area is nearly the same as the values attained in the comparison of volume to hydrospire surface area (Fig. 30). This is to be expected since the volume was calculated using the mass. The only difference is the removal of the

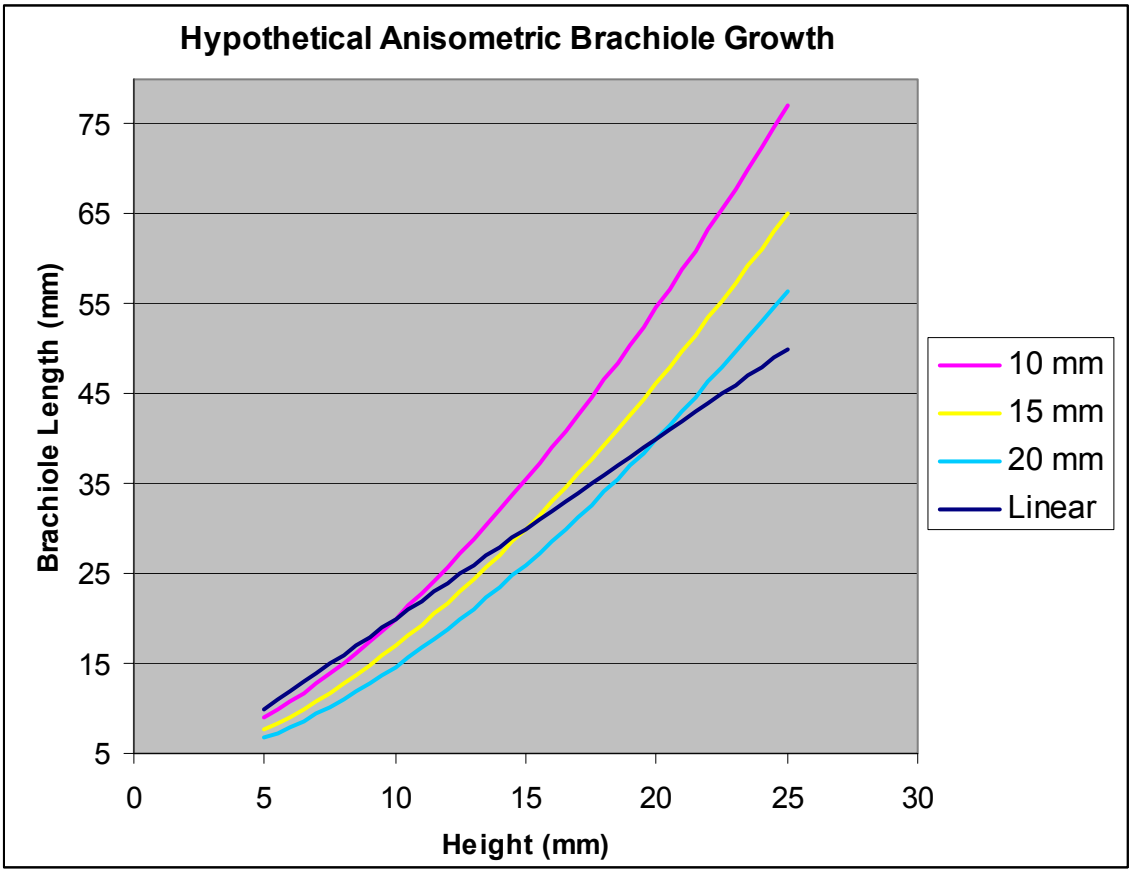

Figure 46: Graphical depiction of brachiole length growth rates utilizing formula derived from hydrospire surface area for *P. godoni*. The constants used for conversion are based on brachiole length equal to twice the thecal height at a height of 10 mm, 15 mm, and 20 mm. Linear growth rate of twice the thecal height through ontogeny as suggested by J. Sprinkle (pers. comm.) was added for comparison.

hydrospire volume from the total volume, which was too small to make much difference in the results between mass and volume to surface area. The comparison of hydrospire surface area to volume produced allometric exponents that showed hydrospire surface area to be slightly lower than volume with reasonable R^2 values (Fig. 29).

The exponent of hydrospire surface area to volume for *P. pyriformis* was 0.84 and for *P. godoni* was 0.88, indicating that volume is increasing more rapidly than surface area through ontogeny. The examination of the line produced by the data of hydrospire surface area to volume had R^2 values that were near to the expected value of unity, with *P. pyriformis* at 0.9832 and *P. godoni* at 0.9839 (Fig. 29). These R^2 values show clearer correlation than those seen in many of the morphometric results, including width and vault ontogeny. Although the results indicate that volume is increasing more rapidly than the hydrospire surface area, the rate of increase is not far off from expected. Another consideration is the lower number of useable samples in the study of the hydrospire surface area relative to the number used in the morphometric analysis. Nearly half the sample population was used (N=48), however the lack of hydrospire preservation in certain samples brought the total number of useable samples down to 33.

It is possible that the volume is exceeding the hydrospire surface area because the total volume calculated is more than is required for metabolism. A more precise measure of the total metabolic requirement for an individual should be the measure of the total visceral volume or the area inside the theca where all the organs are held. The respiratory system is necessary for providing oxygen to all the cells not in contact with seawater, so the external plates, brachioles, stems, and rootlets should be excluded. When total

visceral volume is compared to hydrospire surface area, the results are the same as the results attained for total thecal volume (Fig. 32). In *Pentremites pyriformis*, the allometric exponent for hydrospire surface area to visceral volume is 0.84 (Table 1). In *Pentremites godoni*, the allometric exponent for visceral volume is 0.88 (Table 2). The comparison between visceral volume and hydrospire surface area was expected to be much close to one than total thecal volume. However, the visceral cavity is not composed entirely of organic matter. From modern echinoderms, it can be reasonably assumed that there are organs within the visceral cavity responsible for the transportation of coelomic fluids carrying oxygen and nutrients to other cells within the theca. The digestive system is open to the external water column just like the hydrospires. These fluid filled areas would not add to the total metabolic requirement as they lack cells. Since these structures are not preserved and the entire visceral cavity was measured, the visceral volume is likely exaggerated.

Another issue to consider is that all ontogenetic stages are considered in the volume to hydrospire surface area calculation. Hydrospires go through a developmental stage from the later juvenile samples to early adult samples (Figs. 34 to 36 and Figs. 38 to 40). It is also believed that blastoids had a free swimming larval stage before they metamorphosed into their stalked stage and devolped hydrospires (Sevastopulo, 2005). The minute size of these early stages would have allowed oxygen to diffuse directly into the visceral cavity, and it is likely that diffusion through the plates provided oxygen even into the later juvenile stages. By focusing on the juvenile stages, it is apparent that the hydrospire surface area reaches zero well before height does (Fig. 47).

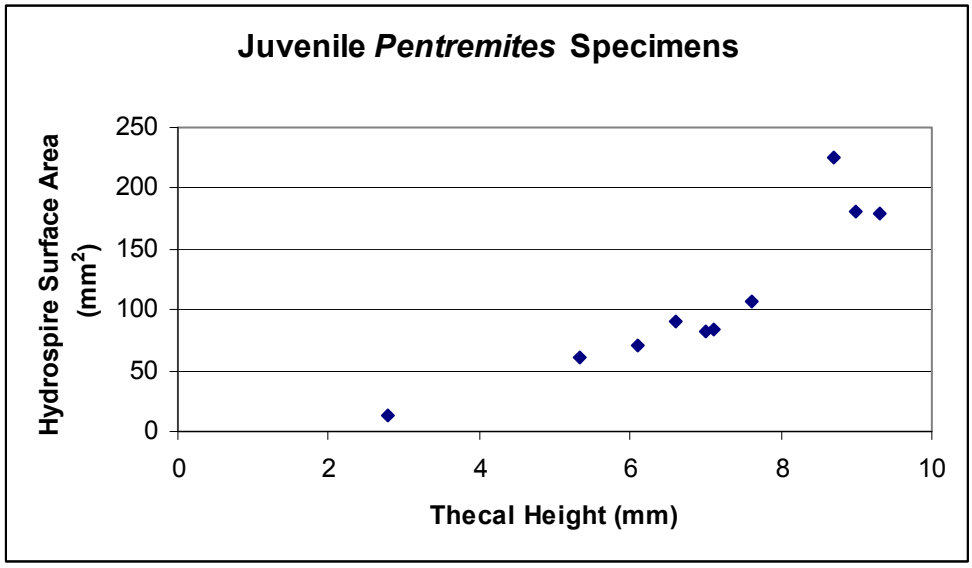

Figure 47: Juvenile Samples from both *Pentremites* species comparing hydrospire surface area to thecal height.

Because of the lack of hydrospires in the early post larval stages, the addition of the juveniles likely decreases the precision of the volume to hydrospire surface area relationship in adult forms. By removing the juveniles, which were determined as having a thecal height of less than 8 mm, the relationship approaches expected values (Fig. 48). The allometric exponent for the hydrospire surface area is 0.91 in *P. godoni* and 0.88 in *P. pyriformis*. The R^2 value for the linear relationship remains approximately the same, with 0.9804 in *P. godoni* and 0.9798 in *P. pyriformis* (Fig. 48).

When the hydrospire surface area of the adult specimens are compared to total visceral volume the results are farther from expected than with total thecal volume (Fig. 49). In mature *Pentremites pyriformis*, the allometric exponent for visceral volume was 0.83, whereas the total thecal volume was 0.88. In mature *Pentremites godoni*, the allometric exponent for visceral volume is 0.86 compared to 0.91 for thecal volume. Both values indicate that the visceral volume is increasing at a more rapid rate than hydrospire surface area. One possible explanation of this is the increased proportion of the visceral volume necessary for respiration. Respiration likely occurs with the transportation of coelomic fluid within the visceral cavity in a counter-current direction relative to the adoral fluid transportation in the hydrospires. With the increasing hydrospire surface area, there should be an equivalent increase in the visceral cavity for the water vascular system running alongside the hydrospires. This system would be primarily fluid filled, and the lack of preservation of soft parts prevents measuring these structures. The visceral cavity must also increase the digestive system to accommodate increased nutrient uptake from the brachioles. Both structures are included in the visceral volume

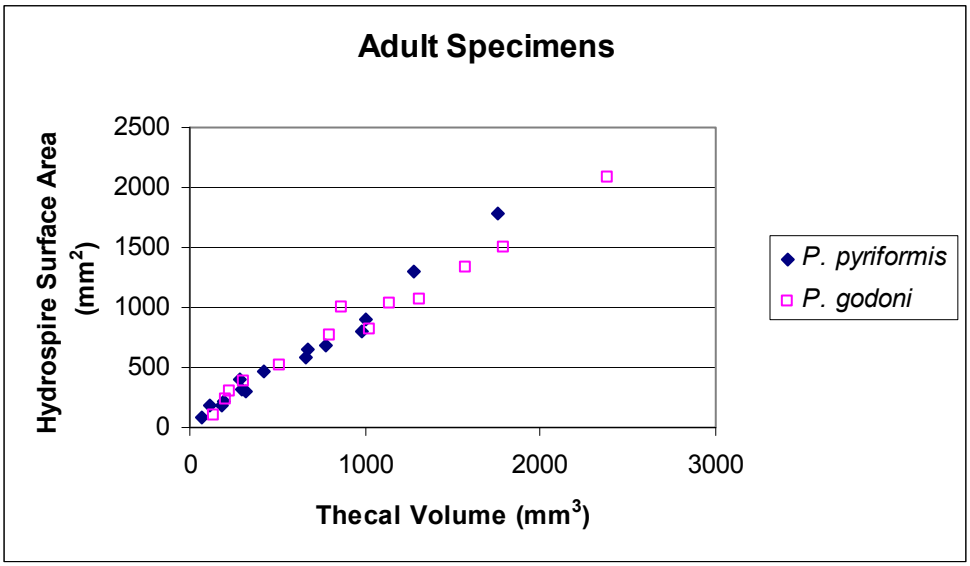

Figure 48: Hydrospire surface area to thecal volume comparison between species using samples considered to be at an adult stage.

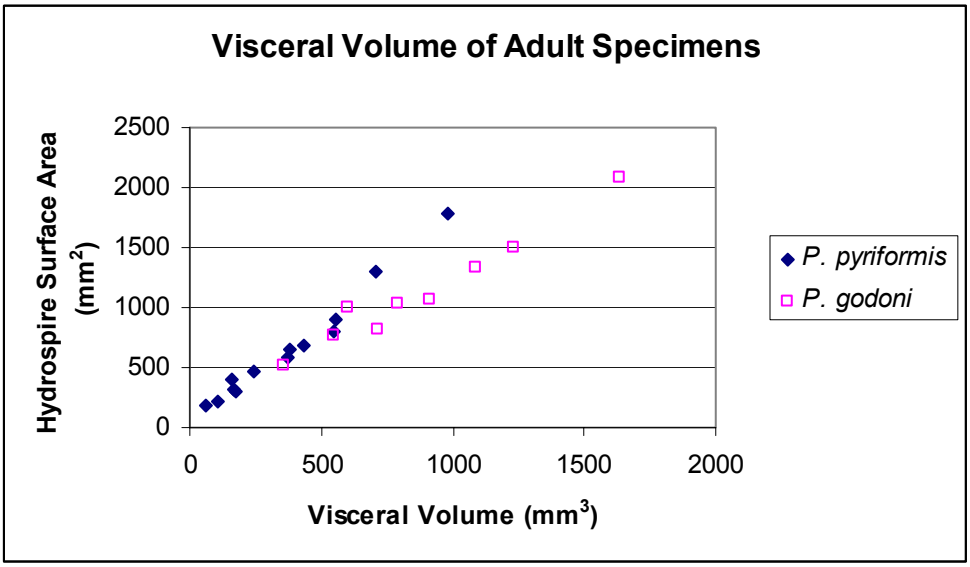

Figure 49: Comparison of hydrospire surface area to visceral volume using mature specimens.

measurements and may explain why the visceral volume is increasing at a faster rate than the hydrospire surface area.

Even without the removal of the juvenile samples, the one to one linear relationship between hydrospire surface area and volume as seen in the allometric exponents are to close to one to be coincidence. This suggests a number of things about the mechanics of respiration in blastoids. The brachioles were not necessary in the maintenance of metabolism and likely did not transport oxygen into the body. Since hydrospire surface area did not surpass the rate of volume increase, structures external to the theca (brachioles, root, and stem) likely required no oxygen from the hydrospires and probably respired through simple diffusion with the external water column. The metabolic requirements are exceeded in younger individuals; however, the older stages still need increasing hydrospire surface area to survive.

It seems unlikely that the metabolic rate of the individual changes through ontogeny since metabolic rate is determined by the volume of the organic matter and the hydrospire surface area matches volume. It is possible that the rate of plate growth in blastoids decreases with maturity, thus decreasing the total metabolic requirement. Since life stage was determined by height in this study, it is not possible to ascertain rate of growth through ontogeny.

The data could not confirm or deny the possibility that oxygen diffusion becomes more efficient at older stages as flow rate through the wider hydrospire pores becomes less restricted. Since the allometric exponent between hydrospire surface area and volume was slightly less than 1.0, it is possible that the extra oxygen may come from increased

water flow rate. However, the hydrospire surface area in *P. godoni* was a closer match to volume than *P. pyriformis*. *Pentremites godoni* also had the longer ambulacra which mean an increased number of hydrospire pores. If a decrease in restriction in the hydrospire pores allowed for an increase in oxygen uptake, *P. godoni* would be expected to have less surface area relative to volume than *P. pyriformis*. Since this is not the case, it appears as though hydrodynamic flow remains unchanged through ontogeny.

Morphological Differences

Part of what determines the hydrospire surface area is the length of the hydrospires. The hydrospires extend from a little below the spiracles to the bottom of the ambulacra. The ambulacra are appreciably longer in *P. godoni* than in *P. pyriformis* (Figs. 7 and 8). This is also characterized in the substantial increase in vault to pelvis ratio in *P. godoni* compared to virtually no change in P/V ratio in *P. pyriformis* through ontogeny (Waters et al., 1985). This morphological difference between the two species brings about different methods of attaining hydrospire surface area. With its longer ambulacra, *P. godoni* have longer hydrospires in contrast to *P. pyriformis*.

Certain photographs contained questionable hydrospire folds or partial bulbs along the interradial side of the hydrospire (Fig. 50). These are likely the beginnings of new folds and indicate that the folds develop from the ambulacra side and add folds toward the interradial side. This is supported by the larger surface area of the hydrospire folds on the ambulacral side of the hydrospire pair relative to the folds on the interradial side.

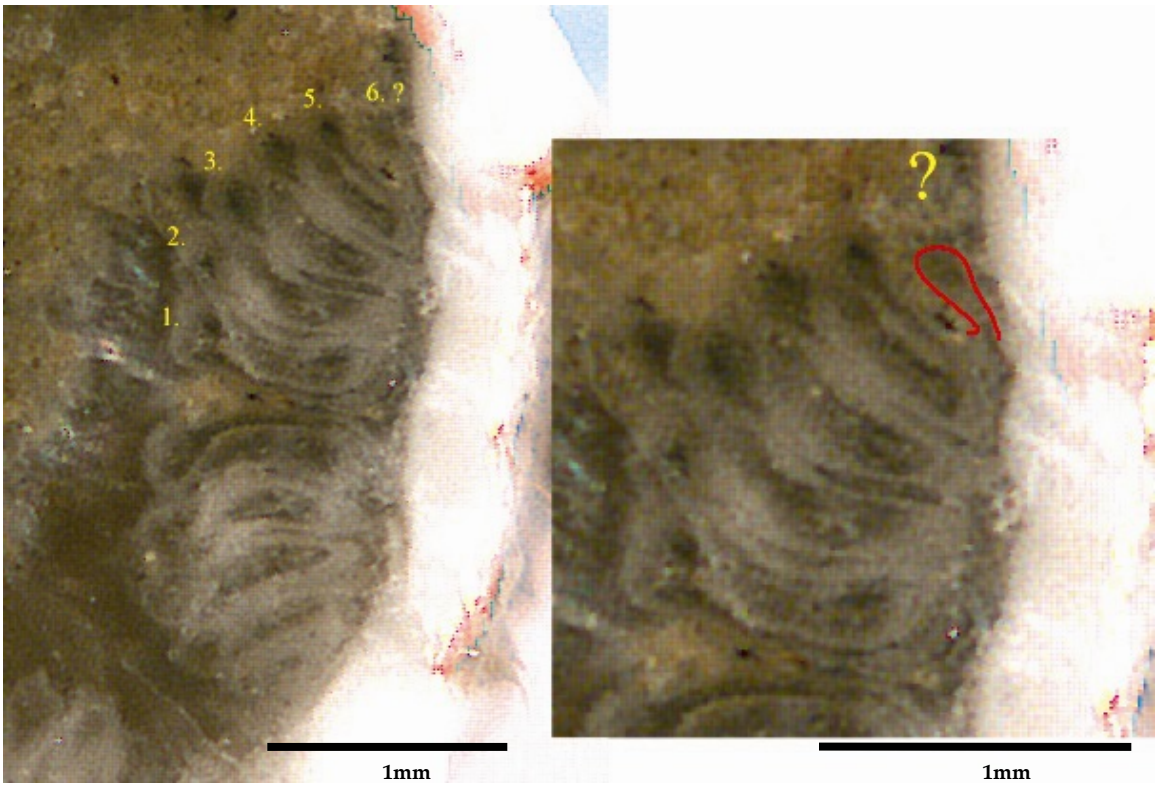

Figure 50: Photograph of a hydrospire showing a questionable fold that may be the early development of a new hydrospire fold (Sample S14).

Both species develop five hydrospire folds early in there development (Figs. 34 through 40). *Pentremites pyriformis* compensates for the shorter hydrospires by increasing the number of hydrospire folds beyond five (Figs. 41, 42, and 43). This is contrary to the previous investigations suggesting hydrospire fold number tends to remain constant through ontogeny (Macurda, 1967, Beaver, 1967, J. Sprinkle, pers. comm.). Any occurrence of increasing hydrospire fold number had previously been observed only in certain fissiculate blastoids (Macurda, 1967). In *P. pyriformis*, fold number increased to a maximum of eight in the useable samples.

This suggests that the two morphotypes of the compared species are utilizing two distinct methods of accommodating increased respiratory requirements. In *Pentremites godoni*, the ambulacra have increased in length which allows the hydrospire length to be increased (Fig. 10). Hydrospire fold number is maintained as hydrospire length increases through ontogeny (Fig. 33). In *Pentremites pyriformis*, the ambulacra increase in surface area at a decreased rate relative to *P. godoni* through ontogeny (Fig. 10). This creates a decrease in length of the hydrospires relative to *P. godoni*. With shorter hydrospires, *P. pyriformis* increases the hydrospire surface area through ontogeny by adding additional hydrospire folds as necessary.

Methodological Issues

A number of issues presented themselves during this study that may have biased the results. Sample selection was not entirely random. The total population from which the samples were selected had to meet certain requirements to be of use to the study. Samples had to be complete, they could not be flattened or deformed, and they had to

have little to no silicification. This was done to ensure accurate morphological measurements (most importantly volume) and to increase the likelihood of visible hydrospires within the theca. Furthermore, from the complete samples an entire ontogenetic series was required for the study. Differential preservation of immature samples to mature samples made gathering a complete ontogenetic series through random selection unlikely. Since a number of juveniles and very mature adults were needed to complete the entire ontogeny of both species, selection of the sample population could not be completely random. Because of the limited number of juveniles and mature adults, almost all were incorporated into the sample population. The sample population was then completed by choosing at random middle-sized adults.

In order to calculate the hydrospire surface area, the hydrospires had to be visible within the photographs. Useable samples had secondary precipitation of large sparry calcite crystals within the visceral cavity that preserved the traces of internal structure. Problems with individuals obscured the visibility of the hydrospires included geopedal micrite fill, poor preservation, or partial dissolution of the internal cavity including the hydrospires. Dissolution could destroy anything from an individual fold to a number of hydrospires. Micrite is an opaque mud that filled both the hydrospires and the visceral cavity obscuring the distinction between fold and cavity. Both issues prevented the measurement of a number of hydrospires, increasing the error within each cross section measurement. The sample was considered unusable unless at least three hydrospires were visible.

Finally, the measurements of volume do not include the visceral volume. The visceral volume is extremely difficult to calculate since it extends aborally into the basals. This would have left little room to mount the theca for cross sectioning. Furthermore, adding an additional measurement inside the theca would have brought about the possibility of that characteristic having poor photographic resolution thus increasing the likelihood of acquiring bad samples. Computed tomography (CT) scans would have greatly improved resolution of both the viscera and the hydrospires, however the cost of CT scanning would have greatly exceeded the funding for this project.

7. Conclusions

Hydrospires increase in surface area through ontogeny in a manner that nearly matches the cubic rate of increase in volume. This suggests that the hydrospires are indeed structures designed primarily for respiration. No additional structures are necessary for the individual to maintain its metabolic requirements through ontogeny, and the external structures did not require oxygen from the theca. Blastoid morphology affects the manner in which this positive allometry in hydrospire surface area is attained. For *Pentremites godoni*, positive allometry of the ambulacra allows for positive allometry of the hydrospire length. In *Pentremites pyriformis*, ambulacral length does not increase markedly through ontogeny. *Pentremites pyriformis* accommodates the isometric ambulacral and therefore hydrospire length by increasing the number of hydrospire folds through ontogeny.

There are a number of Paleozoic echinoderms that utilize internal canal structures for respiration, including glyptocystitoid rhombiferans, hemicosmitid rhombiferans, parablastoids, and certain "rhomb" bearing crinoids. The near one to one relationship between volume and respiratory structure surface area from this study would be expected for the adult stages of these other groups of echinoderms. By measuring volume and the surface area of the respiratory canals of only a few individuals, a line could be interpolated to determine likely respiratory canal surface area for any individual with a known volume. The number of respiratory canals is not as consistent as the ten hydrospires in blastoids. Knowing the surface area of one of the respiratory canals allows the calculation of total number of canals to be expected on an individual once total

respiratory surface area is extrapolated. There is evidence that the respiratory canals in glyptocystitid rhombiferans increase number through ontogeny at a disproportionate rate, having a far greater number later in life than would be expected with a isometric increase (Sumrall and Schumacher, 2002, Sumralland Sprinkle, 1999). Furthermore, the nearly perfect allometry of cubic increase between height and volume in this study would also allow for the development of a graph illustrating ontogeny to volume in these other groups of echinoderms. Respiratory canal surface area could be determined with only the measurement of ontogenetic stage (height or width depending on the group) since ontogenetic stage fairly accurately reveals the volume of the individual. This is highly useful in these groups since preservation is rare and the samples are usually fragmented and incomplete.

List of References

Beaver, Harold H. 1996. Hydrospire meshwork of the Carboniferous blastoid *Pentremites* Say. Journal of Paleontology, Vol. 70 (2): pp. 333-335.

Beaver, Harold H. 1967. Morphology. in Treatise on Invertabrate Paleontology: Echinodermata, 1. The University of Kansas and the Geological Society of America. Part S.,Vol. 2: pp.300-344.

Beaver, Harold H. 1967a. Paleoecology. in Treatise on Invertabrate Paleontology: Echinodermata, 1. The University of Kansas and the Geological Society of America. Part S.,Vol. 2: pp.382-384.

Beaver, Harold H and Fabian, Alexander J. 1998. Color patterns in Mississippian (Chesterian) blastoids. Journal of Paleontology, Vol. 72 (2): pp. 332-338.

Becker, Wayne M., Kleinsmith, Lweis J., and Hardin, Jeff. 2000. Cells and Organelles. in The World of the Cell: Fourth Edition. The Benjamin/Cummings Publishing Company: pp. 78-105.

Blake, Daniel B. and Elliott, Dan R. 2003. Ossicular homologies, systematics, and phylogenetic implications of certain North American Carboniferous asteroids (Echinodermata). Journal of Paleontology, Vol. 77 (3): pp. 476-489.

Bodenbender, Brian E., and Fisher, Daniel C. 2001. Stratocladistic analysis of blastoid phylogeny. Journal of Paleontology, Vol. 75 (2): pp. 351-369.

Brett, Carlton E., Frest, Terrence J., Sprinkle, James T., and Clement, Craig R. 1983. Coronoidea; A new class of blastozoan echinoderms based on taxonomic reevaluation of *Stephanocrinus*. Journal of Paleontology, Vol. 57: pp. 627-651.

Briemer, A. and Macurda, D.B. 1972. The Phylogeny of Fissiculate Blastoids. North Holland Publishing. Amsterdam: pp.159-179.

Brower, James C. 1987. The relations between allometry, phylogeny and functional morphology in some calceocrinid crinoids. Journal of Paleontology, Vol. 61 (5): pp. 999-1032.

Brower, James C. In Press. Ontogeny of the food-gathering system in Ordovician crinoids. Journal of Paleontology.

Campbell, Neil A. 1996. Circulation and gas exchange. in Biology: Fourth Edition. The Benjamin/Cummings Publishing Company: pp. 819-851.

Fay, Robert O. 1967. Introduction. in Treatise on Invertabrate Paleontology: Echinodermata, 1. The University of Kansas and the Geological Society of America. Part S.,Vol. 2: pp. 298-300.

Fay, Robert O. 1967a. Phylogeny and evolution. in Treatise on Invertabrate Paleontology: Echinodermata, 1. The University of Kansas and the Geological Society of America. Part S.,Vol. 2: pp. 298-300.

Fay, Robert O. and Wanner, Johannes.1967. Systematic descriptions. in Treatise on Invertabrate Paleontology: Echinodermata, 1. The University of Kansas and the Geological Society of America. Part S.,Vol. 2: pp. 396-445.

Galloway, Jesse J. and Kaska, Harold V. 1957. Genus *Pentrimites* and its Species. Geological Society of America. New York: pp. 69-99.

Katz, Stephen G. and Sprinkle, James T. 1976. Fossilized eggs in a Pennsylvanian blastoid. Science, Vol. 192: pp. 1137-1139.

Koverman, Kimberly S. and Sumrall, Colin D. 2003. Phylogeny of Early Paleozoic echinoderms and the origin of blastoids. Geological Society of America Abstracts with Programs, Vol. 34 (6): p. 267.

Macurda, Donald B. 1975. The *Pentremites* (Blastoidea) of the Burlington Limestone (Mississippian). Journal of Paleontology, Vol. 49: pp. 346-373.

Macurda, Donald B. 1967. Development and hydrodynamics. in Treatise on Invertabrate Paleontology: Echinodermata, 1. The University of Kansas and the Geological Society of America. Part S.,Vol. 2: pp.356-381.

Macurda, Donald B. 1967a. Stratigraphic and geographic distribution. in Treatise on Invertabrate Paleontology: Echinodermata, 1. The University of Kansas and the Geological Society of America. Part S.,Vol. 2: pp.385-387.

Macurda, Donald B. 1967b. A Permian blastoid from the Canadian arctic. Journal of Paleontology, Vol. 41 (5): pp. 1282-1284.

Macurda, Donald B. 1965. The hydrodynamics of the Mississippian blastoid genus *Globoblastus*. Journal of Paleontology, Vol. 39: pp.1209-1217.

Paul, Christopher R.C. 1968. Morphology and function of dichoporite pore-structures in cystoids. Palaeontology, Vol. 11 (5): pp. 697-730.

Sevastopulo, George D. 2005. The early ontogeny of blastoids. Geological Journal, Vol. 40: pp. 351-362.

Sprinkle, James. 1980. Origin of blastoids; A new look at an old problem. Geological Society of America Abstracts with Programs, Vol. 12: p. 528.

Sprinkle, James. 1980a. An overview of the fossil record. in Echinoderms: Notes for a Short Course, co-edited by Thomas W. Broadhead and Johnny A. Waters, The University of Tennessee, Knoxville, TN: pp. 15-93.

Sprinkle, James. 1973. Morphology and evolution of blastozoan echinoderms. The Museum of Comparative Zoology, Special Publication. Harvard University, Cambridge, MA: pp. 21-27.

Sumrall, Colin D. 1997. The role of fossils in the phylogenetic reconstruction of Echinodermata. In J. A. Waters and C. G. Maples (eds.) Paleontological Society Papers Volume 3, Geobiology of Echinoderms. The Paleontological Society, Pittsburgh: pp.267-288.

Sumrall, Colin D., and Brochu,Christopher A. 2003. Resolution, sampling, higher taxa and assumptions in stratocladistic analysis. Journal of Paleontology, Vol. 71 (1): pp. 189-194.

Sumrall, Colin D., and Schumacher, Gregory A. 2002. *Cheirocystis Fultonensis*, a new glyptocystitoid rhombiferan from the Upper Ordovician of the Cincinnati Arch-Comments on cheirocrinid ontogeny. Journal of Paleontology, Vol. 76 (5): pp. 843-851.

Sumrall, Colin D., and Sprinkle, James. 1999. Early ontogeny of the glyptocystitid rhombiferan *Lepadocystis moorie*. Candia Carnevali and Bonasoro (eds). Balkema, Rotterdam: pp. 409-414.

Sumrall, Colin D., and Waters, Johnny A. 2006. Deltoid and oral plate homologies in blastoids - Insights from primitive crinoids and modern crinoid development. Geological Society of America; *Abstracts with Programs*, Vol. 38 (3): p. 23.

Waters, Johnny A., Horowitz, Alan S, and Macurda, Donald B. 1985. Ontongeny and phylogeny of the Carboniferous blastoid *Pentrimites*. Journal of Paleontology, Vol. 59 (3): pp. 701-712.

Appendix

Table 5: External thecal measurements of *Pentremites pyriformis* for morphometric analyses.

Sample Number	Thecal Height (mm)	Thecal Width (mm)	Vault Height (mm)	Pelvis Height (mm)	Radial Plate Length (mm)	Radial Plate Width (mm)	RR Suture Length (mm)	RD Suture Length (mm)
S1	31.9	24.1	17.3	14.6	22.5	14.6	16.8	4
S2	25.8	18	13.1	12.7	16.8	10.4	13.1	2.7
S3	23.5	13.8	11.5	12	16.5	7.9	13	1.6
S4	18.8	13.5	7.4	11.4	11.2	7.7	9.9	1.5
S5	17.2	12.7	6.7	10.5	11.2	7.6	8.7	1.4
S6	16.7	12.3	8.2	8.5	11.1	7	9.1	1.4
S7	16.5	11.6	9.4	7.1	10.5	6.9	8.7	1.2
S8	14.7	11.2	9	5.7	9.2	6.7	7.6	2.28
S9	14.7	11.1	6.1	8.6	10.6	6.6	8.7	0.92
S10	14.5	10.1	6	8.5	9	6	6.9	0.58
S11	14.2	10.3	6.2	8	10.1	6.5	7.1	0.5
S12	14.1	9.4	6.1	8	10.1	5.9	8	0.54
S13	12.1	7.9	5.4	6.7	8.7	5.4	7.4	0.5
S14	12	8.1	4.8	7.2	8	5.2	7.1	0.46
S15	10.8	6.9	4	6.8	7.2	4.2	6	N/A*
S16	9.3	5.7	3.6	5.7	6.3	3.8	5.2	0.42
S17	9.1	5.8	3.1	6	6	2.9	4.7	0.39
S18	7.8	5.4	2.8	5	4.6	2.7	5	0.23
S19	6.3	4.1	3.7	2.6	3.7	2.4	3.6	N/A*
S20	4.7	3.4	2.8	1.9	2	1.9	2.8	N/A*

*Deltoid plates absent from poor preservation or lack of development.

Table 5: Continued.

Sample Number	Thecal Height (mm)	Thecal Width (mm)	Vault Height (mm)	Pelvis Height (mm)	Radial Plate Length (mm)	Radial Plate Width (mm)	RR Suture Length (mm)	RD Suture Length (mm)
SA1	16.7	10.7	7.3	9.4	10.5	6.6	7.4	0.9
SA2	14.8	11.2	7.6	7.2	9.8	7.3	7.6	1.2
SA3	14.5	9.9	7.5	7	8.4	6	7.2	0.9
SA4	14.9	9.9	5.7	9.2	8.9	5.9	7.2	1.1
SA5	13.3	9.7	6.1	7.2	8.4	5.7	6.5	0.9
SA6	13.5	9.3	6.5	7	8.7	5.9	6.8	0.9
SA7	8.9	5.4	3.3	5.6	5	3.4	2.94	0.63
SA8	8.7	6.4	3.6	5.1	5.4	3.8	3.88	0.38
SA9	7	4.6	2.4	4.6	4.4	3	2.81	0.75
SA10	11.1	7.1	3.3	7.8	6.6	4.9	4.88	0.94
SA11	10.7	7.8	4	6.7	6.8	4.9	4.44	0.75
SA12	7.4	5.8	4	3.4	4.6	4	3.31	0.69
SA13	6.1	4.4	2.6	3.5	3.7	3	2.50	0.38
SA14	6.6	4.6	2.4	4.2	3.6	3	2.81	0.38
SB1	13.2	9.1	5.2	8	8.6	5.3	6.8	0.9
SB2	15	11.3	6.4	8.6	10.6	6.5	7.8	1.5
SB3	12.2	10.5	5.7	6.5	8.1	6.1	7.2	0.9
SB4	13	10.2	6.3	6.7	8.7	5.8	6.3	1.2
SB5	13.6	7.9	4.2	9.4	9.3	4.4	6.5	1.2
SB6	9	7.4	3.2	5.8	6.4	4.3	4.5	0.9

Table 5: Continued.

Sample Number	Thecal Height (mm)	Thecal Width (mm)	Vault Height (mm)	Pelvis Height (mm)	Radial Plate Length (mm)	Radial Plate Width (mm)	RR Suture Length (mm)	RD Suture Length (mm)
SB7	8.6	7.2	4.3	4.3	5.6	4.2	4.8	0.8
SB8	8.1	6.2	3.1	5	5.6	3.8	4.2	0.8
SB9	10.2	7.9	4.2	6	6	4.8	4.8	0.7
SB10	8.5	6.6	3.5	5	5.8	3.6	4	0.8
SB11	7.1	5.3	2.4	4.7	4.5	3.3	4.2	0.4
SB12	7.9	5.1	2.1	5.8	4.4	3.2	3.9	0.5
SB13	7.5	4.8	1.8	5.7	4.4	3.1	4.2	0.4
SB14	6.7	4.7	2.5	4.2	4	3.2	3.2	0.6
SB15	7	4.1	1.6	5.4	4.2	2.8	2.5	0.7
SB16	6.8	5.1	2.4	4.4	4.5	3.1	3.3	0.7

Table 6: Ambulacral and miscellaneous measurements of *Pentremites pyriformis* for analyses.

Sample Number	Ambulacral Length (mm)	Ambulacral Width (mm)	Side Plates per Ambulacra	Side Plates per millimeter	Total Brachiole Number	Pelvis Angle (º)	Mass (g)	Volume (mm^3)
S1	20.9	6.4	102	3	510	85	20.1660	7441.3284
S2	15	5.1	72	3	360	71	8.5331	3148.7454
S3	13.4	4.5	68	3	340	63	4.9763	1836.2731
S4	10	4.5	48	3	240	76	3.6288	1339.0406
S5	9.5	4	44	3	220	82	2.7424	1011.9557
S6	10.8	3.9	56	3	280	89	2.8486	1051.1439
S7	10.1	3.6	50	3	250	86	2.1537	794.7232
S8	9.3	3.8	48	3	240	87	1.8808	694.0221
S9	7.5	3.4	42	3	210	80	1.9392	715.5720
S10	7.2	3.2	36	3	180	70	1.4315	528.2288
S11	7.9	3.3	38	3	190	72	1.5697	579.2251
S12	7.1	3.2	40	3	200	69	1.3868	511.7343
S13	6.8	2.3	36	3	180	69	0.8240	304.0590
S14	6	2.2	34	3	170	68	0.8332	307.4539
S15	5.1	2.5	30	3	150	59	0.5329	196.6421
S16	4.5	2.1	26	3	130	62	0.3330	122.8782
S17	5.9	2	24	4	120	60	0.3111	114.7970
S18	5	2.3	28	4	140	72	0.2395	88.3764
S19	4.1	1.8	22	4	110	68	0.1226	45.2399
S20	3.6	1.6	20	5	100	71	0.0628	23.1734

Table 6: Continued.

Sample Number	Ambulacral Length (mm)	Ambulacral Width (mm)	Side Plates per Ambulacra	Side Plates per millimeter	Total Brachiole Number	Pelvis Angle (º)	Mass (g)	Volume (mm^3)
SA1	9.8	4.1	48	3	240	71	2.0574	759.1882
SA2	9.3	4.4	48	3	240	92	2.1226	783.2472
SA3	8.2	3.8	46	3	230	84	1.4658	540.8856
SA4	7	4.2	34	3	170	67	1.4640	540.2214
SA5	6.9	4.2	32	3	160	77	1.1809	435.7565
SA6	7.3	4	42	3.5	210	83	1.2019	443.5055
SA7	4.2	2.5	24	4	120	58	0.2507	92.5092
SA8	5	3.1	30	4	150	69	0.3505	129.3358
SA9	3.7	2.2	18	4	90	63	0.1615	59.5941
SA10	5.5	3	22	3.5	110	62	0.5709	210.6642
SA11	5.1	3.3	22	3.5	110	71	0.6412	236.6052
SA12	4.6	2.9	32	4	160	76	0.2588	95.4982
SA13	3.3	2.3	20	4	100	74	0.1295	47.7860
SA14	3.6	2.8	26	4	130	67	0.1599	59.0037
SB1	7.4	4.3	32	3	160	78	1.0939	403.6531
SB2	9.3	4.2	48	3	240	83	1.8480	681.9188
SB3	8.6	4.2	54	3.5	270	95	1.4473	534.0590
SB4	8.2	4.2	48	3	240	88	1.2982	479.0406
SB5	6.5	3.5	28	4	140	56	0.8763	323.3579
SB6	5	3.6	22	3	110	78	0.5116	188.7823

Table 6: Continued.

Sample Number	Ambulacral Length (mm)	Ambulacral Width (mm)	Side Plates per Ambulacra	Side Plates per millimeter	Total Brachiole Number	Pelvis Angle (º)	Mass (g)	Volume (mm^3)
SB7	5.3	3.2	32	4	160	86	0.4988	184.0590
SB8	4.4	3.1	28	3.5	140	73	0.3225	119.0037
SB9	6.6	3.8	38	3	190	80	0.6237	230.1476
SB10	5.3	2.9	32	4	160	68	0.3166	116.8266
SB11	4.4	2.5	26	4	130	74	0.1991	73.4686
SB12	3.7	2.8	20	4	100	73	0.1847	68.1550
SB13	3.4	2.5	18	4	90	56	0.1737	64.0959
SB14	3.3	2.5	22	4	110	68	0.1469	54.2066
SB15	2.8	2.2	14	4	70	51	0.1265	46.6790
SB16	3.8	2.9	24	4	120	73	0.1769	65.2768

Table 7: External thecal measurements of *Pentremites godoni* used for morphometric analyses.

Sample Number	Thecal Height (mm)	Thecal Width (mm)	Vault Height (mm)	Pelvis Height (mm)	Radial Plate Length (mm)	Radial Plate Width (mm)	RR Suture Length (mm)	RD Suture Length (mm)
F1	21.1	19.2	16.2	4.9	12.9	10.5	9.7	3.73
F2	20.3	19.3	18.1	2.2	14.1	10.8	10.5	3.82
F3	16.7	13.9	12.9	3.8	10.9	8.1	8.2	2.64
F4	15.7	14.1	11.5	4.2	10.2	8.8	8.6	2.09
F5	14.5	12.9	10.9	3.6	9.5	7.1	6.6	2.45
F6	13.9	12	10.1	3.8	8.5	6.4	7.9	1.73
F7	11	10.8	7.6	3.4	8.4	6.2	7.1	1.27
F8	10.3	8.7	6.7	3.6	7.3	5	5.4	1.09
F9	9.2	7.7	5.1	4.1	6	4.5	4.9	1.09
F10	7.6	6.9	3.8	3.8	5.1	4	2.3	0.82
F11	5.333	5.273	2.061	3.273	3.576	2.909	2.727	0.727
F12	4.485	4.424	2.242	2.242	2.909	2.364	2.727	0.485
F13	2.792	2.792	1.245	1.547	2.848	2.061	2.424	0.364
F14	5.212	4.727	3.030	2.182	3.576	2.545	2.303	0.788
F15	5.333	4.727	2.667	2.667	3.152	2.485	2.121	0.364
FA1	8.1	6	3.9	4.2	4.17	3.42	3.17	0.67
FA2	6.2	5.2	2.1	4.1	3.50	2.92	2.17	0.67
FA3	6.1	5.1	3	3.1	2.83	2.83	2.42	0.50
FA4	7.5	6.4	4.2	3.3	3.92	3.42	3.50	0.58
FA5	7.1	6.6	3.4	3.7	3.58	3.42	2.58	0.67

Table 7: Continued.

Sample Number	Thecal Height (mm)	Thecal Width (mm)	Vault Height (mm)	Pelvis Height (mm)	Radial Plate Length (mm)	Radial Plate Width (mm)	RR Suture Length (mm)	RD Suture Length (mm)
FA6	7.4	6.2	3.4	4	3.17	2.92	2.17	0.67
FA7	5.6	5.4	2.4	3.2	2.83	2.75	2.42	0.50
FA8	6.3	5.8	2.1	4.2	3.42	2.92	2.92	0.58
FA9	5.8	6.8	2.4	3.4	3.25	2.92	2.17	0.75
FA10	6.2	5	2.5	3.7	3.00	2.75	2.83	0.50
FA11	6.4	5.5	2.5	3.9	3.17	2.92	2.17	0.50
FB1	18.4	18.3	14.8	3.6	12.1	8.8	7.7	3.3
FB2	17.6	16.2	11.6	6	11.2	9.3	9.3	3
FB3	14.9	13.3	11.9	3	10	8.2	8	2.1
FB4	17	12.1	9.3	7.7	11.3	7.2	7.3	2.1
FB5	14.4	11.8	10.7	3.7	9	7	7	1.64
FB6	13.4	12.2	9.5	3.9	8.7	6.8	7.1	1.27
FB7	16	13.7	12.1	3.9	11.8	8	7.3	2.4
FB8	12	10.8	7.1	4.9	7.7	6.1	6.3	1.82
FB9	10.9	9.5	7.2	3.7	7.1	6.1	5.2	2.00
FB10	9.9	9.1	6.5	3.4	6.1	5.5	4.7	1.45
FB11	8.5	8	5	3.5	5.6	5.1	4.5	1.09
FB12	8.7	8.2	5.4	3.3	5	4.9	4.1	1.09
FB13	13	9.5	5.7	7.3	7.5	6.1	6.6	1.64
FB14	11.9	7.8	5.8	6.1	7.1	5.6	5.9	1.18

Table 7: Continued.

Sample Number	Thecal Height (mm)	Thecal Width (mm)	Vault Height (mm)	Pelvis Height (mm)	Radial Plate Length (mm)	Radial Plate Width (mm)	RR Suture Length (mm)	RD Suture Length (mm)
FB15	10.4	8.5	5.7	4.7	7.7	5.8	5.9	1.18
FB16	10.8	8.7	6.1	4.7	7.5	5.2	5.7	1.09
FB17	7.6	6.7	4.6	3	5.8	4.4	4.4	N/A*
FB18	8.7	8	4.2	4.5	5.7	5.1	5.2	0.64
FB19	7.6	6.7	4.2	3.4	5.4	4.2	4.6	1.18
FB20	8.6	7.5	4.1	4.5	5.6	4.5	4.8	0.82
FB21	7.8	7.8	4.2	3.6	5.6	4.9	4.9	1.09
FB22	12.4	8.9	5.5	6.9	8	6.2	6.9	1.09
FB23	10.6	8.3	6.5	4.1	7.9	5.3	6.6	1.00
FB24	9.8	7.5	3.5	6.3	6.5	4.5	4.3	0.55

*Deltoid plates absent from lack of development.

Table 8: Ambulacral and miscellaneous measurements of *Pentremites godoni* for analyses.

Sample Number	Ambulacral Length (mm)	Ambulacral Width (mm)	Side Plates per Ambulacra	Side Plates per millimeter	Total Brachiole Number	Pelvis Angle (º)	Mass (g)	Volume (mm^3)
F1	19.1	5.5	106	3	530	132	9.7208	3587.0111
F2	18.8	5.4	108	3	540	154	9.5958	3540.8856
F3	14.7	4.5	84	3	420	129	4.4368	1637.1956
F4	11.8	3.9	74	3	370	122	3.2862	1212.6199
F5	11.9	3.6	74	3	370	125	2.8885	1065.8672
F6	11.3	3.5	70	3	350	125	2.2824	842.2140
F7	8.7	3.3	52	4	260	121	1.4337	529.0406
F8	8.1	2.5	44	4	220	114	0.8870	327.3063
F9	6.9	2.9	38	4	190	112	0.6484	239.2620
F10	5.1	2.2	30	4	150	91	0.3940	145.3875
F11	1.879	2.727	22	4.5	110	103	0.1574	58.0812
F12	2.485	2.364	18	4	90	116	0.0978	36.0886
F13	1.132	1.132	12	4.5	60	73	0.0227	8.3764
F14	2.970	2.121	22	4.5	110	103	0.1241	45.7934
F15	2.606	2.182	18	4	90	98	0.1277	47.1218
FA1	4.2	2.83	28	4	140	75	0.3239	119.5203
FA2	4	2.17	22	4	110	97	0.2004	73.9483
FA3	4	2.26	28	4	140	101	0.2033	75.0185
FA4	5.5	2.52	32	4	160	110	0.3848	141.9926
FA5	5.4	2.57	32	3.5	160	118	0.3474	128.1919

Table 8: Continued.

Sample Number	Ambulacral Length (mm)	Ambulacral Width (mm)	Side Plates per Ambulacra	Side Plates per millimeter	Total Brachiole Number	Pelvis Angle (º)	Mass (g)	Volume (mm^3)
FA6	5	2.48	30	4	150	115	0.3459	127.6384
FA7	3.7	2.26	22	4	110	114	0.1886	69.5941
FA8	4.2	2.26	24	4	120	91	0.2133	78.7085
FA9	4.1	2.43	26	4	130	112	0.2054	75.7934
FA10	4	2.30	22	4.5	110	81	0.1830	67.5277
FA11	3.8	2.39	26	4	130	90	0.2256	83.2472
FB1	16.5	5.18	78	3	390	138	6.8786	2538.2288
FB2	13.6	4.91	76	3	380	110	5.1354	1894.9815
FB3	13.6	4.64	72	3.5	360	135	3.2625	1203.8745
FB4	10.8	3.27	52	3	260	81	2.5794	951.8081
FB5	11.9	3.91	64	3.5	320	132	2.4618	908.4133
FB6	10.8	3.91	66	3	330	131	2.2238	820.5904
FB7	13.6	4.00	74	3	370	119	3.6813	1358.4133
FB8	9.4	3.36	52	3	260	109	1.4806	546.3469
FB9	8.7	3.09	54	3	270	108	1.1899	439.0775
FB10	8.3	2.91	48	3.5	240	113	1.0680	394.0959
FB11	6.9	2.91	46	3.5	230	118	0.6992	258.0074
FB12	7	2.82	42	3.5	210	125	0.6432	237.3432
FB13	7.6	3.27	34	3	170	81	1.2459	459.7417
FB14	7.5	2.91	42	3	210	82	0.8143	300.4797

Table 8: Continued.

Sample Number	Ambulacral Length (mm)	Ambulacral Width (mm)	Side Plates per Ambulacra	Side Plates per millimeter	Total Brachiole Number	Pelvis Angle (º)	Mass (g)	Volume (mm^3)
FB15	8.2	3.27	42	3.5	210	118	0.9494	350.3321
FB16	7.3	3.36	48	3.5	240	94	0.8951	330.2952
FB17	5.9	2.45	32	3	160	125	0.4432	163.5424
FB18	5.8	2.82	38	3.5	190	112	0.5582	205.9779
FB19	4.5	2.64	30	3.5	150	91	0.3551	131.0332
FB20	5.4	2.91	34	3.5	170	92	0.4971	183.4317
FB21	5.8	2.64	40	3.5	200	118	0.5751	212.2140
FB22	6.5	3.09	28	2.5	140	82	1.0471	386.3838
FB23	8.1	3.09	46	3	230	112	0.9363	345.4982
FB24	4.7	2.45	24	3	120	76	0.4960	183.0258
GRand1*							1.2265	452.5830

*Sample used for visceral volume requiring mass and volume only so no other measurements were taken.

Table 9: Internal thecal measurements of *Pentremites pyriformis*.

Sample Number	Hydrospire Volume (mm^3)	Hydrospire Surface Area (mm^2)	Total Volume (mm^3)†	Visceral Volume (mm^3)	Total Visceral Volume (mm^3)†	Hydrospire Fold Number
SA13	1.3568	70.7793	46.4292	28.8591	27.5023	3
SA14	1.9401	90.5008	57.0635	35.6337	33.6936	4
SB15	1.7238	82.1657	44.9552	28.1905	26.4668	5
SB11	2.1415	83.3672	71.3271	44.3694	42.2279	4
SB6	5.2467	180.3542	183.5356	114.0101	108.7634	5
S16	7.9093	179.6647	114.9690	74.2091	66.2998	5
S15	7.4591	221.9768	189.1829	118.7568	111.2976	5
S14	10.3315	322.3989	297.1224	185.6786	175.3472	6
S13	18.0675	394.9849	285.9916	183.6284	165.5609	5
SA6	15.8540	461.6289	427.6516	267.8434	251.9894	5
SB5	8.4849	292.0069	314.8731	195.2835	186.7986	6
S8	22.8819	649.1561	671.1402	419.1363	396.2544	6
SB2	22.9208	590.7841	658.9980	411.8268	388.9060	5
S7	24.7306	688.2751	769.9926	479.9520	455.2214	6
S6	49.6770	907.2012	1001.4669	634.8105	585.1335	6
S5	33.7981	803.9994	978.1577	611.1438	577.3458	6
S4	64.9130	1293.2165	1274.1276	808.6781	743.7651	7
S3	79.8867	1779.5661	1756.3864	1108.9685	1029.0818	8

† Hydrospire volume subtracted from measurements.

Table 10: Internal thecal measurements of *Pentremites godoni*.

Sample Number	Hydrospire Volume (mm^3)	Hydrospire Surface Area (mm^2)	Total Volume (mm^3)†	Visceral Volume (mm^3)	Total Visceral Volume (mm^3)†	Hydrospire Fold Number
F13	0.3308	13.9562	8.0456	6.3238	5.9929	3
F15	1.2753	60.7564	45.8464	35.5747	34.2993	4
F10	3.8224	106.6726	141.5650	109.7605	105.9381	4
FB18	6.0898	225.3099	199.8881	155.5034	149.4136	5
F9	8.9496	297.9174	230.3124	180.6313	171.6817	5
F8	15.9165	383.6102	311.3897	247.1005	231.1839	5
F7	17.1896	514.8635	511.8510	399.4001	382.2105	5
FB6	27.3299	768.6494	793.2605	619.5062	592.1763	5
FB5	38.3626	993.1744	870.0507	685.8082	647.4456	5
F5	36.7552	820.2245	1029.1119	804.6783	767.9231	5
FB3	59.8129	1035.6079	1144.0616	908.8673	849.0543	5
FB7	47.2527	1073.8141	1311.1606	1025.5366	978.2839	5
F3	66.8307	1334.2279	1570.3649	1236.0037	1169.1731	5
FB2	103.0427	1501.5973	1791.9388	1430.6197	1327.5770	5
FB1	151.5993	2075.8935	2386.6295	1916.2404	1764.6411	5

† Hydrospire volume subtracted from measurements.

Table 11: Internal hydrospire measurements for each photograph of *Pentremites pyriformis*.

Sample and Photograph Number	Average Hydrospire Area (mm2)	Average Hydrospire Perimeter (mm)	Section Thickness (mm)‡	Single Hydrospire Volume (mm3)	Single Hydrospire Surface Area (mm2)
S4-2	0.6837	8.9070	0.67	0.4558	5.9379
S4-3	0.7696	12.0006	0.67	0.6413	10.0004
S4-4	1.0537	23.4007	1.00	0.8781	19.5005
S4-5	1.1451	22.5145	0.67	0.7634	15.0095
S4-6	1.2153	24.8068	0.67	0.8102	16.5377
S4-7	1.0731	22.4680	0.67	0.8942	18.7233
S4-9	1.0433	19.2071	1.00	0.6955	12.8047
S4-10	1.0156	19.4139	0.33	0.4232	8.0891
S4-11	0.6942	16.6920	0.50	0.3471	8.3460
S4-12	0.6153	15.1062	0.50	0.3076	7.5531
S4-13	0.3630	9.9276	0.50	0.1815	4.9638
S4-14	0.3741	7.4227	0.50	0.0935	1.8557
S4-Last Cut			0.50		
S6-3	0.5309	10.8172	0.67	0.3539	7.2114
S6-4	0.7063	13.9527	0.67	0.4708	9.3017
S6-5	0.9945	15.5696	0.67	0.6630	10.3797
S6-6	1.1003	19.1378	0.67	0.7335	12.7584
S6-7	1.0636	16.0863	0.67	0.7091	10.7241

‡ Thickness of final section with no remaining hydrospires recorded for calculations.

Table 11: Continued.

Sample and Photograph Number	Average Hydrospire Area (mm2)	Average Hydrospire Perimeter (mm)	Section Thickness (mm)‡	Single Hydrospire Volume (mm3)	Single Hydrospire Surface Area (mm2)
S6-8	0.8065	14.8206	0.67	0.5376	9.8803
S6-9	0.6644	13.8716	0.67	0.4429	9.2477
S6-10	0.5399	11.2791	0.67	0.3600	7.5193
S6-11	0.5151	9.9385	0.67	0.3434	6.6256
S6-12	0.3669	6.9911	0.67	0.2446	4.6607
S6-13	0.2177	4.8227	0.67	0.1088	2.4113
S6-Last Cut			0.33		
S13-3	0.2538	6.4153	0.33	0.0846	2.1384
S13-4	0.3689	8.2904	0.33	0.1230	2.7635
S13-5	0.3137	7.9548	0.33	0.1046	2.6516
S13-6	0.3096	7.4081	0.33	0.1548	3.7040
S13-7	0.5270	10.3036	0.67	0.3513	6.8690
S13-8	0.6577	12.8134	0.67	0.4385	8.5422
S13-9	0.4434	9.7768	0.67	0.2956	6.5178
S13-10	0.3233	7.7398	0.67	0.1617	3.8699
S13-11	0.2195	5.7773	0.33	0.0732	1.9257
S13-12	0.1177	3.0983	0.33	0.0196	0.5164
S13-Last Cut			0.33		

‡ Thickness of final section with no remaining hydrospires recorded for calculations.

Table 11: Continued.

Sample and Photograph Number	Average Hydrospire Area (mm2)	Average Hydrospire Perimeter (mm)	Section Thickness (mm)‡	Single Hydrospire Volume (mm3)	Single Hydrospire Surface Area (mm2)
S16-3	0.1818	4.3676	0.33	0.0606	1.4559
S16-4	0.2197	5.4563	0.33	0.0732	1.8187
S16-5	0.3281	6.9376	0.33	0.1094	2.3125
S16-6	0.3316	7.7354	0.33	0.1105	2.5783
S16-7	0.3415	7.6071	0.33	0.1138	2.5355
S16-8	0.3358	7.4139	0.33	0.1119	2.4713
S16-9	0.2784	5.8531	0.33	0.0928	1.9510
S16-10	0.2329	5.3742	0.33	0.0776	1.7914
S16-11	0.1230	3.1555	0.33	0.0410	1.0518
S16-Last Cut			0.33		
S8-1	0.2695	7.3117	0.33	0.1334	3.6193
S8-2	0.4257	11.4850	0.67	0.2810	7.5801
S8-3	0.4958	12.5307	0.67	0.4115	10.4005
S8-4	0.4207	13.9829	1.00	0.4207	13.9829
S8-5	0.4440	10.9491	1.00	0.3685	9.0877
S8-6	0.4228	10.7835	0.67	0.2790	7.1171
S8-7	0.2671	9.7576	0.67	0.1763	6.4400
S8-8	0.2260	6.7331	0.67	0.1491	4.4438

‡ Thickness of final section with no remaining hydrospires recorded for calculations.

Table 11: Continued.

Sample and Photograph Number	Average Hydrospire Area (mm2)	Average Hydrospire Perimeter (mm)	Section Thickness (mm)‡	Single Hydrospire Volume (mm3)	Single Hydrospire Surface Area (mm2)
S8-9	0.1040	3.4003	0.67	0.0686	2.2442
S8-Last Cut			0.67		
S3-1	0.4676	8.2654	0.67	0.3881	6.8603
S3-2	0.6402	13.1244	1.00	0.6402	13.1244
S3-3	0.7452	17.8839	1.00	0.7452	17.8839
S3-4	1.1434	27.9743	1.00	1.1434	27.9743
S3-5	1.2787	28.2674	1.00	1.2787	28.2674
S3-6	1.2431	26.5381	1.00	1.2431	26.5381
S3-7	1.1005	23.4028	1.00	1.2821	27.2643
S3-8	0.6534	15.3282	1.33	0.7612	17.8574
S3-9	0.4390	10.5626	1.00	0.4390	10.5626
S3-10	0.1354	3.2482	1.00	0.0677	1.6241
S3-Last Cut			1.00		
SA6-1	0.1837	4.8161	0.67	0.1212	3.1786
SA6-2	0.3573	8.0399	0.67	0.2358	5.3064
SA6-3	0.3359	8.1922	0.67	0.2217	5.4069
SA6-4	0.3967	11.4938	0.67	0.2618	7.5859
SA6-5	0.4139	12.8224	0.67	0.2732	8.4628
SA6-6	0.3289	10.7895	0.67	0.2171	7.1211

‡ Thickness of final section with no remaining hydrospires recorded for calculations.

Table 11: Continued.

Sample and Photograph Number	Average Hydrospire Area (mm2)	Average Hydrospire Perimeter (mm)	Section Thickness (mm)‡	Single Hydrospire Volume (mm3)	Single Hydrospire Surface Area (mm2)
SA6-7	0.2487	9.3492	0.67	0.1641	6.1705
SA6-8	0.1098	3.1246	0.67	0.0725	2.0622
SA6-9	0.0545	2.6320	0.67	0.0180	0.8686
SA6-Last Cut			0.67		
SB11-1	0.0232	0.6801	0.33	0.0076	0.2244
SB11-2	0.0919	3.2546	0.33	0.0303	1.0740
SB11-3	0.1085	4.8525	0.33	0.0358	1.6013
SB11-4	0.1448	5.4823	0.33	0.0478	1.8092
SB11-5	0.1532	5.5272	0.33	0.0506	1.8240
SB11-6	0.0977	4.2036	0.33	0.0322	1.3872
SB11-7	0.0596	2.5251	0.33	0.0098	0.4166
SB11-Last Cut			0.33		
SA14-2	0.0315	1.7962	0.20	0.0049	0.2818
SA14-3	0.1017	3.9327	0.12	0.0199	0.7711
SA14-4	0.1184	5.5199	0.27	0.0557	2.5976
SA14-5	0.0891	4.4100	0.67	0.0541	2.6806
SA14-6	0.0833	3.7866	0.55	0.0490	2.2274
SA14-7	0.0329	1.5670	0.63	0.0103	0.4916
SA14-Last Cut			0.34		

‡ Thickness of final section with no remaining hydrospires recorded for calculations.

Table 11: Continued.

Sample and Photograph Number	Average Hydrospire Area (mm2)	Average Hydrospire Perimeter (mm)	Section Thickness (mm)‡	Single Hydrospire Volume (mm3)	Single Hydrospire Surface Area (mm2)
SB15-2	0.0770	3.5385	0.18	0.0142	0.6533
SB15-3	0.0838	4.2159	0.18	0.0129	0.6486
SB15-4	0.1106	4.6837	0.12	0.0119	0.5044
SB15-5	0.1179	5.3884	0.09	0.0145	0.6632
SB15-6	0.1331	6.1266	0.15	0.0205	0.9426
SB15-7	0.1561	7.4550	0.15	0.0288	1.3763
SB15-8	0.1577	6.5649	0.22	0.0315	1.3130
SB15-9	0.1126	5.7656	0.18	0.0243	1.2418
SB15-10	0.0687	4.3673	0.25	0.0137	0.8735
SB15-Last Cut			0.15		
SA13-2	0.0372	1.6303	0.25	0.0074	0.3261
SA13-3	0.0604	3.1865	0.15	0.0139	0.7353
SA13-4	0.0678	3.6122	0.31	0.0167	0.8892
SA13-5	0.0773	3.6774	0.18	0.0155	0.7355
SA13-6	0.0795	4.1135	0.22	0.0232	1.2024
SA13-7	0.0821	4.0600	0.37	0.0227	1.1243
SA13-8	0.0677	3.8495	0.18	0.0250	1.4214

‡ Thickness of final section with no remaining hydrospires recorded for calculations.

Table 11: Continued.

Sample and Photograph Number	Average Hydrospire Area (mm2)	Average Hydrospire Perimeter (mm)	Section Thickness (mm)‡	Single Hydrospire Volume (mm3)	Single Hydrospire Surface Area (mm2)
SA13-10	0.0236	1.3008	0.55	0.0080	0.4403
SA13-11	0.0177	1.0991	0.12	0.0027	0.1691
SA13-12	0.0054	0.3733	0.18	0.0010	0.0672
SA13-Last Cut			0.18		
SB6-2	0.1424	5.5751	0.33	0.0475	1.8582
SB6-3	0.1751	6.3912	0.33	0.0584	2.1302
SB6-4	0.2252	7.4572	0.33	0.0751	2.4855
SB6-5	0.2150	8.2916	0.33	0.0717	2.7636
SB6-6	0.3177	8.7371	0.33	0.1059	2.9121
SB6-7	0.1856	6.3101	0.33	0.0618	2.1031
SB6-8	0.1420	5.4187	0.33	0.0473	1.8060
SB6-9	0.1234	4.3250	0.33	0.0411	1.4415
SB6-10	0.0477	1.6057	0.33	0.0159	0.5352
SB6-Last Cut			0.33		
SB2-1	0.0706	1.7046	0.67	0.0471	1.1363
SB2-2	0.4096	10.1298	0.67	0.2730	6.7525
SB2-3	0.5700	13.5395	0.67	0.3799	9.0254

‡ Thickness of final section with no remaining hydrospires recorded for calculations.

Table 11: Continued.

Sample and Photograph Number	Average Hydrospire Area (mm2)	Average Hydrospire Perimeter (mm)	Section Thickness (mm)‡	Single Hydrospire Volume (mm3)	Single Hydrospire Surface Area (mm2)
SB2-4	0.5299	14.7916	0.67	0.3532	9.8601
SB2-5	0.5618	13.6683	0.67	0.3745	9.1113
SB2-6	0.5483	13.2705	0.67	0.3655	8.8461
SB2-7	0.4513	11.4793	0.67	0.3008	7.6521
SB2-8	0.2060	7.0544	0.67	0.1373	4.7025
SB2-9	0.0910	2.9885	0.67	0.0606	1.9921
SB2-Last Cut			0.67		
SB5-1	0.0838	2.8713	0.33	0.0279	0.9570
SB5-2	0.2016	6.8262	0.33	0.0672	2.2752
SB5-3	0.2148	8.0914	0.33	0.0716	2.6969
SB5-4	0.2771	9.0539	0.33	0.0924	3.0177
SB5-5	0.3582	9.9266	0.33	0.1194	3.3085
SB5-6	0.3132	9.8548	0.33	0.1044	3.2846
SB5-7	0.2728	8.7826	0.33	0.0909	2.9272
SB5-8	0.2660	9.2256	0.33	0.0886	3.0749
SB5-9	0.2487	10.1744	0.33	0.0829	3.3911
SB5-10	0.2082	8.1832	0.33	0.0694	2.7275

‡ Thickness of final section with no remaining hydrospires recorded for calculations.

Table 11: Continued.

Sample and Photograph Number	Average Hydrospire Area (mm2)	Average Hydrospire Perimeter (mm)	Section Thickness (mm)‡	Single Hydrospire Volume (mm3)	Single Hydrospire Surface Area (mm2)
SB5-11	0.0873	3.7419	0.33	0.0291	1.2472
SB5-12	0.0284	1.7579	0.33	0.0047	0.2930
SB5-Last Cut			0.33		
S5-1	0.2014	4.4736	0.33	0.0671	1.4911
S5-2	0.4155	9.5103	0.33	0.1385	3.1699
S5-3	0.4571	10.5605	0.33	0.2286	5.2799
S5-4	0.6590	14.2636	0.67	0.5492	11.8859
S5-5	0.7099	17.2864	1.00	0.7099	17.2864
S5-6	0.6612	15.4294	1.00	0.6612	15.4294
S5-7	0.6372	14.5616	1.00	0.6372	14.5616
S5-8	0.3734	10.3723	1.00	0.3111	8.6432
S5-9	0.1056	3.4521	0.67	0.0704	2.3012
S5-10	0.0201	1.0543	0.67	0.0067	0.3514
S5-Last Cut			0.67		
S7-2	0.2725	8.1937	0.67	0.1816	5.4619
S7-3	0.3474	8.7680	0.67	0.2316	5.8448
S7-4	0.4234	11.4259	0.67	0.2822	7.6168

‡ Thickness of final section with no remaining hydrospires recorded for calculations.

Table 11: Continued.

Sample and Photograph Number	Average Hydrospire Area (mm2)	Average Hydrospire Perimeter (mm)	Section Thickness (mm)‡	Single Hydrospire Volume (mm3)	Single Hydrospire Surface Area (mm2)
S7-5	0.5110	13.7124	0.67	0.3407	9.1415
S7-6	0.4123	13.3068	0.67	0.2748	8.8711
S7-7	0.4929	12.4896	0.67	0.4108	10.4079
S7-8	0.4222	10.8480	1.00	0.4222	10.8480
S7-9	0.2900	9.3690	1.00	0.2900	9.3690
S7-10	0.0782	2.5329	1.00	0.0391	1.2664
S7-Last Cut			1.00		
S15-1	0.0693	0.9511	0.33	0.0231	0.3170
S15-2	0.1452	2.6716	0.33	0.0484	0.8905
S15-3	0.1702	4.8364	0.33	0.0567	1.6120
S15-4	0.2227	6.2303	0.33	0.0742	2.0766
S15-5	0.2402	7.1359	0.33	0.0801	2.3784
S15-6	0.2534	8.0663	0.33	0.0845	2.6885
S15-7	0.3468	9.7061	0.33	0.1156	3.2350
S15-8	0.2515	8.3181	0.33	0.1257	4.1586
S15-9	0.1625	5.6844	0.67	0.1083	3.7892
S15-10	0.0439	1.5780	0.67	0.0293	1.0519
S15-Last Cut			0.67		

‡ Thickness of final section with no remaining hydrospires recorded for calculations.

Table 11: Continued.

Sample and Photograph Number	Average Hydrospire Area (mm2)	Average Hydrospire Perimeter (mm)	Section Thickness (mm)‡	Single Hydrospire Volume (mm3)	Single Hydrospire Surface Area (mm2)
S14-2	0.1106	3.1863	0.33	0.0369	1.0620
S14-3	0.3310	7.9585	0.33	0.1103	2.6526
S14-4	0.3508	9.0458	0.33	0.1169	3.0150
S14-5	0.3510	10.5634	0.33	0.1170	3.5208
S14-6	0.4143	12.1937	0.33	0.1381	4.0642
S14-7	0.3202	10.8919	0.33	0.1067	3.6303
S14-8	0.3173	11.6719	0.33	0.1586	5.8353
S14-9	0.2858	9.7423	0.67	0.1905	6.4942
S14-10	0.1745	5.8974	0.67	0.0582	1.9656
S14-Last Cut			0.67		

‡ Thickness of final section with no remaining hydrospires recorded for calculations.

Table 12: Internal hydrospire measurements for each captured photograph of *Pentremites godoni*.

Sample and Photograph Number	Average Hydrospire Area (mm2)	Average Hydrospire Perimeter (mm)	Section Thickness (mm)‡	Single Hydrospire Volume (mm3)	Single Hydrospire Surface Area (mm2)
F8-2	0.2388	5.4587	0.67	0.1592	3.6391
F8-3	0.3011	7.7680	0.67	0.2008	5.1786
F8-4	0.4651	9.4459	0.67	0.3101	6.2972
F8-5	0.3855	9.6351	0.67	0.2570	6.4233
F8-6	0.3615	8.5499	0.67	0.2410	5.6999
F8-7	0.2832	7.9927	0.67	0.1888	5.3284
F8-8	0.2148	5.5024	0.67	0.1432	3.6682
F8-9	0.1834	4.2526	0.67	0.0917	2.1263
F8-Last Cut			0.33		
F10-2	0.1330	4.5618	0.33	0.0443	1.5206
F10-3	0.2487	6.2635	0.33	0.0829	2.0878
F10-4	0.2308	6.3671	0.33	0.0769	2.1224
F10-5	0.2900	6.6734	0.33	0.0967	2.2244
F10-6	0.1448	4.7063	0.33	0.0483	1.5687
F10-7	0.0994	3.4300	0.33	0.0331	1.1433
F10-Last Cut			0.33		

‡ Thickness of final section with no remaining hydrospires recorded for calculations.

Table 12: Continued.

Sample and Photograph Number	Average Hydrospire Area (mm2)	Average Hydrospire Perimeter (mm)	Section Thickness (mm)‡	Single Hydrospire Volume (mm3)	Single Hydrospire Surface Area (mm2)
FB2-2	0.7776	12.3512	0.67	0.5184	8.2340
FB2-3	0.8449	11.3067	0.67	0.5633	7.5377
FB2-4	1.2133	17.7677	0.67	0.8088	11.8450
FB2-5	1.7157	21.4633	0.67	1.1438	14.3088
FB2-6	1.7102	24.1262	0.67	1.1401	16.0839
FB2-7	1.7911	21.7729	0.67	1.1941	14.5151
FB2-8	1.4564	20.2981	0.67	0.9709	13.5320
FB2-9	1.4438	18.8970	0.67	0.9625	12.5978
FB2-10	1.0639	16.6755	0.67	0.7093	11.1169
FB2-11	0.8972	15.0160	0.67	0.5982	10.0106
FB2-12	0.7513	13.1489	0.67	0.5009	8.7658
FB2-13	0.5880	11.2215	0.67	0.3920	7.4810
FB2-14	0.4518	8.4487	0.67	0.3012	5.6324
FB2-15	0.4613	7.1623	0.67	0.3075	4.7748
FB2-16	0.2901	5.5858	0.67	0.1934	3.7238
FB2-Last Cut			0.67		

‡ Thickness of final section with no remaining hydrospires recorded for calculations.

Table 12: Continued.

Sample and Photograph Number	Average Hydrospire Area (mm2)	Average Hydrospire Perimeter (mm)	Section Thickness (mm)‡	Single Hydrospire Volume (mm3)	Single Hydrospire Surface Area (mm2)
FB3-2	0.8737	10.5259	0.67	0.5824	7.0172
FB3-3	0.8944	12.8881	0.67	0.7453	10.7400
FB3-4	1.0598	16.5223	1.00	1.0598	16.5223
FB3-5	0.9124	15.3387	1.00	0.9124	15.3387
FB3-6	0.9443	13.7944	1.00	0.9443	13.7944
FB3-7	0.5400	10.5191	1.00	0.5400	10.5191
FB3-8	0.5273	10.8833	1.00	0.5273	10.8833
FB3-9	0.3275	9.3493	1.00	0.3275	9.3493
FB3-10	0.2464	6.7013	1.00	0.2045	5.5621
FB3-11	0.2083	5.8098	0.67	0.1375	3.8345
FB3-Last Cut			0.67		
FB5-1	0.2898	6.8451	0.33	0.1434	3.3883
FB5-2	0.4437	11.3896	0.67	0.2928	7.5171
FB5-3	0.7051	15.2388	0.67	0.5853	12.6482
FB5-4	0.5669	16.3880	1.00	0.5669	16.3880
FB5-5	0.6212	17.1988	1.00	0.6212	17.1988
FB5-6	0.5555	14.2465	1.00	0.5555	14.2465
FB5-7	0.5564	13.2930	1.00	0.5564	13.2930

‡ Thickness of final section with no remaining hydrospires recorded for calculations.

Table 12: Continued.

Sample and Photograph Number	Average Hydrospire Area (mm2)	Average Hydrospire Perimeter (mm)	Section Thickness (mm)‡	Single Hydrospire Volume (mm3)	Single Hydrospire Surface Area (mm2)
FB5-8	0.3903	11.0184	1.00	0.3903	11.0184
FB5-9	0.2487	7.2383	1.00	0.1244	3.6192
FB5-Last Cut			0.67		
FB6-2	0.3458	8.2425	0.33	0.1141	2.7200
FB6-3	0.3166	8.6224	0.33	0.1045	2.8454
FB6-4	0.4101	9.7539	0.33	0.2030	4.8282
FB6-5	0.4610	15.4578	0.67	0.3043	10.2021
FB6-6	0.7388	17.5621	0.67	0.6132	14.5765
FB6-7	0.5145	14.7719	1.00	0.4270	12.2607
FB6-8	0.5305	14.1683	0.67	0.4403	11.7597
FB6-9	0.3405	11.0752	1.00	0.3405	11.0752
FB6-10	0.1862	6.5972	1.00	0.1862	6.5972
FB6-Last Cut			1.00		
FB1-1	0.9301	11.2037	0.67	0.6139	7.3945
FB1-2	1.5233	15.9806	0.67	1.2643	13.2639
FB1-3	1.0995	15.8751	1.00	1.0995	15.8751
FB1-4	1.1178	19.3192	1.00	1.3022	22.5068
FB1-5	1.3214	20.7522	1.33	2.2000	34.5523
FB1-6	1.8915	22.2524	2.00	3.7830	44.5048

‡ Thickness of final section with no remaining hydrospires recorded for calculations.

Table 12: Continued.

Sample and Photograph Number	Average Hydrospire Area (mm2)	Average Hydrospire Perimeter (mm)	Section Thickness (mm)‡	Single Hydrospire Volume (mm3)	Single Hydrospire Surface Area (mm2)
FB1-7	1.5032	19.7963	2.00	3.0064	39.5926
FB1-8	0.8626	12.6034	2.00	1.7252	25.2068
FB1-9	0.1654	4.6926	2.00	0.1654	4.6926
FB1-Last Cut			1.00		
F9-1	0.1479	4.9365	0.33	0.0488	1.6290
F9-2	0.2065	7.1021	0.33	0.0681	2.3437
F9-3	0.2365	8.7254	0.33	0.1171	4.3191
F9-4	0.3593	10.4341	0.67	0.2372	6.8865
F9-5	0.2884	9.4970	0.67	0.1903	6.2680
F9-6	0.2008	7.3352	0.67	0.1326	4.8413
F9-7	0.1417	4.8609	0.67	0.0935	3.2082
F9-8	0.0223	0.8967	0.67	0.0073	0.2959
F9-Last Cut			0.67		
F15-2	0.0803	3.4044	0.20	0.0268	1.1348
F15-3	0.1097	4.7317	0.47	0.0430	1.8556
F15-4	0.0967	4.9580	0.31	0.0246	1.2638
F15-5	0.0656	3.5313	0.20	0.0154	0.8309

‡ Thickness of final section with no remaining hydrospires recorded for calculations.

Table 12: Continued.

Sample and Photograph Number	Average Hydrospire Area (mm2)	Average Hydrospire Perimeter (mm)	Section Thickness (mm)‡	Single Hydrospire Volume (mm3)	Single Hydrospire Surface Area (mm2)
F15-6	0.0410	2.2963	0.27	0.0177	0.9906
F15-Last Cut			0.59		
F13-2	0.0503	2.0991	0.27	0.0114	0.4777
F13-3	0.0616	2.6693	0.19	0.0104	0.4514
F13-4	0.0649	2.6989	0.15	0.0112	0.4665
F13-Last Cut			0.20		
F5-1	0.2154	4.0157	0.33	0.0718	1.3384
F5-2	0.4411	8.4599	0.33	0.2205	4.2295
F5-3	0.5411	12.6296	0.67	0.3607	8.4189
F5-4	0.7675	15.3921	0.67	0.6396	12.8262
F5-5	0.7266	15.1121	1.00	0.7266	15.1121
F5-6	0.5631	12.7194	1.00	0.5631	12.7194
F5-7	0.5323	11.8718	1.00	0.5323	11.8718
F5-8	0.3590	9.6465	1.00	0.3590	9.6465
F5-9	0.1090	3.2670	1.00	0.1090	3.2670
F5-10	0.0929	2.5925	1.00	0.0929	2.5925
F5-Last Cut			1.00		

‡ Thickness of final section with no remaining hydrospires recorded for calculations.

Table 12: Continued.

Sample and Photograph Number	Average Hydrospire Area (mm2)	Average Hydrospire Perimeter (mm)	Section Thickness (mm)‡	Single Hydrospire Volume (mm3)	Single Hydrospire Surface Area (mm2)
F3-1	0.4949	9.1318	0.67	0.4124	7.6095
F3-2	0.7752	13.9329	1.00	0.7752	13.9329
F3-3	0.8042	16.3214	1.00	0.8042	16.3214
F3-4	0.9315	18.2805	1.00	0.9315	18.2805
F3-5	0.9055	16.5698	1.00	0.9055	16.5698
F3-6	0.7427	14.6116	1.00	0.7427	14.6116
F3-7	0.7085	13.2482	1.00	0.9446	17.6639
F3-8	0.4592	9.7426	1.67	0.7653	16.2371
F3-9	0.2410	7.3180	1.67	0.4017	12.1962
F3-Last Cut			1.67		
F7-1	0.1879	4.8424	0.67	0.1253	3.2279
F7-2	0.3124	9.9235	0.67	0.2082	6.6150
F7-3	0.3999	11.8809	0.67	0.2665	7.9198
F7-4	0.4030	11.2838	0.67	0.2686	7.5218
F7-5	0.4039	11.1402	0.67	0.2692	7.4261
F7-6	0.3132	10.2604	0.67	0.2088	6.8396
F7-7	0.2764	8.8792	0.67	0.1843	5.9189
F7-8	0.2325	7.0655	0.67	0.1550	4.7098

‡ Thickness of final section with no remaining hydrospires recorded for calculations.

Table 12: Continued.

Sample and Photograph Number	Average Hydrospire Area (mm2)	Average Hydrospire Perimeter (mm)	Section Thickness (mm)‡	Single Hydrospire Volume (mm3)	Single Hydrospire Surface Area (mm2)
F7-9	0.0496	1.9613	0.67	0.0331	1.3074
F7-Last Cut			0.67		
FB7-1	0.4765	9.8278	0.67	0.3176	6.5512
FB7-2	0.5269	13.3513	0.67	0.3512	8.9000
FB7-3	0.6984	15.4125	0.67	0.4656	10.2740
FB7-4	0.7921	17.9557	0.67	0.5280	11.9693
FB7-5	0.8655	17.5315	0.67	0.7212	14.6090
FB7-6	0.7474	15.6735	1.00	0.7474	15.6735
FB7-7	0.7020	13.9480	1.00	0.7020	13.9480
FB7-8	0.4176	11.3093	1.00	0.4176	11.3093
FB7-9	0.2971	8.8302	1.00	0.3466	10.3018
FB7-10	0.0960	2.8841	1.33	0.1281	3.8454
FB7-Last Cut			1.33		
FB18-2	0.1714	5.9376	0.33	0.0571	1.9790
FB18-3	0.1993	7.4676	0.33	0.0664	2.4890
FB18-4	0.2092	8.2594	0.33	0.0697	2.7529
FB18-5	0.2178	7.9128	0.33	0.0726	2.6373

‡ Thickness of final section with no remaining hydrospires recorded for calculations.

Table 12: Continued.

Sample and Photograph Number	Average Hydrospire Area (mm2)	Average Hydrospire Perimeter (mm)	Section Thickness (mm)‡	Single Hydrospire Volume (mm3)	Single Hydrospire Surface Area (mm2)
FB18-6	0.2781	8.7366	0.33	0.0927	2.9119
FB18-7	0.1829	7.4906	0.33	0.0610	2.4966
FB18-8	0.1865	7.3006	0.33	0.0622	2.4333
FB18-9	0.1740	6.4381	0.33	0.0580	2.1458
FB18-10	0.1525	5.4766	0.33	0.0508	1.8254
FB18-11	0.0553	2.5797	0.33	0.0184	0.8598
FB18-Last Cut			0.33		

‡ Thickness of final section with no remaining hydrospires recorded for calculations.

Table 13: Internal measurements of visceral volume calculated for *Pentremites pyriformis*.

Sample Number S10		Sample Number SA1		Sample Number SA7	
Diameter (mm)	Thickness (mm)	Diameter (mm)	Thickness (mm)	Diameter (mm)	Thickness (mm)
	0.1110		0.1277		0.0323
0.3774	0.4071	1.0647	0.4255	0.4194	0.2258
2.8127	0.4071	1.2348	0.4255	1.3875	0.2258
4.2193	0.4071	2.3830	0.4255	1.7419	0.2258
4.9963	0.4071	3.9149	0.4255	1.9032	0.2258
5.5885	0.4071	4.6385	0.4255	2.4839	0.2258
6.0700	0.4071	5.8304	0.4255	2.7744	0.2258
6.6247	0.4071	6.2555	0.4255	3.1935	0.2258
7.1429	0.4071	6.9787	0.4255	3.5808	0.2258
7.5501	0.4071	7.1916	0.4255	3.7419	0.2258
7.6241	0.4071	7.7874	0.4255	3.9679	0.2258
7.8090	0.4071	7.9576	0.4255	4.1292	0.2258
8.1051	0.4071	8.0426	0.4255	4.1613	0.2258
8.0681	0.4071	8.1702	0.4255	4.2903	0.2258
8.1421	0.4071	8.3404	0.4255	4.5161	0.2258
8.1051	0.4071	8.5107	0.4255	4.3872	0.2258
7.8091	0.4071	8.4682	0.4255	4.3227	0.2258
7.3279	0.4071	8.3404	0.4255	4.2581	0.2258
6.8468	0.4071	8.5111	0.4255	4.0324	0.2258
6.4028	0.4071	8.5106	0.4255	3.8711	0.2258

Table 13: Continued.

Sample Number S10		Sample Number SA1		Sample Number SA7	
Diameter (mm)	Thickness (mm)	Diameter (mm)	Thickness (mm)	Diameter (mm)	Thickness (mm)
6.1437	0.4071	8.4682	0.4255	3.6774	0.2258
5.8105	0.4071	8.4256	0.4255	3.4516	0.2258
5.3664	0.4071	7.0214	0.4255	3.3871	0.2258
5.0703	0.4071	6.4681	0.4255	3.1615	0.2258
4.5893	0.4071	6.3406	0.4255	3.0323	0.2258
4.3673	0.4071	5.9149	0.4255	2.8066	0.2258
4.0340	0.4071	5.4468	0.4255	2.5484	0.2258
3.6271	0.4071	5.1917	0.4255	2.4839	0.2258
2.9608	0.4071	4.7660	0.4255	1.9677	0.2258
2.1466	0.4071	4.5534	0.4255	1.4842	0.2258
1.5914	0.4071	4.0434	0.4255	1.4197	0.2258
1.2959	0.4071	3.7447	0.4255	1.0000	0.2258
0.9993	0.4071	2.8511	0.4255	0.7742	0.2258
0.5181	0.4071	2.3845	0.4255	0.4194	0.1613
0.2984	0.4071	1.8723	0.4255		
0.1110	0.3351	1.1489	0.4255		
		0.5973	0.2979		

Table 13: Continued.

Sample Number SB9	
Diameter (mm)	Thickness (mm)
	0.1584
0.8318	0.2377
2.3767	0.2377
3.4066	0.2377
3.8027	0.2377
4.0008	0.2377
4.1989	0.2377
4.3573	0.2377
4.6744	0.2377
4.9911	0.2377
5.1101	0.2377
5.2684	0.2377
5.4664	0.2377
5.4666	0.2377
5.4268	0.2377
5.5853	0.2377
5.5062	0.2377
5.4664	0.2377
5.4666	0.2377
4.4365	0.2377
4.1989	0.2377
3.8423	0.2377
3.7235	0.2377
3.5651	0.2377
3.4066	0.2377
3.2086	0.2377
3.0501	0.2377
2.8523	0.2377
2.4559	0.2377
1.6642	0.2377
1.2280	0.2377
1.0695	0.2377
0.5942	0.1584

Table 14: Internal measurements of the visceral volume calculated for *Pentremites godoni*.

Sample Number F2		Sample Number FB4		Sample Number FB19	
Diameter (mm)	Thickness (mm)	Diameter (mm)	Thickness (mm)	Diameter (mm)	Thickness (mm)
	0.3717		0.2301		0.1024
1.3937	0.5110	0.9212	0.3835	0.6909	0.1791
5.5749	0.5110	2.4931	0.3835	0.9468	0.1791
8.5948	0.5110	2.7613	0.3835	1.4844	0.1791
10.0348	0.5110	3.4132	0.3835	2.3797	0.1791
11.1034	0.5110	4.6021	0.3835	2.8147	0.1791
12.0791	0.5110	4.9856	0.3835	3.3009	0.1791
12.7759	0.5110	5.5227	0.3835	3.8128	0.1791
13.4263	0.5110	5.9445	0.3835	4.0687	0.1791
13.7515	0.5110	6.3280	0.3835	4.2734	0.1791
14.5415	0.5110	6.5964	0.3835	4.4780	0.1791
15.1917	0.5110	6.9803	0.3835	4.7595	0.1791
15.7957	0.5110	7.2101	0.3835	5.0666	0.1791
16.1209	0.5110	7.5169	0.3835	5.2201	0.1791
16.4925	0.5110	7.6702	0.3835	5.5015	0.1791
16.8644	0.5110	7.9771	0.3835	5.5784	0.1791
16.9570	0.5110	8.3605	0.3835	5.7574	0.1791
17.0502	0.5110	8.5907	0.3835	5.7575	0.1791

Table 14: Continued.

Sample Number F2		Sample Number FB4		Sample Number FB19	
Diameter (mm)	Thickness (mm)	Diameter (mm)	Thickness (mm)	Diameter (mm)	Thickness (mm)
16.9108	0.5110	8.6293	0.3835	5.8087	0.1791
16.7713	0.5110	8.7057	0.3835	5.8086	0.1791
16.7715	0.5110	8.8207	0.3835	5.2968	0.1791
16.8642	0.5110	8.7057	0.3835	5.0921	0.1791
16.8177	0.5110	8.6674	0.3835	4.9642	0.1791
16.6318	0.5110	8.4756	0.3835	4.8875	0.1791
16.7250	0.5110	8.5906	0.3835	4.8106	0.1791
16.6783	0.5110	7.0182	0.3835	4.5804	0.1791
16.3067	0.5110	6.5965	0.3835	4.4269	0.1791
16.1673	0.5110	6.3663	0.3835	4.2989	0.1791
15.8421	0.5110	6.2513	0.3835	4.0431	0.1791
15.0523	0.5110	5.7148	0.3835	3.8895	0.1791
12.7295	0.5110	5.3309	0.3835	3.7360	0.1791
11.8935	0.5110	4.7178	0.3835	3.5056	0.1791
10.4994	0.5110	4.1421	0.3835	3.0450	0.1791
9.1057	0.5110	3.6435	0.3835	2.4821	0.1791
6.5507	0.5110	2.7240	0.3835	1.5867	0.1791
1.3937	0.1915	1.9175	0.3835	1.1003	0.1024

Table 14: Continued**.**

Sample Number FB23		Sample Number GRand1	
Diameter (mm)	Thickness (mm)	Diameter (mm)	Thickness (mm)
	0.0727		0.1172
0.1024	0.2544	0.5274	0.2653
0.1535	0.2544	0.9380	0.2653
0.2063	0.2544	1.7287	0.2653
0.2047	0.2544	2.1096	0.2653
0.1791	0.2544	2.9891	0.2653
0.1791	0.2544	3.6928	0.2653
0.4376	0.2544	4.8345	0.2653
1.0544	0.2544	5.1571	0.2653
2.3256	0.2544	5.5084	0.2653
3.3069	0.2544	6.0065	0.2653
3.8156	0.2544	6.3873	0.2653
4.9420	0.2544	6.6218	0.2653
5.2331	0.2544	7.0320	0.2653
5.6323	0.2544	7.1201	0.2653
5.7777	0.2544	7.2957	0.2653
6.1773	0.2544	7.3835	0.2653
6.4317	0.2544	7.4128	0.2653
6.5044	0.2544	7.4422	0.2653
6.7225	0.2544	7.5593	0.2653

Table 14: Continued.

Sample Number FB23		Sample Number GRand1	
Diameter (mm)	Thickness (mm)	Diameter (mm)	Thickness (mm)
6.7587	0.2544	7.7059	0.2653
6.7225	0.2544	7.5007	0.2653
6.7952	0.2544	7.5301	0.2653
6.8677	0.2544	7.5007	0.2653
7.0494	0.2544	7.4129	0.2653
7.0495	0.2544	7.3543	0.2653
6.9041	0.2544	7.2370	0.2653
7.0495	0.2544	6.5925	0.2653
6.8678	0.2544	5.7721	0.2653
6.5408	0.2544	5.2740	0.2653
5.9593	0.2544	5.3033	0.2653
5.4869	0.2544	4.5415	0.2653
5.2690	0.2544	4.3365	0.2653
4.9420	0.2544	3.8090	0.2653
4.4333	0.2544	3.2230	0.2653
3.8156	0.2544	1.8754	0.2653
3.2342	0.2544		
2.7253	0.2544		
1.6356	0.2544		

Vita

Troy Anthony Dexter was born and raised in the small suburban area known as New Jersey on June 28th in the year of our Lord, 1977. He was born into a loving family, conceived by Elizabeth G. Patullo and fathered by Andrew G. Dexter. Troy's fascination with paleontology began at an early age despite the fact that there was no money to be made in such a career. The sciences were always the primary focus of his studies in school, and he later gained particular interest in evolutionary theory. Despite attending Bound Brook High School, he was accepted into Albright College in Reading, PA in 1995. He later received a bachelor of science in biology and graduated Albright in May of 1999. After receiving his degree, he moved to Brumphus, New Jersey to work a number of laboratory jobs, including scanning electron microscopist and artificial flavor technician. His most notable job was working in the Consumer Products Division of Johnson & Johnson compounding a number of familiar products, including Baby Lotion, Baby Powder, and K-Y Warming Liquid (the secret ingredient is honey). Tiring of the corporate grind, Troy returned to academia to study evolution using the fossils that once fascinated him as a child. He arrived at the Earth and Planetary Sciences Department of the University of Tennessee in the fall of 2003 to work in the field of paleobiology using the extinct echinoderm clade Blastoidea. After distinguishing himself with his exceptional Master's thesis, Troy plans on continuing his education in the PhD program at Virginia Polytechnic Institute's Paleobiology Group.